NASA/CR—2001-210882

20010038803

52 8760
Pg 156



System Report for the Optical Properties Monitor (OPM) Experiment

L. Hummer
AZ Technology, Inc., Huntsville, AL 35806



Prepared for Marshall Space Flight Center
under Contract NAS8–39237

March 2001

The NASA STI Program Office...in Profile

Since its founding, NASA has been dedicated to the advancement of aeronautics and space science. The NASA Scientific and Technical Information (STI) Program Office plays a key part in helping NASA maintain this important role.

The NASA STI Program Office is operated by Langley Research Center, the lead center for NASA's scientific and technical information. The NASA STI Program Office provides access to the NASA STI Database, the largest collection of aeronautical and space science STI in the world. The Program Office is also NASA's institutional mechanism for disseminating the results of its research and development activities. These results are published by NASA in the NASA STI Report Series, which includes the following report types:

- TECHNICAL PUBLICATION. Reports of completed research or a major significant phase of research that present the results of NASA programs and include extensive data or theoretical analysis. Includes compilations of significant scientific and technical data and information deemed to be of continuing reference value. NASA's counterpart of peer-reviewed formal professional papers but has less stringent limitations on manuscript length and extent of graphic presentations.

- TECHNICAL MEMORANDUM. Scientific and technical findings that are preliminary or of specialized interest, e.g., quick release reports, working papers, and bibliographies that contain minimal annotation. Does not contain extensive analysis.

- CONTRACTOR REPORT. Scientific and technical findings by NASA-sponsored contractors and grantees.

- CONFERENCE PUBLICATION. Collected papers from scientific and technical conferences, symposia, seminars, or other meetings sponsored or cosponsored by NASA.

- SPECIAL PUBLICATION. Scientific, technical, or historical information from NASA programs, projects, and mission, often concerned with subjects having substantial public interest.

- TECHNICAL TRANSLATION. English-language translations of foreign scientific and technical material pertinent to NASA's mission.

Specialized services that complement the STI Program Office's diverse offerings include creating custom thesauri, building customized databases, organizing and publishing research results...even providing videos.

For more information about the NASA STI Program Office, see the following:

- Access the NASA STI Program Home Page at ***http://www.sti.nasa.gov***

- E-mail your question via the Internet to help@sti.nasa.gov

- Fax your question to the NASA Access Help Desk at (301) 621–0134

- Telephone the NASA Access Help Desk at (301) 621–0390

- Write to:
  NASA Access Help Desk
  NASA Center for AeroSpace Information
  7121 Standard Drive
  Hanover, MD 21076–1320

NASA/CR—2001-210882



System Report for the Optical Properties Monitor (OPM) Experiment

L. Hummer
AZ Technology, Inc., Huntsville, AL 35806

National Aeronautics
and Space Administration

Prepared for Marshall Space Flight Center•MSFC, Alabama 35812

March 2001

Page intentionally left blank

Page intentionally left blank

TABLE OF CONTENTS

1.0 OPM EXPERIMENT OVERVIEW 1

1.1 Background 1

1.2 Requirements 2

1.3 Design/Integration 4

1.4 Environmental Testing 5
1.4.1 Vibration Testing 6
1.4.2 Thermal Vacuum 9
1.4.3 EMI/EMC 11
1.4.4 Toxicity 12

1.5 Russian Acceptance Testing 12

1.6 Launch (STS-81) 13

1.7 Mission 15
1.7.1 Events on Mir 16
1.7.1.1 Docking Module Condensation Pools 16
1.7.1.2 Mir Fire 17
1.7.1.3 OPM EVA Deployment 17
1.7.1.4 The Progress Resupply Vehicle Collision into Spektr 19
1.7.1.5 Retrieval 19
1.7.2 Power On/Off Status Charts 20
1.7.3 Timeline/Data Status 20

1.7 Return to Ground (STS-89) 27

2.0 OPM SYSTEMS DESCRIPTION AND MISSION PERFORMANCE 28

2.1 Structure 28
2.1.1 Mission Performance 28

2.2 Thermal Control 29
2.2.1 Mission Performance 31

2.3 Power/Control System 33
2.3.1 Power Supply Center (PSC) 35
2.3.2 Power Amplifier Center (PAC) 37
2.3.3 Data Acquisition and Control System (DACS) 38
2.3.4 Power Timeline 40
2.3.5 Mission Performance 43

2.4 Carousel Drive Assembly 43
2.4.1 Sample Carousel 44
2.4.2 Carousel Drive Motor 48
2.4.3 Cable Management System 49

TABLE OF CONTENTS

2.4.3 Cable Management System 49
2.4.4 Mission Performance 49

2.5 Software 50
2.5.1 Design 50
2.5.1.1 Flight Software 50
2.5.1.2 Ground Software 62
2.5.1.3 MIPS Software 66
2.5.2 Software Test and Verification 70
2.5.2.1 Flight Software 70
2.5.2.2 MIPS Software 71
2.5.3 Mission Performance 71
2.5.3.1 Flight Software Anomalies 71
2.5.3.2 MIPS Software Anomalies 72

2.6 Data Acquisition and Analysis 72
2.6.1 Overview 72
2.6.1.1 Single Event Upsets, Double Event Upsets 74
2.6.2 Data Log Formats 76
2.6.2.1 Instrument Sample Numbering 76
2.6.2.2 AO Monitor Data 76
2.6.2.3 Radiometer Data 77
2.6.3 DACS Health and Status Data 77
2.6.3.1 Overview 77
2.6.3.2 Reduced OPM Data File Types 77
2.6.3.3 OPM Voltage Measurements 78
2.6.3.4 System Time 78
2.6.3.5 Events 79
2.6.4 Temperature Data 81
2.6.4.1 OPM Thermistor Placement 81

2.7 Harness/Cabling 82
2.7.1 OPM Harness 82
2.7.2 EVA Cable 82
2.7.3 IVA Cable 83
2.7.4 Mission Performance 83

3.0 OPM INSTRUMENT/MONITORING SUBSYSTEM DESCRIPTIONS AND MISSION PERFORMANCE 85

3.1 Reflectometer 85
3.1.1 Instrument Description 86
3.1.1.1 Operation 86
3.1.2 Instrument Design 86
3.1.2.1 Optical Design 87

TABLE OF CONTENTS

3.1.2.2 Electronics Design 88
3.1.2.3 Mechanical Design 92
3.1.2.4 Software Design 93
3.1.3 Testing 94
3.1.4 Mission Status 95
3.1.4.1 Flight Performance 95
3.1.4.2 Flight Anomalies 97

3.2 Vacuum Ultraviolet (VUV) Spectrometer 97
3.2.1 Instrument Description 97
3.2.1.1 Operation 97
3.2.2 Instrument Design 98
3.2.2.1 Optical Design 98
3.2.2.2 Electrical Design 100
3.2.2.3 Mechanical Design 103
3.2.2.4 Software Design 104
3.2.3 Testing 104
3.2.4 Mission Status 104
3.2.4.1 Flight Performance 104
3.2.4.2 Flight Anomalies 105

3.3 Total Integrated Scatter [1,2] (TIS) 106
3.3.1 Instrument Description 106
3.3.1.1 Operation 106
3.3.2 Instrument Design 109
3.3.2.1 Optical Design 109
3.3.2.2 Electronics Design 110
3.3.2.3 Mechanical Design 112
3.3.2.4 Software Design 113
3.3.3 Testing 114
3.3.4 Mission Status 114
3.3.4.1 Flight Performance 114
3.3.4.2 Flight Anomalies 115

3.4 Molecular Contamination Monitor 117
3.4.1 TQCM Design 117
3.4.1.1 TQCM Electrical Design 118
3.4.1.2 TQCM Mechanical Design 118
3.4.1.3 TQCM Software Design 119
3.4.2 Testing 119
3.4.3 Mission Status 119
3.4.3.1 Flight Performance 119
3.4.3.2 Flight Anomalies 121

TABLE OF CONTENTS

3.5 Atomic Oxygen (AO) Monitor 121
3.5.1 AO Monitor Design 121
3.5.1.1 AO Monitor Electrical Design 123
3.5.1.2 AO Monitor Mechanical Design 124
3.5.1.3 AO Monitor Software Design 124
3.5.2 Testing 125
3.5.3 Mission Status 125
3.5.3.1 Flight Performance 125
3.5.3.2 Flight Anomalies 126

3.6 Irradiance Monitors 126
3.6.1 Radiometer Design 126
3.6.1.1 Radiometer Electrical Design 127
3.6.1.2 Radiometer Mechanical Design 127
3.6.1.3 Radiometer Software Design 129
3.6.2 Testing 129
3.6.3 Mission Status 129
3.6.3.1 Flight Performance 129
3.6.3.2 Flight Anomalies 129

4.0 POST-FLIGHT STATUS 131

4.1 Hardware Returned From Flight 131

4.2 Post-Flight Functional Test at the SPPF 132

4.3 Post-Flight Functional Test at AZ Technology 132

4.4 Status Checks and Anomaly Investigations 132

5.0 SUMMARY 134

ATTACHMENT 1 ..... A-1

LIST OF FIGURES v

LIST OF TABLES vii

ACRONYMS & ABBREVIATIONS viii

LIST OF FIGURES

Figure 1-1. OPM on the Vibration Test Stand....6
Figure 1-2. X_{OPM} - Axis Power Spectral Density....7
Figure 1-3. Y_{OPM} - Axis Power Spectral Density....8
Figure 1-4. Z_{OPM} - Axis Power Spectral Density....8
Figure 1-5. OPM Thermal Vacuum Test Cycles....10
Figure 1-6. OPM in the Thermal Vacuum Chamber....10
Figure 1-7. OPM Being Placed in the Toxicity Chamber for Test....13
Figure 1-8. Hardware Transferred to Mir....14
Figure 1-9. OPM Launch Configuration in the SpaceHab Double Rack....15
Figure 1-10. OPM on MIR (Docking Module-End View)....18
Figure 1-11. OPM Mounting Orientation on the Mir....18
Figure 1-12. OPM "ON" TIME - Measurement Timeline....21
Figure 2-1. OPM Design Configuration....29
Figure 2-2. OPM Reflectometer Thermal Profile for the Measurement Sequence....30
Figure 2-3. Effects of UV Vacuum Exposure on Non-etched Side of 500F I/B....32
Figure 2-4. Effects of UV Vacuum Exposure on Etched Side of 500F I/B....32
Figure 2-5. OPM MIR Power/Data Interface....34
Figure 2-6. OPM Power/Data System Architecture....34
Figure 2-7. Power Supply Center (PSC)....36
Figure 2-8. PAC Architecture....37
Figure 2-9. DACS Mother Board....40
Figure 2-10. DACS Daughter Board....41
Figure 2-11. OPM Power Profile....42
Figure 2-12. OPM Order of Instrument Operation....42
Figure 2-13. Sample Carousel....44
Figure 2-14. Calorimeter Sample Holder (Reflectometer Sample)....46
Figure 2-15. Test Sample Assembly VUV, TIS, and Passive Sample....47
Figure 2-16. Sample FOV....48
Figure 2-17. OPM Control Program State Transition Diagram....52
Figure 2.18. Mass Memory Layout....62
Figure 2-19. Reflectometer PC-Based Test Program (REFCTL)....64
Figure 2-20. OPM/DACS Test Configurations....64
Figure 2-21. ESU Configuration....65
Figure 2-22. User Interface....66
Figure 2-23. OPM-MIPS-Mir Data Transfer....67
Figure 2-24. OPM Data Collection Timeline....73
Figure 3-1. Reflectometer Optical Schematic....86
Figure 3-2. Integrating Sphere Reflectometer Subsystem....89
Figure 3-3. Synchronous Detector Block Diagram....90
Figure 3-4. Signal and Noise versus Frequency....90
Figure 3-5. Demodulated Signal and Noise....91
Figure 3-6 Photograph of the Reflectometer Assembly....92
Figure 3-7. Drawing of the Reflectometer Assembly....94

LIST OF FIGURES

Figure 3-8. Instrument Assembly Integrated into OPM 95
Figure 3-9. Pre- and Post-flight Data for Precontaminated Z93 95
Figure 3-10. VUV Spectrometer Optical Schematic. 97
Figure 3-11. Assembled VUV Instrument. 98
Figure 3-12. VUV Spectrometer Subsystem 101
Figure 3-13. Schematic of a TIS Instrument. 106
Figure 3-14. Relationship between TIS and Wavelength. 108
Figure 3-15. Calibration (left) and Test Sample (right) Layout. 108
Figure 3-16. TIS Flight Assembly. 111
Figure 3-17. TIS Subsystem 112
Figure 3-18. Examples of TIS Data. 115
Figure 3-19. TIS Flight and Post-Flight Data for AlMgF Mirror 116
Figure 3-20. Comparison of TQCM and Attitude Data 119
Figure 3-21. AO Sensor Assembly. 121
Figure 3-22. AO Monitor Assembly 122
Figure 3-23. AO Sensor Plate Assembly. 124
Figure 3-24. Solar Radiometer. 127
Figure 3-25. Earth IR Radiometer. 127

LIST OF TABLES

Table 1-1 OPM Sine Sweep Loads. 7
Table 1-2 SPACEHAB Random Vibration Requirements for OPM. 9
Table 1-3 EMI/EMC Testing 12
Table 1-4 OPM Data Collection/Telemetry History. 25
Table 2-1. Normal and Extended Measurement Timeline Durations 56
Table 2-2. Crew Manual Control Program Menus 69
Table 2-3. Telemetry Data Types, Sizes, and Rates 74
Table 2-4. Mass Memory Usage 74
Table 2-5. OPM Memory Upset Frequency 75
Table 2-6. AO data listed in the OPM Telemetry Data Files 77
Table 2-7. REDUCETV.EXE generated files 78
Table 2-8. Voltage Samples in OPM 79
Table 2-9. Event Id and Description 79
Table 2-10. Thermistor Placement in OPM 81
Table 4-1. OPM TPS Log 132

ACRONYMS & ABBREVIATIONS

A2D	Analog-to-Digital
ADDR	Address
AO	Announcement of Opportunity, Atomic Oxygen
ASCII	American Standard Code for Information Interchange
BFO	Beat Frequency Oscillator
BOL	Beginning-of-Life
C	Celsius
CD	Compact Disk
CDA	Carousel Drive Assembly
CDT	Central Daylight Time
Co-Proc	Co-Processor
COTS	Commercial-Off-the-Shelf
CP	Control Program
CPSHORT	Control Program Short
CPU	Central Processing Unit
CSV	Control Separated Value
CW	Continuous Wave
CR	Carriage Return
D2A	Digital-to-Analog
DACS	Data Acquisition and Control System
DB	Decibel
DC	Direct Current
DEU	Double Event Upset
DMT	Decreed Moscow Time
DPA	Destructive Physical Analysis
DRAM	Dynamic Random Access Memory
EEE	Electrical, Electronic, and Electromechanical
EEPROM	Electrically Erasable Programmable Read Only Memory
EDAC	Error Detection and Correction
EMC/EMI	Electromagnetic Compatibility/Electromagnetic Interference
EOL	End-of-Life
ESH	Equivalent Sun Hours
ESU	Electrical Simulation Unit
EURECA	European Retrievable Carrier
EVA	Extravehicular Activity
F	Fahrenheit

ACRONYMS & ABBREVIATIONS

FEM	Finite Element Model
FEU	Functionally Equivalent Unit
FOV	Field-of-View
gm	Grams
g_{rms}	Gravity
GSE	Ground Support Equipment
GUI	Graphical-User Interface
hr	Hour
Hz	Hertz
I	Current
IC	Integrated Circuit
ICE	In-Circuit Emulator
I/F	Interface
I/O	Input/Output
Init	Initialize
In-lb	Inch-Pound
IN-STEP	In Space Technologies Experiment Program
ISR	Interrupt Service Routine
ISS	International Space Station
ISTAR	Integrating Sphere Transmitometer and Reflectometer
IVA	Intravehicular Activity
JSC	Johnson Space Center
K	Thermal Conductivity
KHz	Kilohertz
KSC	Kennedy Space Center
kW	Kilowatt
kWh	Kilowatt-hour
LASER	Light Amplification by Stimulated Emission of Radiation
LDEF	Long Duration Exposure Facility
LEO	Low Earth Orbit
LF	Line Feed
LISN	Line Impedence Simulation Network
LPSR	Laboratory Portable SpectroReflectometer
M&P	Material and Processes
mA	Milliamp
MAPTIS	Materials and Processes Technical Information System

ACRONYMS & ABBREVIATIONS

Mbyte	Megabyte
MCS	Motion Control System
MD	Mission Day
MEEP	Mir Environmental and Effects Payload
MET	Mission Elapsed Time
MHz	Megahertz
MIL	Military
min	Minute
MIPS	Mir Interface to Payload System
MIUL	Materials Identification and Usage List
MLI	Multilayer Insulation
mm	Millimeters
MM	Mass Memory
MSFC	Marshall Space Flight Center
MUA	Material Usage Agreement
MUX	Multiplexer
mW	Milliwatt
N/A	Not Applicable
NAR	Non-Advocate Review
NASA	National Aeronautics and Space Administration
NHB	NASA Handbook
nm	Nanometers
NSPAR	Non-Standard Parts Approval Request
OAST	Office of Aeronautics and Space Technology
OPM	Optical Properties Monitor
OWS	Optical Witness Samples
PAC	Power Amplifier Center
PbS	Lead Sulfide
PCA	Printed Circuit Assembly
PCB	Printed Circuit Board
PFA	Perfluoralkoxy
PGA	Programmable Gain Amplifier
PI	Principal Investigator
PIND	Particle Impact Noise Detection
PRT	Platinum Resistance Thermistor
PSC	Power Supply Center
PSD	Power Spectral Density
R	Resistance
RAM	Random Access Memory

ACRONYMS & ABBREVIATIONS

RAU	Remote Acquisition Unit
RE	Reaction Efficiency
REFL	Reflectometer
RME	Risk Mitigation Experiment
RSC E	Russian Space Company - Energia
RTS	Request to Send
S/C	Spacecraft
SEU	Single Event Upset
Si	Silicon
SINDA	Systems Improved Numerical Differencing Analyzer
SMT	Surface Mount Technology
SMART	Safety and Mission Assurance Review Team
SPPF	SpaceHab Payload Processing Facility
SRAM	Static Random Access Memory
SSPC	Solid-State Power Controller
SSR	Solid-State Relay
STD	Standard
STS	Space Transportation System
S/W	Software
SwRI	Southwest Research Institute
TE	Thermo-Electric
TED	Thermo-Electric Device
TFLC	Tuning Fork Light Chopper
TIS	Total Integrated Scatter
TPFE	Tetrapolyfluorolethylene
TPS	Test Preparation Sheet
TRASYS	Thermal Radiation Analysis System
TQCM	Temperature-Controlled Quartz Crystal Microbalance
UART	Universal Asynchronous Receiver/Transmitter
U.S.	United States
UV	Ultraviolet
UV EPROM	Ultraviolet Erasable Programmable Read Only Memory
V	Volts
VCMO	Volatile Condensible Materials - Optics
VDA	Vapor Deposited Aluminum
VDC	Volts Direct Current
VUV	Vacuum Ultraviolet
xceiver	Transceiver

ACRONYMS & ABBREVIATIONS

xfer	Transfer
xmission	Transmission

1.0 OPM EXPERIMENT OVERVIEW

This Systems Report is an engineering document that contains information describing how the Optical Properties Monitor (OPM) experiment was developed. Section 1 defines the pertinent OPM design parameters, environmental testing performed, mission information, and system requirements. Section 2 details the systems description (that is, those common core systems) and its performance during the mission. The core systems are defined as those components that are not specifically associated with the OPM instruments, environmental monitors, or flight samples. Section 3 describes the instrument and monitor subsystems and performance during the mission. The instrument and monitor subsystems include the Reflectometer, Vacuum Ultraviolet (VUV), Total Integrated Scatter (TIS), Atomic Oxygen (AO) Monitor, Irradiance Monitor, and Molecular Contamination Monitor. Section 4 contains a brief overview of the OPM post-flight status. Section 5 contains a brief summary of the OPM Phase I Risk Mitigation Experiment (RME) Mission. The *OPM Science Data Report, AZ Technology Report No. 91-1-118-169*, has been written to address the OPM flight samples and data.

1.1 Background

In 1986, the National Aeronautics and Space Administration (NASA) Office of Aeronautics and Space Technology (OAST) released an Announcement of Opportunity (AO) under the In-Space Technologies Experiment Program (IN-STEP). The objective of the IN-STEP program was to demonstrate new space technology on space experiments. In response to this AO, the OPM experiment was proposed as an in-space materials laboratory to measure in-situ the effects of the space environment on thermal control materials, optical materials, and other materials of interest to the aerospace community. The OPM was selected for a Phase A study to determine technical feasibility of the experiment, technical approach, and the estimated cost. The Marshall Space Flight Center (MSFC) in Huntsville, Alabama was selected by the NASA/OAST to manage the project. A second AO was issued by NASA/OAST for the development phase of the IN-STEP experiments. OPM was selected under this solicitation for development and flight. A Phase B (Preliminary Design) was funded to develop the OPM design and cost parameters, and consider available payload carriers suitable for an OPM mission. In late 1992 a peer review, called the Non-Advocate Review (NAR), was held to verify the need and design of the experiment prior to further funding. The OPM was subsequently approved for further development, and the final Phase C/D (Final Design through Mission Support/Data Analyses) funded in April 1993. Between April 1993 and September 1996, the OPM was designed, fabricated, integrated, tested, and delivered to MSFC.

The OPM was launched on the Space Shuttle STS-81 on January 12, 1997, mounted in a SpaceHab Double Rack. The OPM was transferred into the Mir Space Station on January 16, 1997 by Intravehicular Activity (IVA) and stowed inside the Mir for three and one-half months. The OPM was deployed on the Mir Docking Module (DM) and powered up by the first joint Russian-American Extravehicular Activity (EVA) on April 29, 1997. On June 25, 1997, the OPM lost power because of the Progress collision into Mir's Spektr module and did not regain

operational status until September 12, 1997. The OPM continued operation until January 2, 1998 when the OPM was powered down in preparation of the January 8, 1998 EVA to retrieve the OPM. The OPM was retrieved from the DM by Russian EVA on January 8, 1998. The OPM was stowed inside the Mir and later transferred into the Shuttle (STS-89) which returned to Kennedy Space Center (KSC) on January 31, 1998.

1.2 Requirements

The basic premise for the OPM experiment was established by contract early in the program to be commensurate with a low-cost approach to flying Principal Investigator (PI) proto-flight hardware. However, certain documentation requirements were levied to assure an appropriate level of success (i.e., reliability) was achieved. Cost and schedule were very important factors in management of the program. Within this management structure, NASA/MSFC delegated to AZ Technology certain management functions with the caveat that overall cost and schedule could not be impacted without NASA oversight and approval. Spares were kept to a minimum as a means of cost containment, but were purchased when determined necessary for program requirements, dictated to hedge against potential schedule impact by loss of the component, or when quantity discounts took precedence over small orders.

The OPM is an in-space optical laboratory to study the behavior of materials in the space environment. There were three independent optical instruments, three environmental monitors, and common systems of power, data, thermal control, housing (structure), and sample positioning. Because of the optical nature of the experiment, contamination control and prevention requirements were implemented to maintain cleanliness levels and prevent "self-contamination" during the mission. This required materials to be used that were inherently low outgassing. Available data from the NASA/MSFC Materials and Processes Technical Information System (MAPTIS) database were reviewed for materials selection, plus new materials were tested for Volatile Condensable Materials - Optics (VCMO). VCMO, per MSFC-SPEC-1443, became the criteria for materials selection for the OPM experiment.

Other requirements were "tailored" toward a PI-type program. Costs were considered as a factor to balance requirement versus result. If a requirement could not be justified to impose on the contract, or if the requirement could be reduced to effect the same end result or intent, then this cost savings measure was adapted by the program with MSFC concurrence. Specific areas considered under this criteria included quality, testing, parts control, verification, and safety. These areas are briefly discussed in the following paragraphs.

The deliverance of a "Quality" product was paramount. Given the OPM was to fly in space, safety and quality assurance were "built-in" where appropriate by mandating that NASA Handbook (NHB) 5300.4(1C) was required for safety critical structures, but only used as a guideline for non-safety critical hardware. This measure reduced cost where possible but kept rigid requirements for Class I hardware (i.e. hardware that would impact crew safety, shuttle schedule, instrument performance, etc). However, AZ Technology was given authority to control

Class II hardware and was given authority for its own Configuration Control Board to determine disposition of non-critical hardware.

The OPM was designated as a Class D payload with Class C environmental testing. This meant primarily that the experiment success was classified as "PI risk." However, mission success was to be enhanced by conducting environmental tests on the proto-flight hardware. These tests included vibration, thermal vacuum, Electromagnetic Compatibility/Electromagnetic Interference (EMC/EMI), and toxicity. The test levels imposed were commensurate with the launch, mission, and/or landing requirements. The purpose of these tests was to simulate the actual mission environments on the OPM hardware, conduct operational tests while in these environments, and determine the hardware's success of operating while subjected to or from these environments. For proto-flight hardware, the acceptance and qualification test levels were combined into a single test with levels expected during the mission lifecycle. The main purpose of the tests was to verify performance, safety and interfaces.

A Parts Control Plan was implemented to use the most reliable parts available for both the electrical and mechanical disciplines. For the selection of standard Electrical, Electronic, and Electromechanical (EEE) parts, MIL-STD-975 was required. Cavity devices were required to be further up screened to a Class 2+ status by conducting Particle Impact Noise Detection (PIND), X-Ray, and Destructive Physical Analysis (DPA). Parts approved after upscreening were marked for positive identification. DPA was performed only on expensive parts when electrically rejected parts could not be procured from the vendor for DPA as long as the part was from the same lot and date code of those purchased for the OPM. Standard parts were listed in an EEE Parts List and non-standard parts were listed on a Non-Standard Parts Approval Requests (NSPAR). Both lists were submitted and approved by NASA/MSFC for use in the OPM.

For the selection of mechanical parts, the primary concerns were structural integrity, stress corrosion cracking, and fatigue as well as the potential contamination of the optical components of the OPM. Parts processing (i.e. alodine, anodize, passivation, or thermal control coatings) was performed based on usage, material compatibility, thermal environment, and/or environmental exposure. All mechanical parts were approved by NASA/MSFC by submitting Materials Identification and Usage Lists (MIUL) and Material Usage Agreements (MUA) forms. MUAs were submitted for materials not meeting the explicit program requirements per MSFC-HDBK-527.

The OPM verifications were taken from contractual, Extravehicular Activity (EVA), Russian Space Company - Energia (RSC E) (Mir), and SpaceHab (carrier) requirements. All verification requirements were cross-referenced to determine common verifications and identify the most stringent requirement. This enabled one verification to be performed for all agencies' requirements.

The OPM experiment was approved for safety by both the Johnson Space Center (JSC) Safety Panel for Shuttle and the JSC Mir Safety and Mission Assurance Review Team

(SMART). Multiple reviews by each panel were held to determine crew and carrier safety issues, resolve those issues to the satisfaction of each panel, and obtain approval for flight. Some design changes were implemented to obtain panel approval, while procedural changes were processed to meet others. All safety issues were successfully addressed prior to flight.

1.3 Design/Integration

The OPM was designed for multiple missions. The OPM can be reflown with a new materials complement or by retrofitting new instruments suitable to investigate phenomenon for a particular mission. For a mission requiring the potential of new instruments, this suggests that any instrument or monitor should be capable of being removed from the OPM and another inserted in its place. Each instrument has its own independent row of samples that the sample carousel rotated under its measurement aperture. Therefore, the instruments were designed to be modular - that is, capable of being removed as an entity. However, there are some aspects that reduce the modularity without imposing other internal changes; those being power and data, limited volume and area constraints, and thermal loads. Any new instrument would have to be within similar constraints of the instrument it replaces because of existing power and data requirements. Finally, the OPM has one main cable harness that connects the instruments, monitors, and system components together. Each component had its own internal cable system to permit it to be removed from the OPM.

To enhance modularity, the OPM was designed to enable the accessibility of the instruments and major system components. Should an instrument or system component require repair, rework, or replacement, it should be accessible to minimize "down-time." The OPM had removable side panels that bolted to the main structure and a removable top cover that permitted access to the optical instruments. Further, the structure had one removable member that enabled one instrument to be removed easily. In addition, the power supply is bolted to the frame for ease of access.

The modularity and accessibility issues promoted the integration of the components. Being modular, the instruments and monitors were checked out prior to integration into the OPM. If the instrument or monitor did not work once integrated in the OPM, then the resolution of the problem most likely lie in the OPM systems.

The OPM was originally to be launched on the reflight of the European Retrievable Carrier (EURECA) on a Shuttle ferry flight. The EURECA was to be deployed for a six to nine month mission and retrieved on a subsequent Shuttle mission. However, the EURECA was not reflown. Therefore, the OPM was manifested for launch as an unpowered payload in the SpaceHab Module for EVA deployment on the Mir Space Station for an approximate nine-month mission. Selected as part of the International Space Station (ISS) Phase I program of RMEs, the OPM was to be a part of the learning process of how to work with international partners in addition to obtaining science data for the ISS.

However, design changes were required to accommodate this mission change. Several of the more challenging changes are listed here followed by descriptions of the issues. First, the OPM was too large to fit through the Mir hatches. Second, the OPM was to be launched in the habitable crew environment requiring a proven containment design for frangible materials. Third, now that the OPM would be EVA deployed, the OPM had to be "EVA-friendly"; conform to EVA requirements (i.e. handrails, no sharp edges, tethers, etc.), and consider the crew interface issues for power, data, and mounting to Mir. The thermal control changed from being grouped with multiple payloads under a common Multilayer Insulation (MLI) blanket (EURECA) to being isolated on the Mir.

The original OPM design concept was based on a similar shape and volume to the Long Duration Exposure Facility (LDEF) experiments. This generous volume enabled sufficient room for instrument placement and potential growth. OPM was first downsized to fit the EURECA area constraints. Instrument and subsystem component placements were revised to accommodate this design change. For the Mir mission, the OPM was again downsized to fit the Mir hatch constraints. The design revisions required changing instrument and subsystem placement to integrate the total complement of science into the volume constraints. The final design reflects chamfered sides and top, minimal clearances between instruments, reduced samples on the carousel, a sample cover to protect the sample exposure area, and EVA-friendly features (i.e. tethers, soft dock mechanisms, labels, and handrails).

The design changes for Mir included interfacing to a Russian "solar array latch" for mounting to the Mir Docking Module, development of EVA and Intravehicular Activity (IVA) compatible power and data cables, and crew procedures defining how to assemble the OPM hardware 'on-orbit' plus data collection/troubleshooting by the IVA crew.

The OPM integration effort became more involved with the launch in the SpaceHab Module and deployment on the Russian Mir Space Station. A new interface to the SpaceHab Module was required to mount the OPM in a Double Rack for launch and landing. Crew training was required to demonstrate how the OPM would be removed and installed in the rack. The Mir integration effort required obtaining a "solar array latch" (called the OPM/Mir Interface Adapter) from Russia to ensure the mechanical interface to the latch, substantial coordination between the United States (U.S.) and Russian engineers for developing the EVA and IVA power and data cables, and crew training for the EVA deployment and retrieval.

1.4 Environmental Testing

Environmental tests were performed at the "System" level for the OPM experiment to demonstrate the capability of the hardware to survive expected mission environments. Vibration, thermal vacuum (including contamination), EMI/EMC, and toxicity tests were required to certify the OPM as "flight-qualified." The main objective of testing was to verify safety and interfaces. The specific test levels and general details are synopsized in the following sections. Detailed test procedures and reports are listed in Attachment 1 and are available upon request.

To determine if the OPM successfully passed a particular environmental test, a short functional test was performed prior to and preceding each test. During this functional test, each instrument, environmental monitor, and housekeeping sensor was exercised in a short mission simulation to verify proper operation. If an anomaly was detected, the problem was corrected and the system retested.

Some instrument and monitor subsystems were environmentally tested prior to integration in the OPM to verify performance and suitability to the environment of space. These tests added confidence to the expectation of a successful operation while on mission to Mir. Test specifics are included in the respective sections of this report.

1.4.1 Vibration Testing

The vibration tests were conducted at the expected load levels for the OPM mounted in the SpaceHab Double Rack. The tested loads included the sine sweep and vibro-acoustic environment associated with launch. McDonnell Douglas Aerospace (now part of Boeing Aerospace Company) developed the approximate loads for the OPM from a Finite Element Model (FEM) given to them for this purpose. A sine sweep of 0.25gm from 5 to 2,000Hz was performed in each axis to determine the fundamental frequency. A random vibration was performed to simulate the vibro-acoustic loads for launch. The OPM could not be tested in an actual Double Rack because the fixture would be too large to mount to available vibration tables. AZ Technology designed a fixture, that when coupled with the OPM, closely modeled the expected loads for a Double Rack mounted OPM payload. Figure 1-1 is the OPM on the vibration test stand. Note that the OPM is "bagged" to minimize its contamination from the test environment. The OPM passed all vibration tests and sustained no damage.

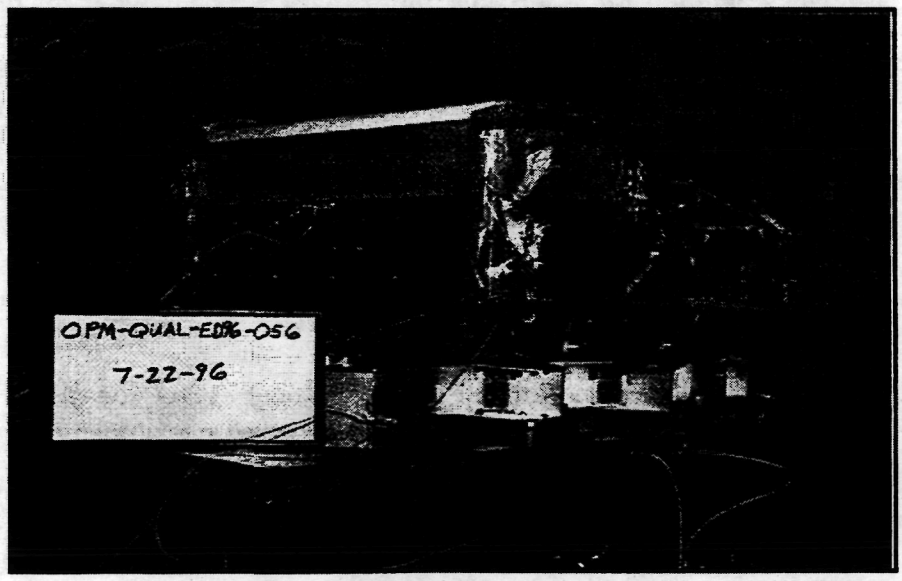


Figure 1-1. OPM on the Vibration Test Stand.

The sine sweep loads applied to the OPM are given in Table 1-1.

Table 1-1 OPM Sine Sweep Loads.

Axis	Sine Sweep
X	5 - 2,000Hz, 0.25g, at 1 octave/minute
Y	5 - 2,000Hz, 0.25g, at 1 octave/minute
Z	5 - 2,000Hz, 0.25g, at 1 octave/minute

The vibro-acoustic loads applied to the OPM are given in Figures 1-2 through 1-4 and Table 1-2.

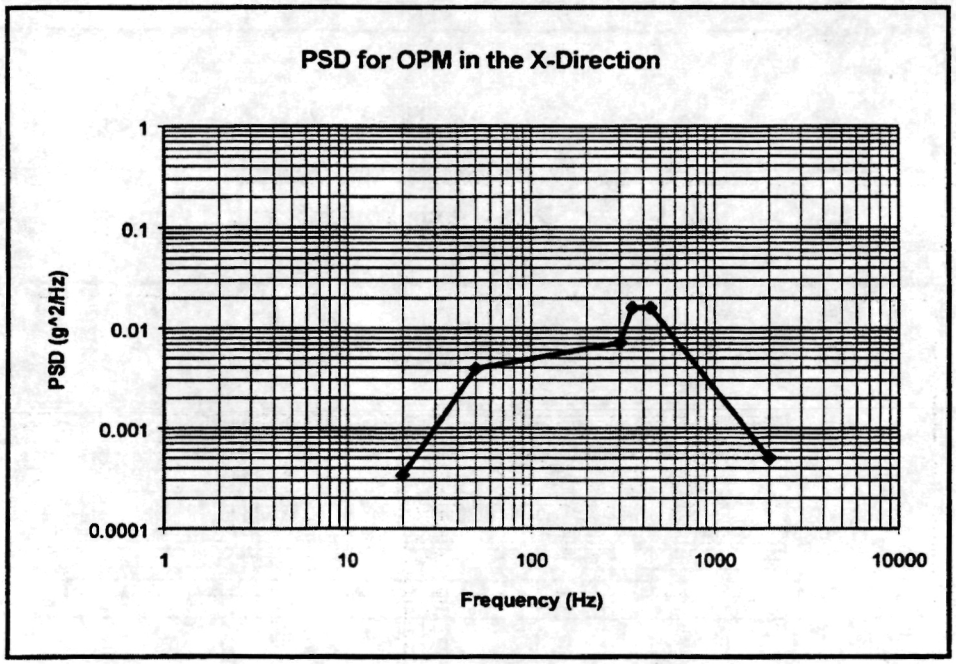


Figure 1-2. X_{OPM} - Axis Power Spectral Density.

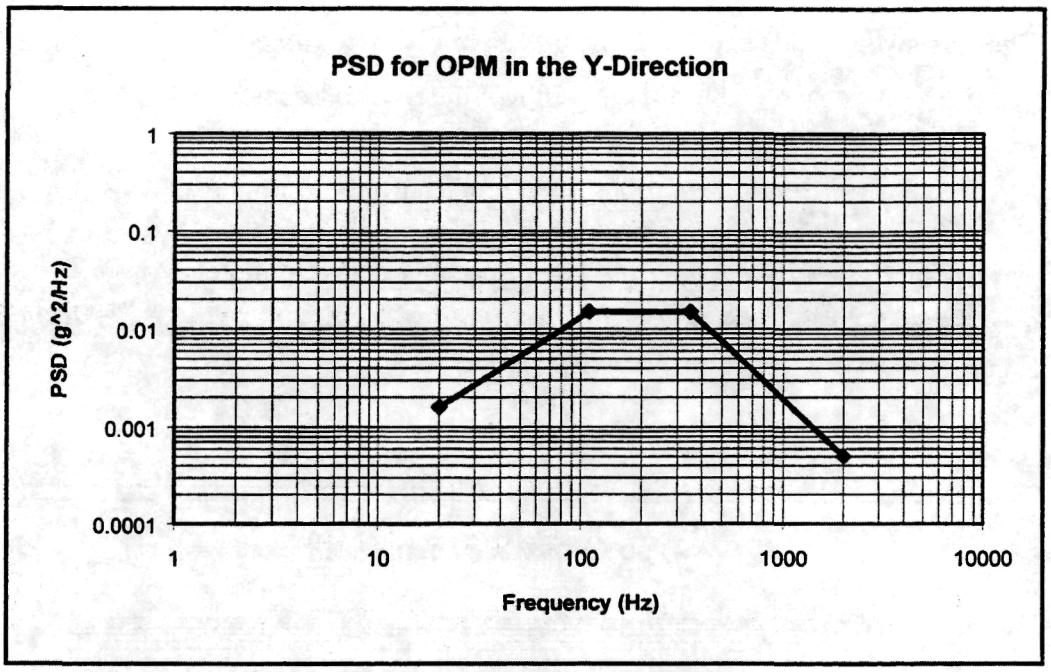


Figure 1-3. Y_{OPM} - Axis Power Spectral Density.

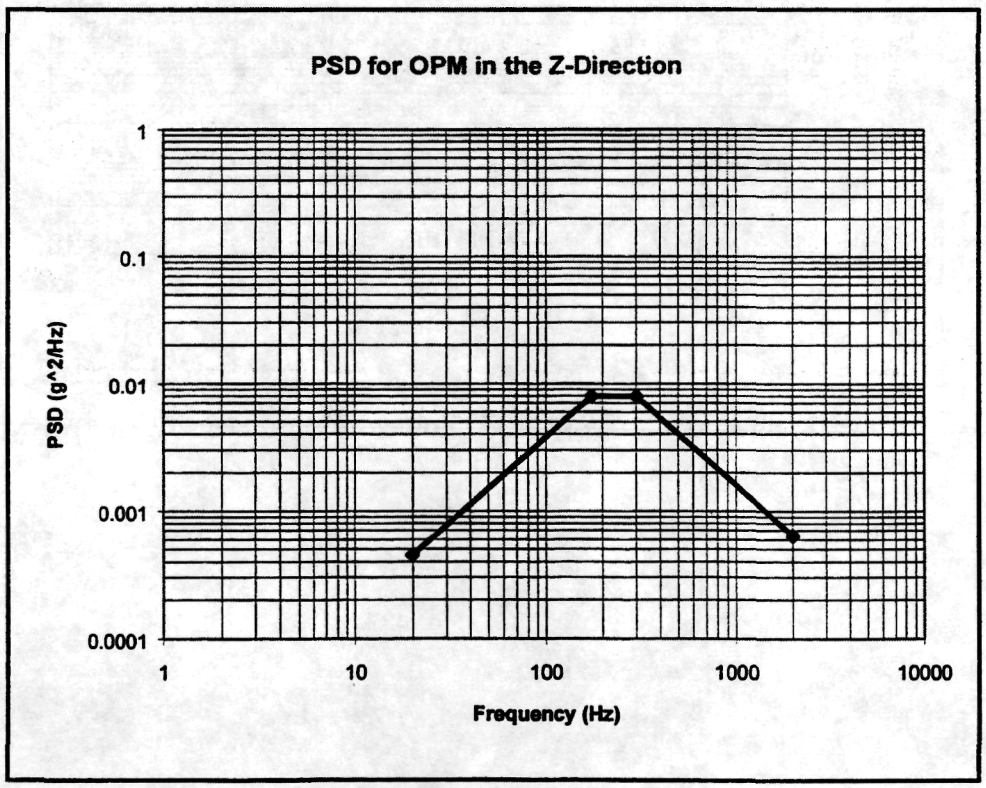


Figure 1-4. Z_{OPM} - Axis Power Spectral Density.

Table 1-2 SPACEHAB Random Vibration Requirements for OPM.

Parameter Zone	Axis	Frequency (Hz)	Level
OPM Mounted in Double Rack, Center Post Removed (defined at the rack post to OPM interface)	X_{OPM}-Axis (Y_{ORB}-Axis)	20 - 50 50 - 300 300 - 350 350 - 440 440 - 2000	+8 dB/octave +1 dB/octave +16 dB/octave 0.016 g^2/Hz -7 dB/octave
		Composite = 2.87 g_{rms}	
	Y_{OPM}-Axis (X_{ORB}-Axis)	20 - 110 110 - 350 350 - 2000	+4 dB/octave 0.015 g^2/Hz -6 dB/octave
		Composite = 2.94 g_{rms}	
	Z_{OPM}-Axis (Z_{ORB}-Axis)	20 - 175 175 - 300 300 - 2000	+4 dB/octave 0.008 g^2/Hz -4 dB/octave
		Composite = 2.24 g_{rms}	

1.4.2 Thermal Vacuum

The OPM was designed for passive thermal control with supplemental active resistance heating to maintain an internal thermal environment between 0 and 40°C. The anticipated and documented Mir attitude orientation was gravity gradient for seventy to eighty percent of the time. To simulate this environment, the OPM was placed in a thermal vacuum chamber. Heat lamps were used to simulate the incident solar energy on the OPM. Based on thermal analyses for the OPM mounted on the Mir Docking Module, minimum and maximum operating temperatures (thermal set points) were predicted for the "mission." These thermal set points corresponded to OPM Base Plate temperatures of -5 and +5°C at the beginning of a measurement cycle. Multiple thermal cycles were conducted while at vacuum with functional tests performed at the minimum and maximum set points. Figure 1-5 illustrates the OPM Thermal Vacuum Test Cycles. Figure 1-6 is the OPM in the thermal vacuum chamber.

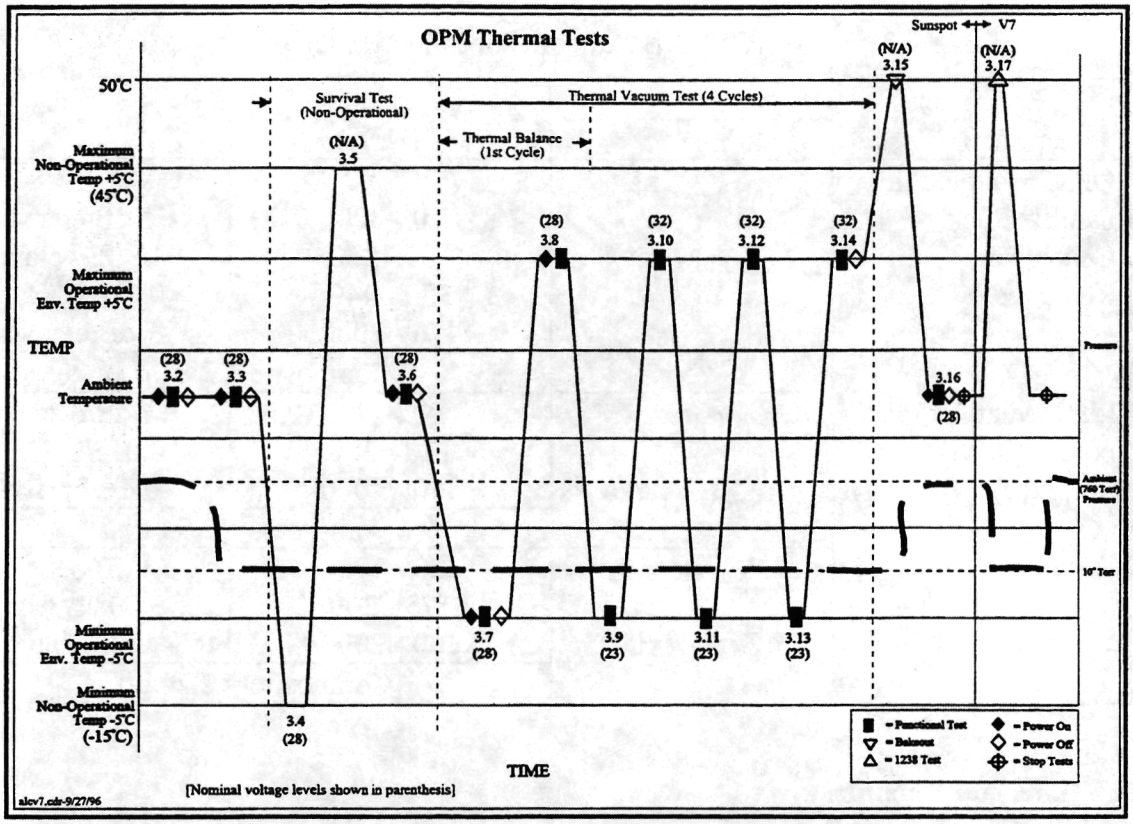


Figure 1-5. OPM Thermal Vacuum Test Cycles.

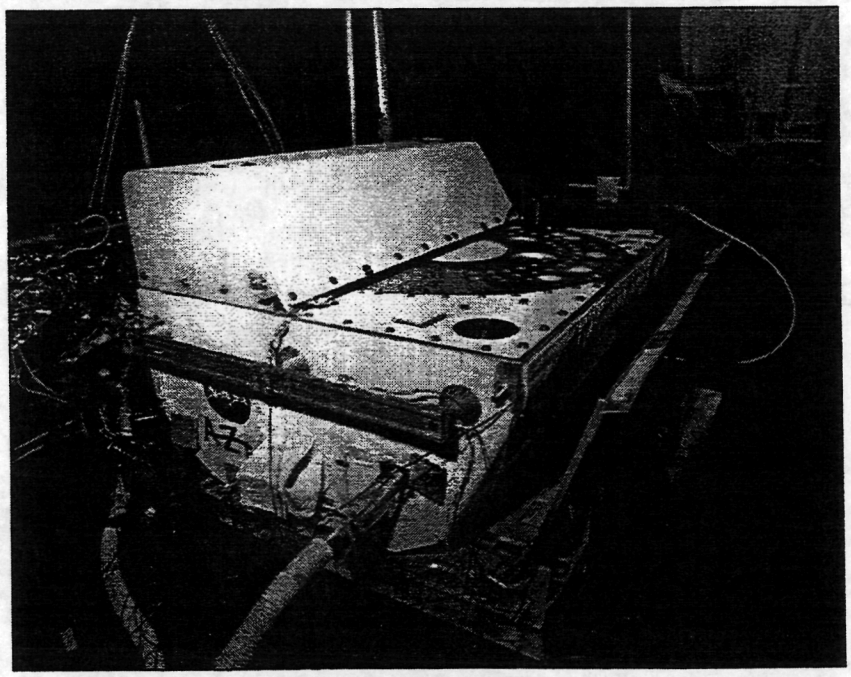


Figure 1-6. OPM in the Thermal Vacuum Chamber.

The thermal vacuum chamber was tested for cleanliness prior to installing the OPM by checking Temperature-Controlled Quartz Crystal Microbalance (TQCM) output over a twelve hour time span and using Optical Witness Samples (OWS) to monitor contamination levels by pre- and post-test analyses. The chamber acceptance required the TQCM to register less than 5 Hz/hr over the monitoring period and the OWS have less than three percent change in reflectance at 121.6 nanometers (nm).

The thermal vacuum test began with a functional test at ambient pressure and temperature to ensure the OPM systems were setup and working properly. The chamber was evacuated to test pressure of at least $1x10^{-5}$ Torr (typically $3x10^{-6}$ Torr) and a second functional test conducted to check experiment operation at vacuum prior to beginning testing. The OPM was subjected to hot and cold survival temperatures, while non-operational, followed by a functional test at ambient temperature. Four thermal cycles were conducted, with the first concurrent with a thermal balance check to calibrate the thermal analyses to the actual hardware performance. At the conclusion of thermal cycling, an OWS was again installed in the chamber and the chamber again evacuated to $1x10^{-5}$ Torr, the chamber temperature set to +50°C, and a thermal bakeout conducted for thirty-six hours to "cleanup" any remaining volatiles. The goal was to have the chamber TQCMs register less than 5 Hz/hr to terminate the test. After thirty-six hours of bakeout the OWS sample temperature was lowered to -10°C and an additional twenty-four hour soak at +50°C bakeout temperature was performed.

The OPM proto-flight hardware successfully passed the thermal vacuum and contamination tests.

1.4.3 EMI/EMC

The EMI/EMC test requirements, see Table 1-3, were based on the Russian Mir environment which had been negotiated between NASA/MSFC and the Russian EMI/EMC engineers. Radiated emission and susceptibility, conducted emission and susceptibility, and a transient test were performed on the OPM experiment while it was in an anechoic chamber. A Russian Line Impedence Simulation Network (LISN) was used to test the OPM per Russian requirements. The OPM was not allowed to conduct noise emissions back onto the Russian power line nor radiate noise back to the Mir Station at levels that exceeded Russian limits. Further, the OPM was tested to ensure that it was not susceptible to Mir noise, either conducted through the power line or radiated from Mir. Transients at power up were required to be within set limits for Russian acceptance.

Table 1-3 EMI/EMC Testing

Test	Requirement
Conducted Emission Tests	CE01, CE03
Radiated Emission Test	RE02
Radiated Susceptibility	RS02
Conducted Susceptibility Tests	CS01, CS02, CS06
DC Power Bus Transients Test	TT01

Initially, OPM passed three out of the eight tests performed. After installing inductive filters, the EMC/EMI tests were completed successfully with the exception of tests CE03 and RE02 where there were minor excellencies. These two tests were subsequently approved for "use as is." Russian EMC experts concurred with approval of these test data. EMI tests demonstrated that OPM would survive the conducted and radiated emissions environments and would not significantly add to the surrounding EMC environments. Pre- and Post-Functional tests successfully demonstrated that OPM did not sustain damage during the tests. OPM successfully demonstrated its ability to function and perform its intended mission in the Mir electromagnetic environments as tested.

1.4.4 Toxicity

All OPM flight hardware was launched in a habitable crew area. Therefore, a toxicity test was required to ensure that no toxic gases could be released from the flight hardware. Further, the Russian toxicological limits had to be met in addition to the United States (U.S.) requirements because the hardware was to be transferred to Mir. The only test acceptable to both the US and Russian agencies was NHB 8060.1C, Test 7 (Determination of Offgassed Products). Figure 1-7 shows the OPM being placed in the Toxicity Chamber for test.

The Toxicity test was a three-day test. The hardware was placed in a sealed chamber and brought to a test temperature of 120°F and maintained for 72 hours. At the end of the test, a sample of the "air" was taken for analyses to determine the concentration levels of specified gaseous constituents. The resulting analyses indicated that the measured levels were within the acceptable toxicological limits of both spacecraft. The OPM hardware passed all these tests.

1.5 Russian Acceptance Testing

A Russian Acceptance Test was performed in September 1996 for the Russian and U.S. engineering representatives. The purpose of the test was to demonstrate that the as-built hardware performed to design requirements, the hardware was complete and ready for flight, the drawings were in compliance with the as-built hardware configuration, and that the mechanical and electrical interfaces were correct and complete. This test was the only time when the Russian engineers were able to review the OPM hardware and certify it for flight. This test

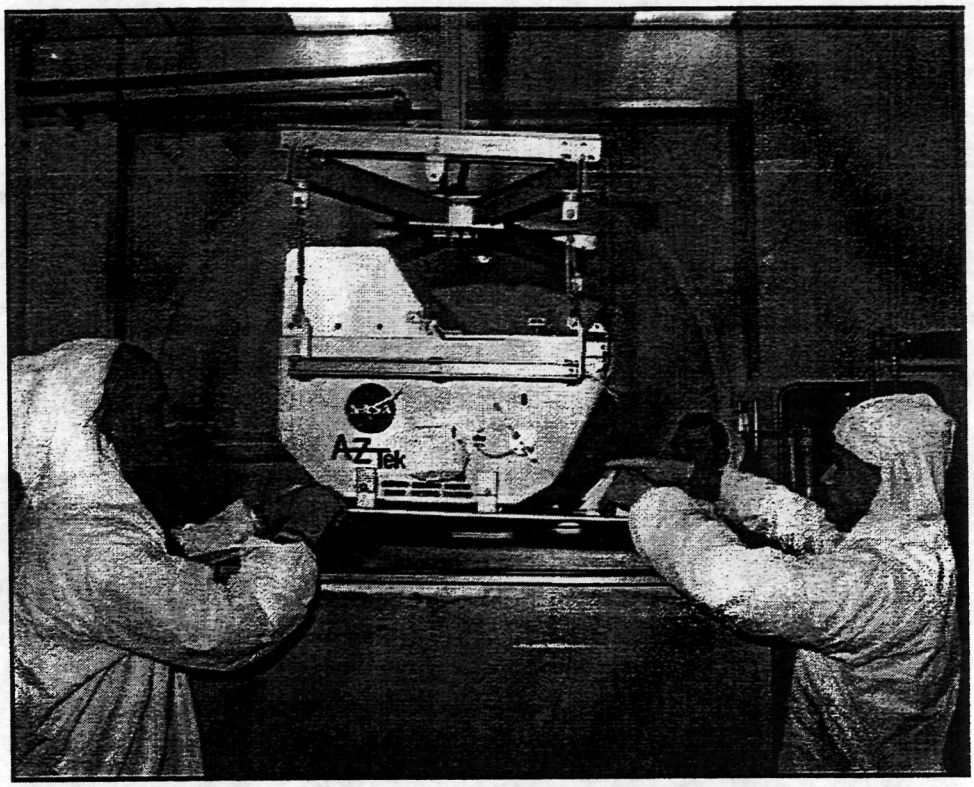


Figure 1-7. OPM Being Placed in the Toxicity Chamber for Test.

included all hardware that was to fly to Mir (see Figure 1-8), including the OPM protoflight unit, the Mir Interface Plate, the OPM/Mir Interface Adapter, the EVA/IVA cables, the flight cable bags, and the OPM flight bag. The OPM Flight bag was comprised of a closed-cell foam covered with Nomex to protect the OPM during launch, IVA transfer, its subsequent stowage on Mir and return to ground. It was removed prior to EVA and later placed back on the OPM after EVA retrieval. The bolted structure, comprised of the OPM/Mir Interface Adapter and the OPM/Mir Interface Plate, was called the OPM/Mir Interface Assembly.

As part of the testing, a short functional test was conducted at ambient temperature and pressure to demonstrate the OPM performed to the design requirements. All three instruments, all three environmental monitors, and all housekeeping functions were checked for proper operation. In addition, the data from the optical measurements, environmental monitors, and power/temperature housekeeping sensors were reviewed and approved.

At the conclusion of the testing, the OPM was approved for flight and certified to be in compliance with all documentation requirements.

1.6 Launch (STS-81)

The OPM experiment hardware was launched on STS-81 on January 12, 1997. The OPM was mounted in a dedicated SpaceHab Double Rack. Also, mounted to this Rack was the

OPM/Mir Interface Assembly. Figure 1-9 illustrates the launch configuration in the SpaceHab Double Rack. AZ Technology designed, built, and integrated the rack structure in the Double Rack that supported the OPM hardware. The OPM EVA/IVA Cables and a backup software program were packed in a crew transfer bag and stowed in the SpaceHab Module. On January 16, 1997, the OPM hardware was IVA transferred into the Mir Space Station and stowed awaiting an EVA scheduled for February 1997. The EVA was postponed until April 29, 1997. The OPM was stowed in Mir for almost three and one-half months awaiting EVA deployment. Just prior to the EVA, the crew removed the OPM Flight Bag, integrated the OPM to the OPM/Mir Interface Assembly, and attached the EVA cable to the OPM.

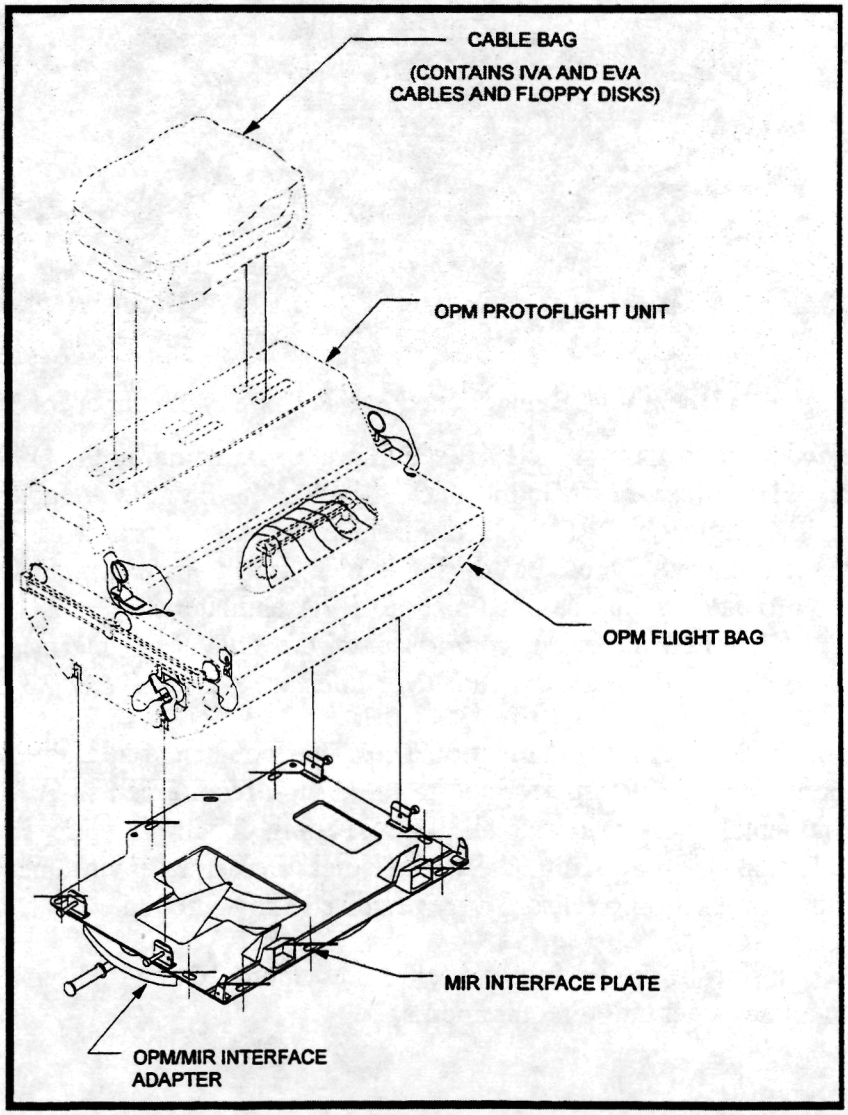


Figure 1-8. Hardware Transferred to Mir

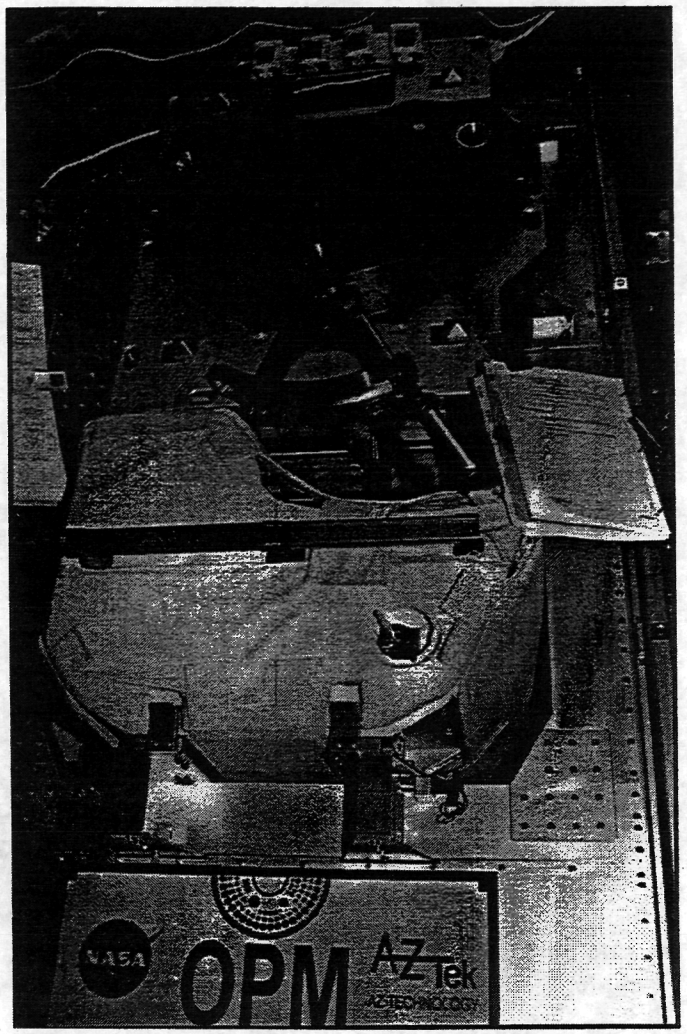


Figure 1-9. OPM Launch Configuration in the SpaceHab Double Rack.

1.7 Mission

The Mir Mission was designed for autonomous operation and minimal Mir crew support. Once the OPM was deployed and powered on, the OPM software "timeline" took control of the experiment and its operations. The software timeline was comprised of one nineteen-hour measurement sequence followed by 149 hours of environmental monitoring and housekeeping status checks. See Section 2.3.4 (Figures 2-11 and 2-12) for additional Timeline information. The OPM conducted in-situ measurements with the three optical instruments to assess the material optical and thermal properties under test. The measurement sequence began with the TIS instrument, followed by the VUV spectrometer, and the reflectometer. Next, a calorimetric measurement process measured the temperature change of each colorimeter sample for post-flight calculation of its thermal emittance. After completing the calorimetric measurements, the flight samples were rotated back out into the environment to begin another week of exposure. The first timeline occurred one hour after power up. If power were ever lost to the OPM, the

OPM internal clock would stop. At power on, the internal clock would resume and count to the next scheduled measurement sequence. Software was available to the IVA crew to initiate a measurement cycle and/or reset the internal clock, if necessary. The crew was to communicate with the OPM Data Acquisition and Control System (DACS) once a week to download stored data and telemeter it to ground.

The OPM timeline was developed based on parameters received from Russian documentation and telecons. However, given a flight environment with unexpected situations that arise quite suddenly, some parameters were different than expected.

For example, the environmental monitor measurement parameters were tuned to an expected Mir attitude and orientation. Therefore, the AO monitor exposure time was minimized for what was anticipated to be a large AO flux and total fluence for a mostly gravity gradient attitude. This was not the case. The flight orientation actually was a solar inertial attitude most of the time. In retrospect, the AO sensors could have been left exposed for all of the mission time.

Another interesting aspect was the thermal loading. Since the actual Mir attitude was mostly solar inertial, the OPM became much hotter than expected during the few days of maximum solar exposure. This happened twice during the mission. The temperatures that resulted exceeded the predicted mission temperatures and the qualification test temperatures by 5 to 25°C. However, the most sensitive components, i.e., stepper motors and LASER components, continued to work after these exposures.

Further, the crew time allocated to the OPM for data collection was approximately one to two hours per week. The OPM DACS data storage was planned to allow for up to three weeks of no data collection before loss of data (due to memory overwrite). There were periods when the OPM data was not collected for up to three weeks because the crew simply did not have time to download OPM data. In retrospect, a way to communicate directly with the OPM from the ground would have been most beneficial.

1.7.1 Events on Mir

The twelve months OPM was on the Mir Space Station happened during a critical period of stability for the crew life support systems. Some of the more interesting events are detailed in the following paragraphs.

1.7.1.1 Docking Module Condensation Pools

The OPM was initially stowed in the Docking Module. It usually had cooler temperatures than other Mir modules, and tended to support condensation "pools" in some areas. When these pools were mentioned during one of the Mir Daily Activity Reports, AZ Technology requested the OPM be moved to another module where condensation was not suspected to be a

problem. There was concern among the OPM Team members of moisture migrating onto the optical components inside the OPM and contaminating them.

1.7.1.2 Mir Fire

On February 23, 1997, a fire started on board the Mir Station while trying to supplement the oxygen for six crewmembers. Lithium perchlorate canisters were being used to release oxygen during the chemical "burn" and the heat of the process melted the outside container. A fire resulted that nearly caused the evacuation of the Mir Station, and took several days for the particulates to settle. This proved to be an unexpected contamination source for the OPM experiment. From the safety perspective, the exposed OPM materials had been flammability tested prior to flight and proven not to be an ignition source.

1.7.1.3 OPM EVA Deployment

The EVA Deployment was delayed several times while the crew worked on station issues. The EVA occurred on April 29, 1997, and it was the first joint Russian - US EVA. The crew performed a nominal EVA, and powered up the OPM. Within one hour of power up, the OPM initiated its first measurement sequence. Figure 1-10 is a photograph of the deployed OPM. OPM is seen near the 2 o'clock position on the Docking Module. The OPM was mounted on the Mir Space Station with customized interface hardware. The Russians supplied a latch that mechanically interfaced to standard interfaces used on the Mir exterior modules. This latch, called the OPM/Mir Interface Adapter, used a three ball magnetic latch as an EVA 'soft dock' feature plus the movement of a handle to 'hard dock' the latch to the Mir interface. The hard dock featured a cam-driven device that locked the latch in place just below the centerline of the ball on the Mir interface. AZ Technology designed an Interface Plate to interface the OPM to this latch. This Plate mounted to the bolt pattern of the latch and provided an interface to the OPM structure. Both the Russian latch and the Interface Plate were designed to permit just one correct mounting orientation by the placement location of the interfaces to the respective hardware.

The OPM hardware and the OPM/Mir Interface Assembly were mated just prior to the EVA. Once mated, the OPM was placed on the starboard side of the Mir Docking Module. This oriented the OPM assembly to face the Mir Core module and to the space environment for determining the effects of the space environment and the Mir induced environment on the flight samples. Figure 1-11 illustrates the OPM mounting orientation on the Mir Space Station.

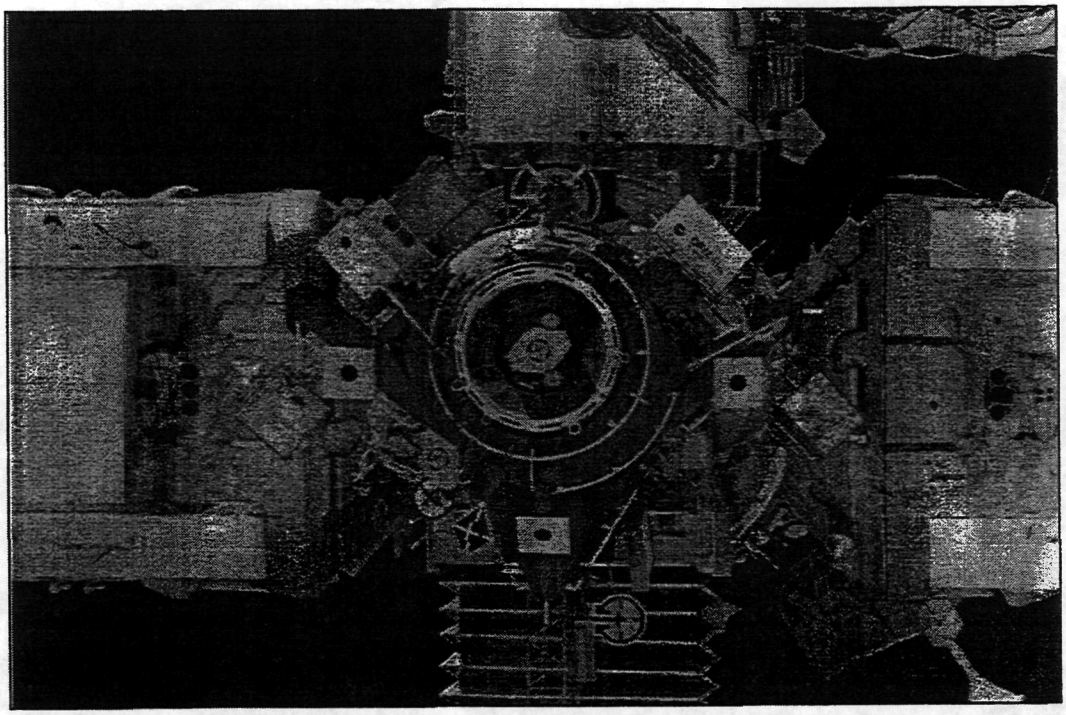


Figure 1-10. OPM on MIR (Docking Module-End View).

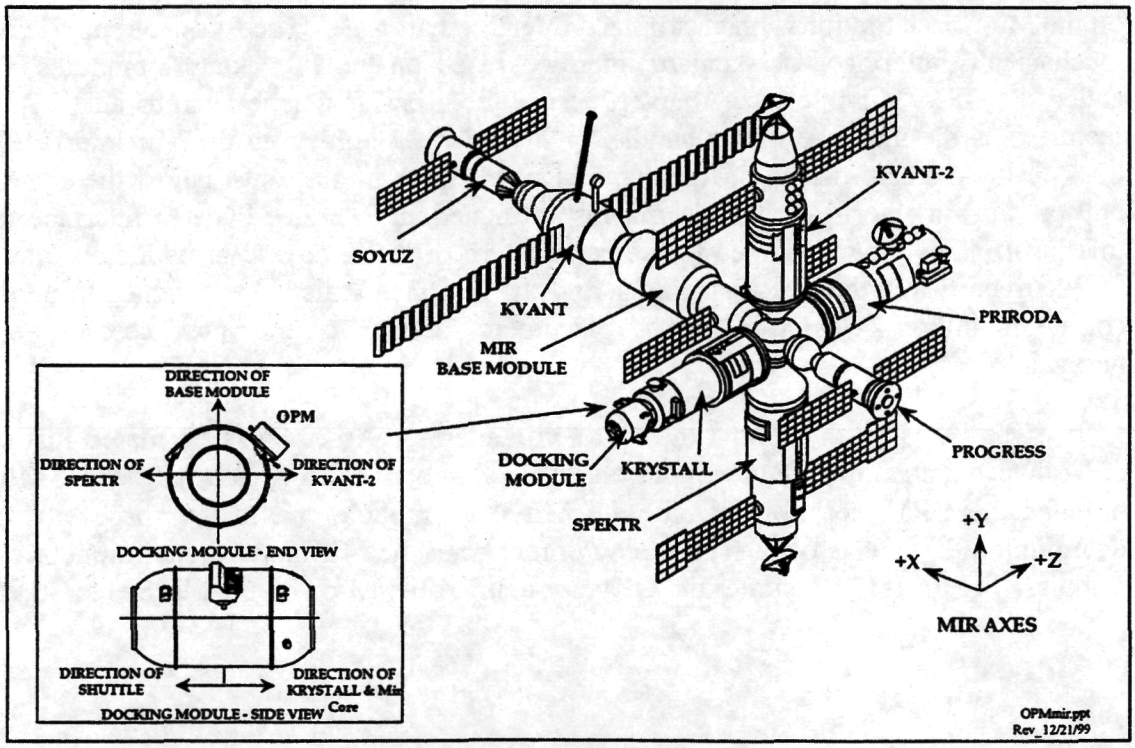


Figure 1-11. OPM Mounting Orientation on the Mir.

1.7.1.4 The Progress Resupply Vehicle Collision into Spektr

The collision occurred on June 25, 1997 on the Mir Station while practicing manual rendezvous procedures. Upon collision, the crew reacted quickly to seal off the leaking Spektr module and to conserve power. At that time there was no battery power on the Krystall Module, and the OPM power was severed in order to conserve battery power. The power remained off until September 12, 1997, when the OPM was officially repowered. Later, it was discovered that the OPM power was not shut down by turning the OPM power breaker to the "Off" position in the Docking but was powered down when all Docking Module (DM) power was shut off. When the Krystall module was repowered, so was the OPM. Therefore, the OPM experiment was powered up whenever the Mir Station entered the sunlight, and went off (unpowered) when it entered the earth's shadow. When this was realized, the OPM was powered down at the power breaker until ready for official power up. Figures 1-12.1 through 1-12.4 show the estimated power on/off status chart beginning with the restart date. The OPM did not have a real-time clock, only an elapsed timer so the exact times cannot be determined. The time is given in Decreed Moscow Time (DMT) - the time used by the Mir crew.

1.7.1.5 Retrieval

The OPM retrieval was dependent upon visual and operational checks. Because the OPM contained frangible material, the crew visually checked for glass particles that might have been emanating from the OPM before the EVA. Second, measurement data was to confirm that during the most recent measurement sequence, the instruments were functioning properly - indicating no frangible material. Third, the crew was to initiate the OPM Deactivation procedure. This procedure checked the optical lamps for operation and returned a message to the crew that the systems were still operational. In the absence of any one of these checks, the OPM could be left outside Mir. Upon reentry into Mir, and after repressurization, the crew was to tape the OPM around the Sample Cover to positively prevent escape of frangible material while inside the habitable area.

Because the VUV lamp never worked on orbit, the procedural checks were somewhat relaxed to bring a more realistic process to the retrieval. In fact, during the STS-86 EVA retrieval of the Mir Environmental and Effects Payload (MEEP) payloads, the EVA crew passed by the OPM and saw nothing suspicious. Therefore, a good visual inspection was conducted by the crew, and the OPM retrieved on January 8, 1998 CDT (January 9,1998, DMT). The two Russian crewmembers brought in the OPM and EVA cables, and taped the Sample Cover shut as planned. The OPM was stowed inside the Mir Kvant2 module until IVA transferred to the Shuttle Space Transportation System (STS-89) in January 1998.

1.7.2 Power On/Off Status Charts

At the conclusion of the EVA deployment in April 1997, the EVA crew powered on the OPM and the OPM began autonomous operation. From that time until June 25, 1997, the OPM

operated continuously. The monitoring data collected from the OPM attest to this fact. However, the collision of the Progress Resupply Module into the Spektr module changed the power "on" status. Figure 1-12 depicts, to the best data available, the status of the OPM power on for the remainder of the Mir mission. There were multiple Motion Control System (MCS) failures plus other times when the OPM had to be shut down to conserve Station power. These data were taken from the accounts listed in the Mir Daily Activity Reports. It is evident that Mir power became more stable as the time from OPM restart increased. The last power down was an unscheduled MCS failure, and based on the OPM elapsed time, the OPM was not re-powered after the MCS until the Deactivation Procedure just prior to the EVA retrieval.

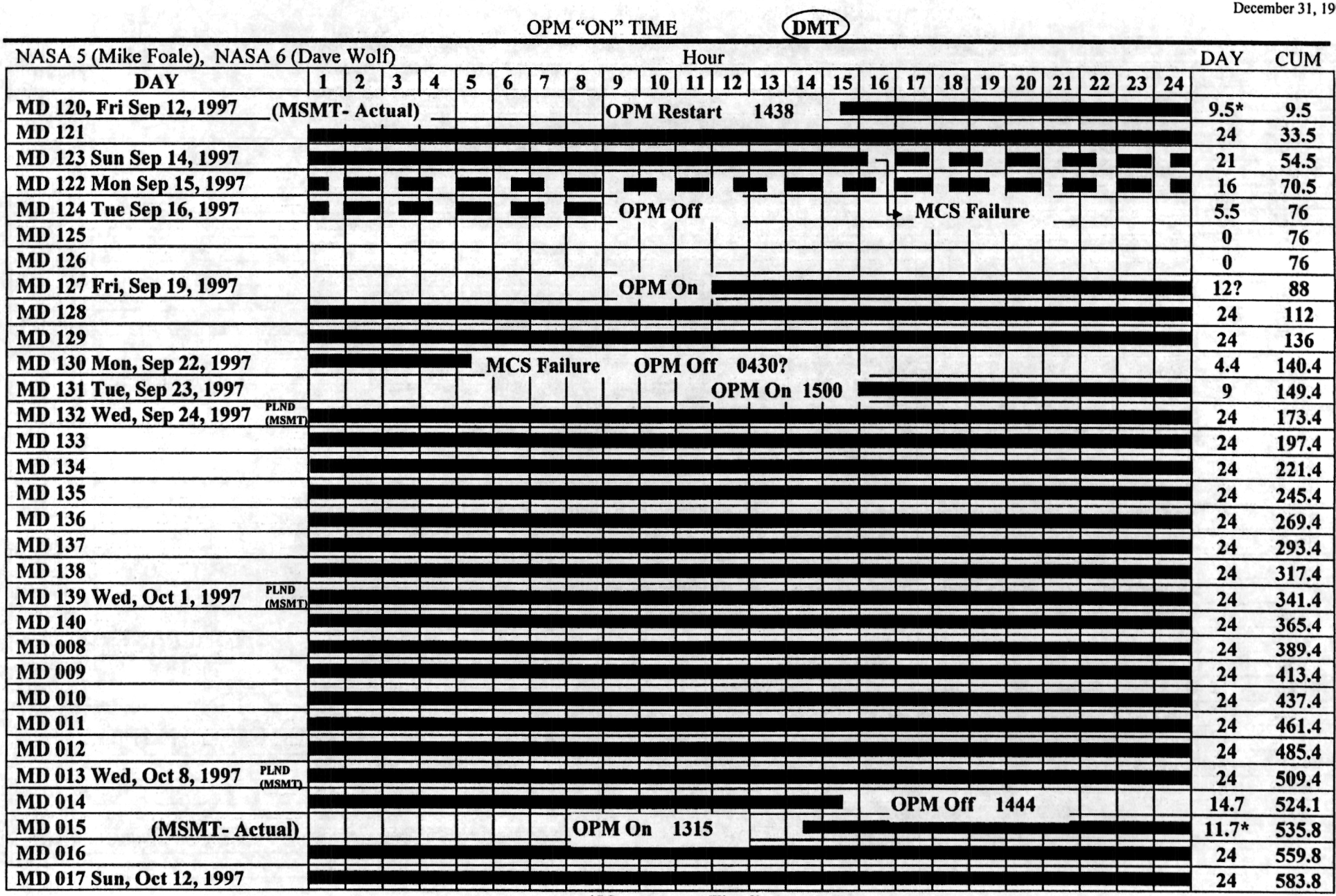
1.7.3 Timeline/Data Status

A chart of the entire mission measurement sequences and data transfers to ground is given in Table 1-4, OPM Data Collection/Telemetry History. This chart contains the scheduled time for each measurement sequence, the actual date for the sequence, the planned date for the data telemetry to ground and the actual date, the number of files that should have been received versus the number actually received, plus a comments or status column. These data help correlate the power on/off status chart to the actual measurement sequences. The two together assist in solving the puzzle of what happened on Mir, and enabled one to track what data were available for download, when the download occurred, and if the data were 'good'. There were multiple times when data received were corrupted by the downlink process, and the data requested for re-transmittal.

The data collection / telemetry history since the EVA on April 29,1997:

1. The Timelines mentioned in Table 1-4 refer to the optical measurement timelines that occurred once per week.
2. Monitoring data was continuously taken during the remainder of the week.
3. MET was Mission Elapsed Time after power up during EVA deployment.

OPM Data collection stopped at EVA Retrieval on January 8, 1998.



*Measurement Timeline

Figure 1-12. OPM "ON" TIME - Measurement Timeline

OPM "ON" TIME (DMT)

NASA 6 (Dave Wolf)

DAY	Hour 1	2	3	4	5	6	7	8	9	10	11	12	13	14	15	16	17	18	19	20	21	22	23	24	DAY	CUM
MD 051 Sat, Nov 15, 1997																									24	1359.4
MD 052																									24	1383.4
MD 053																									24	1407.4
MD 054 Tue, Nov 18, 1997																									24	1431.4
MD 055																									24	1455.4
MD 056																									24	1479.4
MD 057																									24	1503.4
MD 058 Sat, Nov 22, 1997			0200 Power Off - MCS Failure																						2	1505.4
MD 059													1053 Power On												13	1568.4
MD 060																									24	1592.4
MD 061 Tue, Nov 25, 1997																									24	1616.4
MD 062																									24	1640.4
MD 063																									24	1664.4
MD 064																									24	1688.4
MD 065 Sat, Nov 29, 1997																									24	1712.4
MD 066																									24	1736.4
MD 067																									24	1760.4
MD 068 Tue, Dec 2, 1997																									24	1784.4
MD 069																									24	1808.4
MD 070																									24	1832.4
MD 071																									24	1856.4
MD 072 Sat, Dec 6, 1997																									24	1880.4
MD 073																									24	1904.4
MD 074																									24	1928.4
MD 075 Tue, Dec 9, 1997																									24	1952.4
MD 076																									24	1976.4
MD 077																									24	2000.4
MD 078																									24	2024.4
MD 079 Sat, Dec 13, 1997																									24	2048.4
MD 080																									24	2072.4
MD 081																									24	2096.4
MD 082 Tue, Dec 16, 1997																									24	2120.4

Figure 1-12. OPM "ON" TIME - Measurement Timeline (Continued)

OPM "ON" TIME (DMT)

NASA 6 (Dave Wolf)

DAY	Hour 1	2	3	4	5	6	7	8	9	10	11	12	13	14	15	16	17	18	19	20	21	22	23	24	DAY	CUM
MD 083 Wed, Dec 17, 1997																									24	2144.4
MD 084																									24	2168.4
MD 085																									24	2192.4
MD 086 Sat, Dec 20, 1997																									24	2216.4
MD 087																									24	2240.4
MD 088																									24	2264.4
MD 089																									24	2288.4
MD 090 Wed, Dec 24, 1997																									24	2312.4
MD 091																									24	2336.4
MD 092																									24	2360.4
MD 093 Sat, Dec 27, 1997																									24	2384.4
MD 094																									24	2408.4
MD 095																									24	2432.4
MD 096																									24	2456.4
MD 097 Wed, Dec 31, 1997																									24	2480.4
MD 098																									24	2504.4
MD 099					Mir Computer Failure									0345 Hrs											3.6	2508
MD 100 Sat, Jan 3, 1998																										
MD 101																										
MD 102																										
MD 103																										
MD 104 Wed, Jan 7, 1998																										
MD 105 Thur, Jan 8, 1998	OPM EVA Retrieval (stowed inside Mir)																									

Figure 1-12. OPM "ON" TIME - Measurement Timeline (Continued)

Table 1-4 OPM Data Collection/Telemetry History.

Event No:	MET (hrs)	Sched Date	Actual Date	No: Files	# Files Rec'd	Status
1	44	4/29/97	4/29/97			Timeline 1
2		4/30/97	4/30/97	3	3	Data xfer 1, 2nd xmission OK
3	212	5/6/97	5/6/97			Timeline 2, data xfer 2 postponed due to power cable issues.
4	380	5/13/97	5/13/97			Timeline 3
5		5/14/97	5/14/97	25	25	Data xfer 2, 9 files incomplete. Retransmit denied due to upcoming Shuttle docking. Obtain optical disks after STS-84 landing.
6	548	5/20/97	5/20/97			Timeline 4, no data xfer due to shuttle docking.
7	716	5/27/97	5/27/97			Timeline 5
8		5/29/97	5/30/97	26	1	Data xfer 3, 25 files missing. Request to retransmit. Unable to find files on MIPS.
9		6/3/94	6/3/97	7	1 (3 total)	Data xfer 4, 6 files missing. On 6/10 & 6/13, 1 file received, and other 4 found on Mir, but not received.
10	884	6/3/97	6/3/97			Timeline 6
11		6/10/97	6/11/97	1		Data xfer 5 (3&4 repeat). Contingency ops for 1Mb data.
12	1052	6/10/97	6/10/97			Timeline 7
13	1220	6/17/97	6/17/97			Timeline 8
14		6/12/97	6/18/97	1	1	Received Data xfer 5 (1Mb file). Data for 5/14 - 6/11 (but 3 days: 5/31 - 6/2 missing). Small amount of bad data.
15		6/19/97	6/21/97	29	0	Data xfer 6. 29 files Zipped, but unable to unzip. Request retransmit at earliest convenience.
16	1388	6/24/97	6/24/97			Timeline 9
17	~1412		6/25/97			OPM Powered Down at 0500 hrs CDT
18			7/1/97		28	Received Optical Disk data from STS-84 (Data xfers 1 and 2)
19						OPM operates "unofficially" for approx. 85 hours prior to "Restart" on Sep 12.
20	1474	9/12/97	9/12/97			Official OPM Restart at 0638 CDT. Primary memory download to Laptop. Timeline 10.
21	1494		9/13/97			Timeline 11. Crew induced.
22	1524		9/14/97			Timeline 12. Crew induced.
23	1557	9/19/97	9/21 - 24/97			Timeline 13. Timeline slip due to power outages onboard Mir.
24	1726	10/1/97	9/30/97			Timeline 14
25	1894	10/8/97	10/7/97			Timeline 15

Event No:	MET (hrs)	Sched Date	Actual Date	No: Files	# Files Rec'd	Status
26		10/13/97	10/10/97	37		Data download to Laptop. Primary memory.
27	1942		10/10/97			Timeline 16
28			10/17/97	1		Data xfer 7. Rec'd single file of all data. Data for period of 6/24 to 10/8.
29	2110		10/17/97			Timeline 17
30			10/18/97	20	20	Rec'd 20 (000-019) of the 37 segmented files off MIPS-2L from Data xfer 7.
31		10/24/97	10/24/97			Data download to Laptop. Primary memory.
32	2278		10/26/97			Timeline 18
33			10/28/97	35	32	Data xfer 8. Rec'd 32 files (000-034) off MIPS-2L. Files 018 - 020 are missing. Data for 10/10 to 10/24.
34			10/30/97		63	Received Optical Disk data from STS-86 (Data xfers 3 through 6 plus Timeline 9)
35	2446	11/2/97	11/2/97			Timeline 19
36			11/3/97	13	13	Data xfer 9. Rec'd 13 files. 3 partially corrupted. Data for 10/24 to 10/31.
37	2614	11/9/97	11/9/97			Timeline 20
38		11/10/97	11/11/97	13	13	Data xfer 10. Rec'd 13 files. Data for 10/31 to 11/7.
39	2782	11/16/97	11/16/97			Timeline 21
40		11/17/97	12/2/97	11	11	Data xfer 11. Data for 11/7 to 11/14. Missing files: telem001.opm and telem007.opm.
41	2918	11/23/97	11/23/97			Timeline 22
42		11/24/97	12/2/97	13	13	Data xfer 12. Data for 11/14 to 11/21.
43	3086	11/28/97	11/30/97			Timeline 23
44		12/1/97	12/2/97	16	16	Data xfer 13. Data for 11/21 to 11/29.
45	3254	12/5/97	12/7/97			Timeline 24
46		12/8/97	12/7/97	6	2	Data xfer 14. Data for 11/29 to 12/1. Some data corrupt.
47	3422	12/12/97	12/14/97			Timeline 25
48		12/15/97	12/18/97	16	16	Data xfer 15. Data for 12/1 to 12/11
49	3590	12/19/97	12/31/97			Timeline 26
50		12/22/97	12/26/97	19	19	Data xfer 16. Data for 12/11 to 12/21
51	3758	12/26/97	12/28/97	18		Timeline 27
52			1/2/98			OPM powered off due to Mir computer outage.
53			1/8/98			OPM Deactivation Procedure
54			2/26/98		18	Download Timeline 27 data at SPPF
55			3/9/98		180	Rec'd Optical Disk data from STS-89 (Data xfers 7 through 16)

1.7 Return to Ground (STS-89)

The OPM was transferred by IVA to the Shuttle on January 24, 1998. The OPM hardware was mounted in the same SpaceHab Double Rack as launch, secured in place, and returned to ground on January 31, 1998. The transfer and mounting were completed without problem. The OPM/Mir Interface Adapter was left on board the Mir Space Station for future payloads, at the request of the Russians.

In February 1998, the OPM hardware was returned to the SpaceHab Payload Processing Facility (SPPF) at Cape Canaveral, FL for deintegration and post-flight functional tests. Further details are contained in Section 4.0, Post-Flight Status.

2.0 OPM SYSTEMS DESCRIPTION AND MISSION PERFORMANCE

The OPM support Systems were those components remaining in the OPM experiment if the OPM instruments, environmental monitors, and flight samples were to be removed. The systems were comprised of the OPM structure and ancillary hardware, thermal control, power, data, carousel, software, and the internal harness cabling in addition to the OPM EVA and IVA cables. This section will describe these systems and provide mission performance data as appropriate.

2.1 Structure

The structural system consisted of the OPM experiment structure plus the Mir integration hardware. The OPM experiment structure provided the basis for mounting the OPM components, ultimately defined the size and shape of the components, and provided protection to the components during testing, stowage, and crew operations.

The OPM experiment structure was comprised of six main elements: four side panels, an emissitivy plate, and one baseplate. The emissivity plate was so named because it was used as an isothermal element to calculate the emittance of the calorimeters. All other components mounted directly or indirectly to these six elements. Each side panel and the emissivity plate were machined aluminum and alodine processed for electrical bonding. The baseplate was a combination of machined and extruded aluminum that had been riveted together. The side panels and baseplate were riveted together to form the overall structure. The emissivity plate was bolted to this overall structure and became the top structural element. There were no welded components in the main structure. These elements were not fabricated as safety critical hardware because the SpaceHab Module provided containment of the OPM.

A top cover was fabricated to protect the optical instruments and provide some of the passive thermal control radiator surface area. This top cover was geometrically constrained to maximize the Field-of-View (FOV) of the flight samples to the space environment. Figure 2-1 illustrates the final OPM design configuration.

2.1.1 Mission Performance

The mission data collected for the structure was comprised of a visible post-flight evaluation of the condition of the hardware. While the OPM structure appeared to be mechanically intact; there were numerous minor bumps and scratches. These indicate some rough handling either during the preparation for or during the EVA deployment or retrieval activities, or possibly during stowage on Mir. There were no meteoroid or micrometeoroid impacts visible to the naked eye on the OPM. Judging by the condition of the OPM structure and working status of the instruments, it would appear that the structure adequately protected the OPM internal instruments.

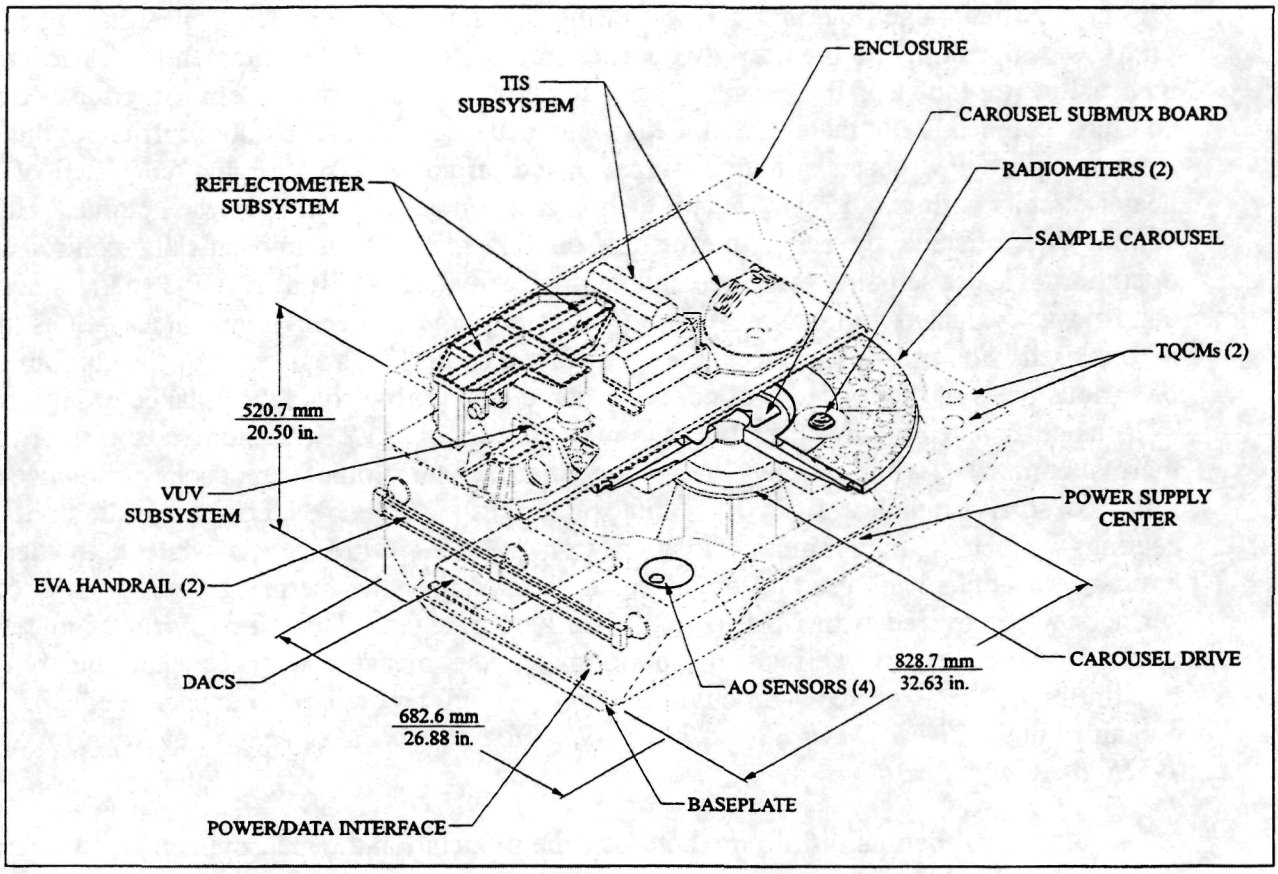


Figure 2-1. OPM Design Configuration.

2.2 Thermal Control

The OPM experiment was modeled using Systems Improved Numerical Differencing Analyzer (SINDA) and Thermal Radiation Analysis System (TRASYS) to calculate the conduction and radiation heat transfer between the internal OPM components as well as its external environment. To assist in the accuracy of the model predictions, the OPM was added to the integrated Mir/Docking Module thermal models obtained from NASA/JSC. The results of the predicted thermal values dictated how the OPM thermal design was achieved for hot, cold, and nominal operating conditions. Further, the OPM timeline was analyzed to minimize peak input power requirements (kilowatts [kW], not kilowatt-hour [kWh]) and assess the internal temperature fluctuations to the OPM. These predicted thermal extremes were not to exceed the component minimum and maximum operating temperatures. Indeed, the OPM timeline was changed to modify the proposed measurement sequence which decreased the component temperature extremes and peak power (kW). However, the measurement sequence duration increased, increasing the total kWh.

Based on model predictions and the modified weekly timeline, the OPM was designed for passive thermal control with active heaters to maintain a minimum temperature of 0°C.

The heaters maintained thermal control during the quiescent periods of operation when the OPM was operating in monitor mode (i.e. not performing measurements). During the measurement sequence, the heaters were switched off and the external thermal control coatings coupled with the thermal capacitance of the OPM provided sufficient thermal control. The OPM heater system design, located on the emissivity plate, consisted of two heater circuits with two 15-watt heater elements mounted in parallel in each circuit. Heater control was effected by using thermistors on this plate to thermostatically control their operation. Heater setpoints were selected at approximately 4°C (on) and 7°C (off). Thermal control was evaluated for materials exposed directly to the space environment as well as those not exposed. For exposed surfaces, the temperature control was achieved by the combination of various types of thermal control coatings, some having low solar absorptance or high solar reflectance coupled with either low thermal emittance (AZTek custom coating) or high thermal emittance (white coating) in order to control absorption of direct solar irradiance and reflected solar irradiance from Mir and/or the earth (Albedo). Low thermal emittance coatings were used to minimize radiation from selected OPM panels while high thermal emittance coatings were used on other panels to maximize the thermal radiation. The other surfaces were covered with MLI to minimize heat transfer. The combination of materials provided the necessary thermal control to match the measurement sequence and overall timeline with the expected Mir environment. A full report of the model predictions is contained in the *Thermal Data Book for the OPM Experiment, AZ Technology Report No. 91-1-118-145.*

A typical thermal profile predicted by the models for the measurement sequence and compared to flight data is shown in Figure 2-2.

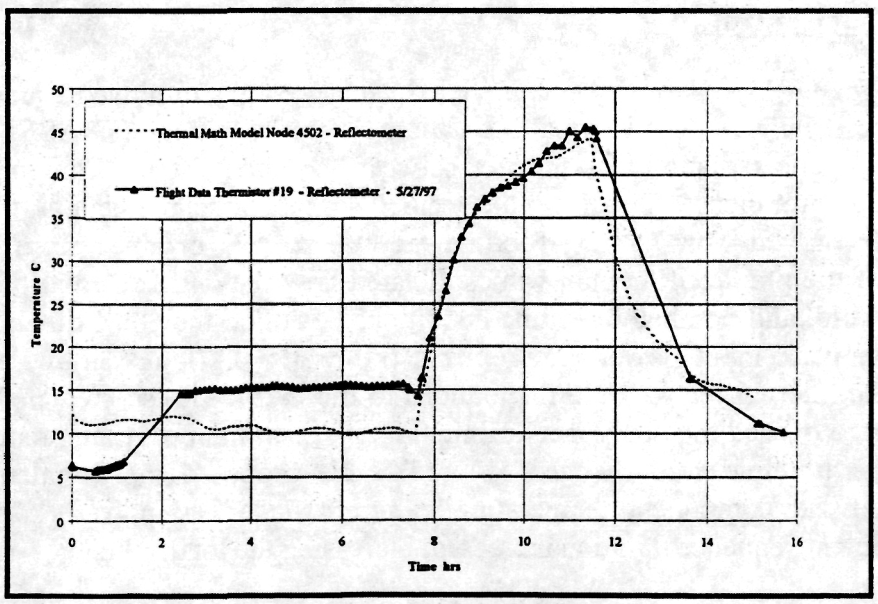


Figure 2-2. OPM Reflectometer Thermal Profile for the Measurement Sequence.

2.2.1 Mission Performance

The actual flight profiles measured and recorded by the OPM DACS closely follow the model predictions. Figure 2-2 illustrates the Reflectometer thermal profile for a measurement sequence performed on May 27. A more detailed report of the OPM Flight Thermal Data has been compiled and is referenced in the *Mission Thermal Data Book, AZ Technology Report No. 91-1-118-166.* The thermal control coatings did provide adequate thermal control of the OPM experiment. However, there were several days when the OPM was subjected to full sun and overheated because of the change in Mir attitude. The thermal model was again used to determine the OPM internal temperatures while the OPM was without power after the Progress collision into the Spektr module. The model predicted the OPM was at or just below the tested minimum temperature. Thermal measurements made at restart verified the predictions. Despite the thermal extremes encountered during the mission, the OPM still functioned within instrument/monitor specifications. Only one component, the solar radiometer sensor, is known to have failed during a full sun attitude. There were no other thermal induced failures or anomalies.

The outside surface of the MLI turned from white to varying shades of brown during the mission. In fact, photographs taken by the STS-84 Shuttle crew, while docked to the Mir Docking Module in May of 1997 after the OPM had been exposed for three weeks, show that the exposed surface of the MLI had already begun to turn brown. An investigation for the reason of the discoloration was begun by AZ Technology and the NASA/MSFC Material and Processes Laboratory (M&P) after the OPM was returned to the ground.

The outer layer of the MLI thermal insulation blanket was a 500F B1 Beta Cloth woven fiberglass material coated with TPFE as supplied by Chemfab Corporation. Samples of the same lot of material as used on OPM were supplied to NASA/MSFC for a 500 Equivalent Sun Hour (ESH) solar ultraviolet space simulation exposure test. Since attitude data was very limited at the time of this test, the 500 ESH level was the first estimate of the level of exposure received by the OPM on Mir and also was a convenient exposure fluence. Actual exposure levels were later found to range from 141 to 2903 ESH for the different sides of the OPM. Two separate ground tests were completed by NASA/MSFC where, in both tests, both sides of the Beta Cloth were exposed to the solar ultraviolet irradiation. After UV vacuum exposure, both sides of the Beta Cloth increased in solar absorptance, with the bondable or "etched" side having a much greater increase. This effect was evidenced by the Beta Cloth visually changing from white to brown. This change in visual solar absorptance of the Beta Cloth test samples demonstrated similar optical characteristics to the material flown on OPM. Figures 2-3 and 2-4 demonstrate the effect of 500 ESH solar ultraviolet had on 500F Beta cloth material. The change in solar absorptance for the data in Figures 2-3 and 2-4 were 14.3% and 40.5% respectively. This percent change in solar absorptance was significant because of the relatively short duration of this ground test. Such surfaces will be exposed to the uncontrolled conditions of space for a much longer duration on ISS. Contamination contribution to the changes in the OPM MLI Beta cloth effects have not yet been evaluated. Further discussion of these data are available in *OPM Science Data Report Number 91-1-118-*

169.

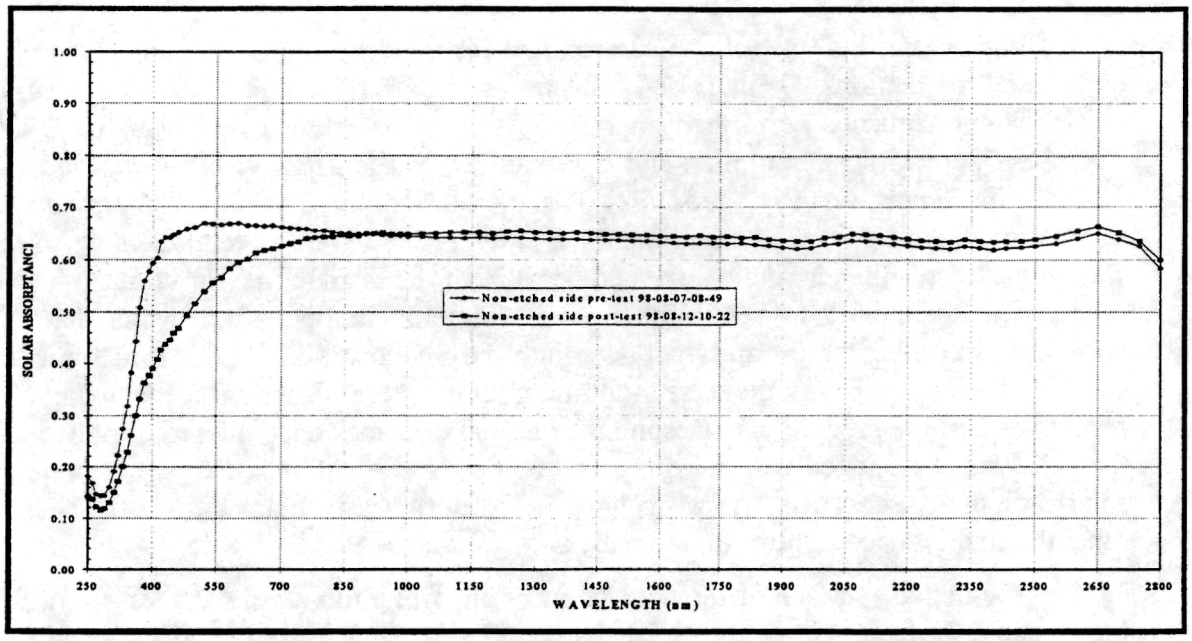


Figure 2-3. Effects of UV Vacuum Exposure on Non-etched Side of 500F I/B

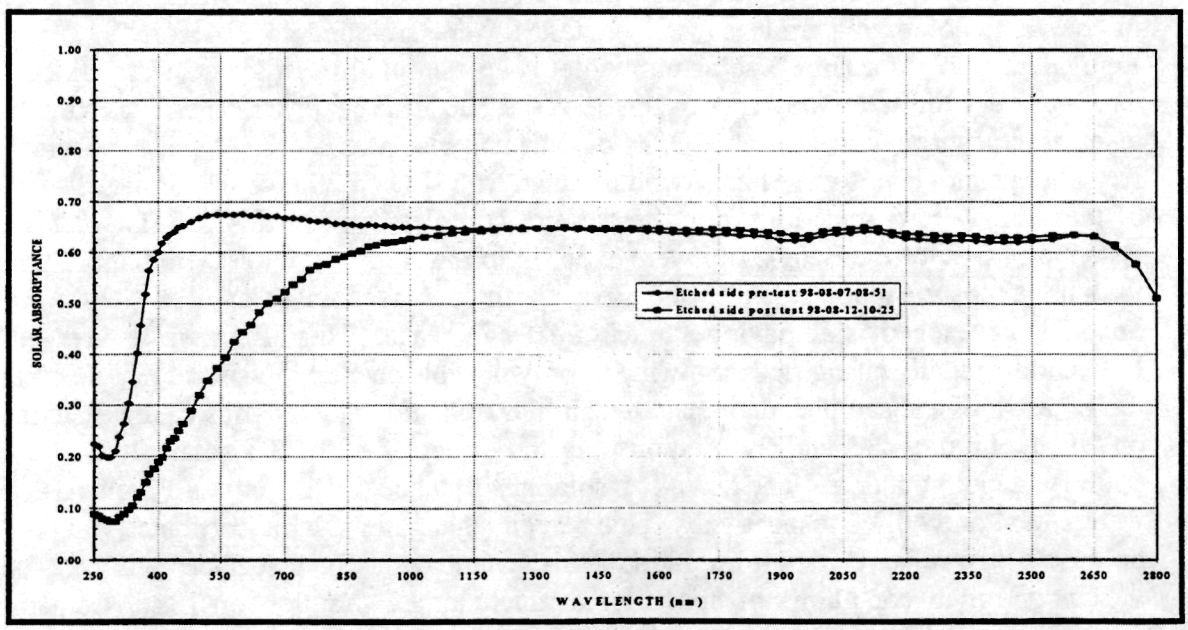


Figure 2-4. Effects of UV Vacuum Exposure on Etched Side of 500F I/B

One probable reason for discoloration was traced to the vendor's processing of the Beta Cloth. The outer layer of the MLI used a Teflon coated glass woven fabric (Beta Cloth) to act as an atomic oxygen AO barrier and provide mechanical protection to the inner layers of the MLI. The Beta Cloth used on OPM contained no silicones. Other Beta Cloth products do contain silicone polymers or additives. The 500F B1 material had one side non-etched and the other "etched" for bonding.

The Beta Cloth with one etched side was requested by AZ Technology to apply marker coatings to meet the Mir hardware marking requirement. Normally, the purpose of this "etched" side was to provide a roughened surface for deposition of VDA or other coatings. A post-flight investigation into the Beta Cloth darkening revealed the roughened surface (etched side) actually was an additional coating deposited onto one side of the Beta Cloth, not a removal of the Teflon as originally thought. This coating, according to the manufacturer, was composed of Perfluoralkoxy (PFA) Teflon and fumed silica (very fine glass). The additional coating on the "etched" side of this fabric is prone to enhanced degradation of its solar absorption properties, as shown in Figure 2-4. This damage was the result of UV exposure in a vacuum (space) environment. The non-etched side of the Beta Cloth also degraded from exposure to solar UV and vacuum environment, but to a lesser extent. Although the percent change in solar absorptance was approximately 1/3 of the processed (etched) side of the Beta Cloth (for 500 ESH) it remains significant considering the expected lifetime of 10 to 15 years for such surfaces on the ISS. A comparative example of a well-known surface material is the ceramic glass thermal control coating Z93. It has demonstrated less than a two percent change in solar absorptance after being in LEO for almost six years and ~11,000 ESH exposure on the LDEF as compared to the 500 ESH exposure of these test samples. As a result of OPM's flight, even common materials like Beta cloth prove to be important "samples" to ISS and other future missions.

2.3 Power/Control System

The OPM was designed to operate with 28 Volts Direct Current (VDC) –9, +12 Volts (V) spacecraft power. The OPM experiment received power from the Mir Station through the Krystall and Docking Module power bus (see Figure 2-5). The Russian ground crew, prior to a Shuttle launch, verified compatibility by connecting the OPM EVA cable to a mockup of the Docking Module bulkhead fitting used for powering external payloads. This cable was used for supplying the OPM power and for OPM data communications with Mir Station.

The OPM power/data system architecture is shown in Figure 2-6. The Power Supply Center (PSC) filtered the 27VDC Russian input power supplied by the Mir Station. The filtered 27VDC was routed to the DACS and through the PSC. The DACS contained a separate, independent Direct Current to Direct Current (DC/DC) converter for the DACS Mother board power. The PSC converted the input power into required voltages and supplied these voltages to the Power Amplifier Center (PAC) and Housekeeping. The PAC contained DACS software controlled drive circuits for the OPM instruments, carousel motor, and

environmental monitors. Housekeeping consisted of internal OPM thermistors for temperature measurements and calorimeters for carousel temperature measurements. The Housekeeping data sampling was software controlled by the DACS.

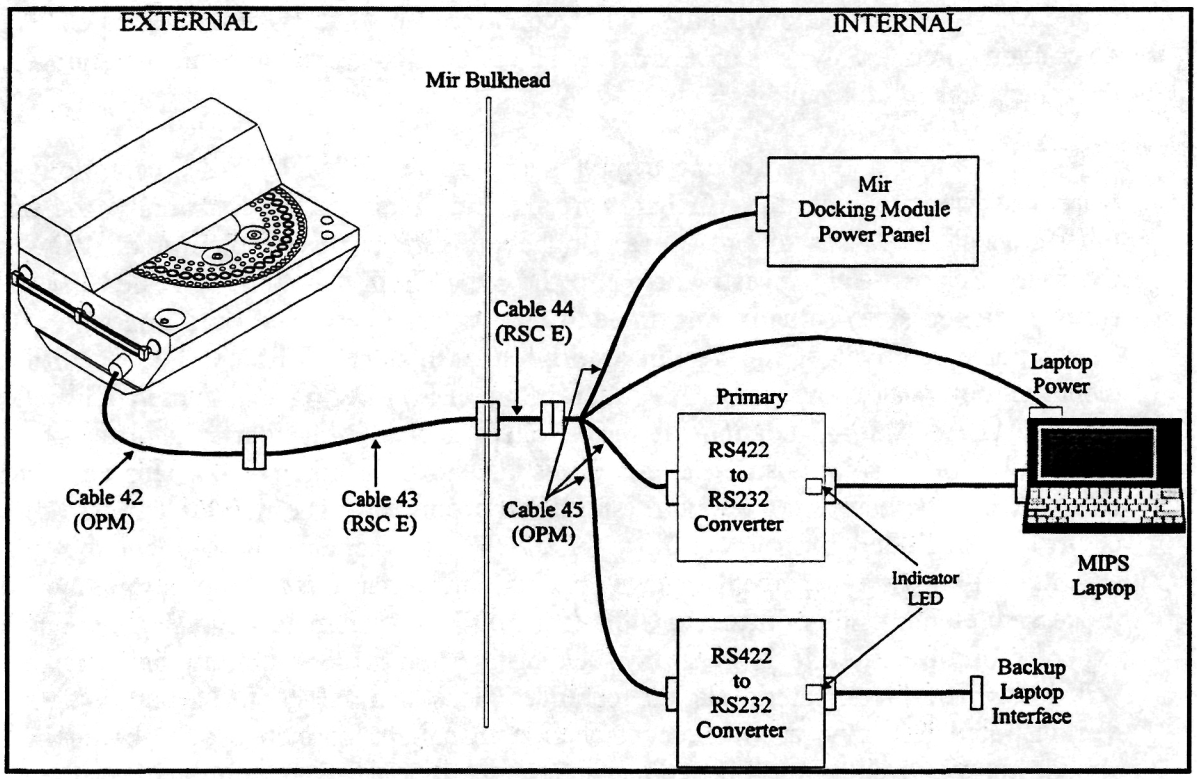


Figure 2-5. OPM MIR Power/Data Interface.

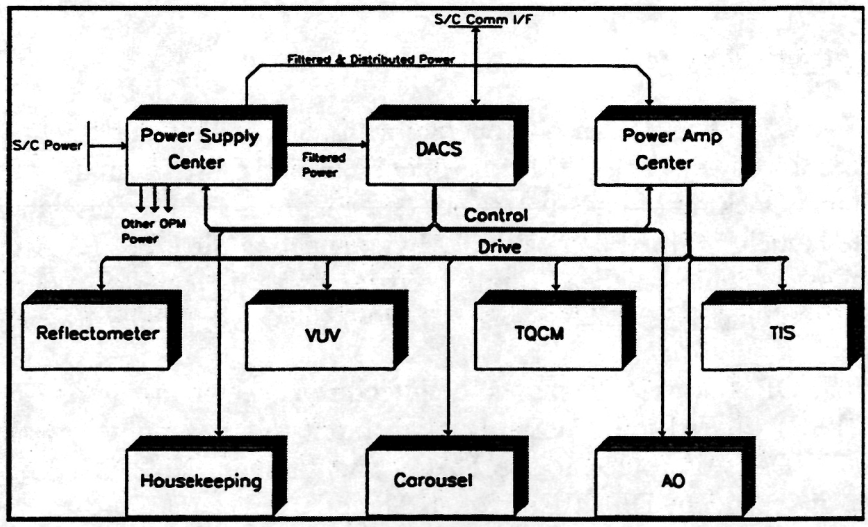


Figure 2-6. OPM Power/Data System Architecture.

The PSC, PAC, and DACS were designed as three separate modular units. The units consisted of box style housings and Printed Circuit Assemblies (PCAs). This design concept reduced EMI/EMC noise, consolidated space, allowed for easy assembly and removal, and was thermally efficient. The housings were designed as self-contained removable rectangular boxes with cutouts on the ends for connections. The boxes were bolted to the internal structure of OPM. PCAs, placed inside the housing, contained the OPM harness input and output connectors on the Printed Circuit Board (PCB) ends. The PCB design required that the heat produced from the EEE parts conduct through the housing to the OPM internal structure. Thermal analysis was performed on all PCBs in the PSC, PAC, and DACS. The PSC and PAC PCAs utilized nickel-plated copper top plate PCB construction to move the heat from the EEE parts to the housing. Wedge locks for each PSC and PAC PCA provided the thermal contact between the PCA and the housing. The DACS PCAs utilized a nickel-plated copper heat sink plate that was sandwiched between two multi-layer PCBs. The plate and the two PCBs were constructed to make a single PCA. The plate extended past the edges of the PCBs and was bolted to the DACS housing to provide thermal contact.

The DACS PCBs were fabricated using Surface Mount Technology (SMT) devices to save space. All other OPM PCBs were fabricated using Pin in Hole devices, for ease of construction and inspection. The size of the PCBs used for hall effect devices were mechanically constrained and SMT parts would have not reduced size. The PAC and PSC used high power parts not readily available in SMT packages.

Since the OPM system architecture was based on a modular design, upgrades or changes could be implemented efficiently at tremendous cost savings. For example, OPM can adapt to a new carrier with a different power requirement such as 120VDC or ISS power. The PSC can be easily removed and redesigned to accommodate the new power requirement. Once upgraded, the upgraded PSC can be re-installed and connected in the OPM.

2.3.1 Power Supply Center (PSC)

The PSC was designed for 28VDC –9, +12V spacecraft power. The spacecraft power entered the OPM through a connection cable and was directly routed to the PSC. The PSC block diagram is outlined in Figure 2-7. The PSC contained three PCAs stacked in a box style housing. Each PCA contained DC/DC converters, EMI filters, remote Solid-State Power Controllers (SSPCs), Solid-State Relays (SSRs), and connectors.

All spacecraft power was routed through a primary SSPC in the PSC. The primary SSPC was designed as the primary switch for OPM power on and off. The carrier selection was not finalized during the PSC design phase. Therefore, the PSC design implemented the primary SSPC with two selectable features. The primary SSPC could enable the spacecraft or carrier to control OPM power on/off from an external signal; or, the control for power on/off could be jumped for power on. The initial carrier was the EURECA, which had capability to turn power

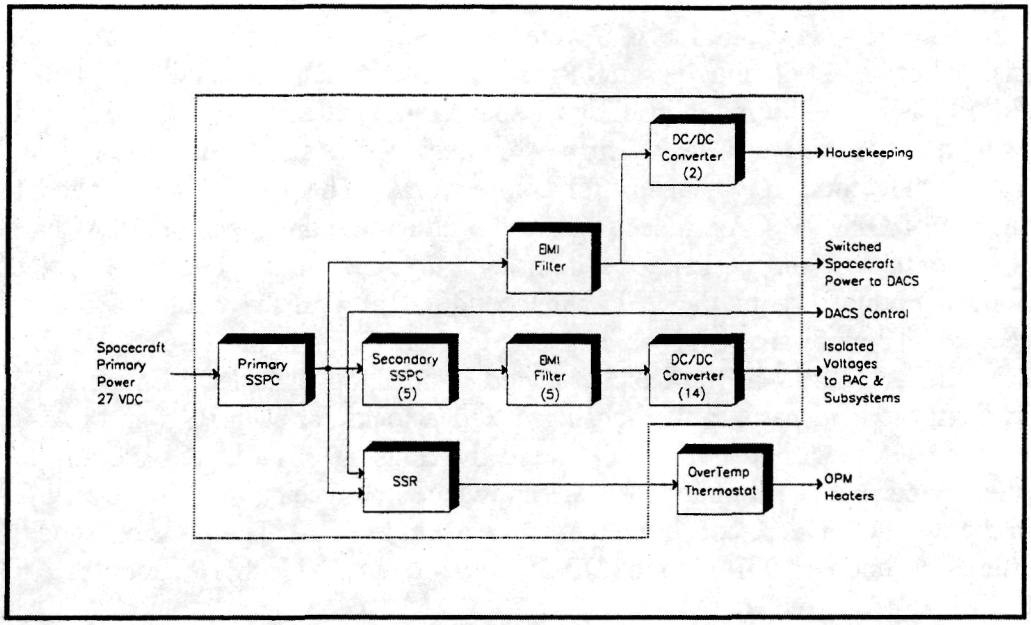


Figure 2-7. Power Supply Center (PSC).

on and off to a payload such as OPM. However, the OPM was manifested later for Mir which did not have payload power on/off capability. Therefore, the latter feature was used. Additionally, the primary SSPC monitored the OPM load current draw and provided short circuit and current overload protection. If a short circuit or current overload condition existed in the OPM, the primary SSPC would disconnect automatically the OPM from spacecraft input power. OPM could then be repowered by cycling input power.

The OPM PSC was designed for efficient power conversion. The DACS, under software control, individually controlled secondary SSPCs designed to power respective DC/DC converters for the different OPM instruments, subsystems, etc. The secondary SSPCs had the same capability as the primary SSPC but at a lower current rating. The secondary SSPCs monitored the respective instruments and subsystems for load current draw. If a short circuit or current overload condition existed in the respective instrument or subsystem, the respective SSPC automatically disconnected the respective load from its input power. These SSPCs could be reset and powered back on under software control. All power routed to the DC/DC converters was EMI filtered. The DC/DC converters converted the filtered 28VDC input power to distributed voltages of ±5, 10, 12, ±15, +24, and 105V. The distributed voltages were routed to the PAC and Housekeeping. Filtered power was routed directly to the DACS.

The PSC was designed to power the heaters inside the OPM. An SSR was implemented in the PSC under DACS software control to turn power on or off to the heaters. This power was unfiltered but monitored by the primary SSPC. Thermistors on the plate where the heaters were mounted were used to control the heaters. The control set point was set at approximately 7°C to cut off the heaters and cut on at 4°C.

2.3.2 Power Amplifier Center (PAC)

The PAC contained four PCAs stacked in a box style housing. The PAC contained drive circuits for the OPM instruments, carousel motor, and environmental monitors. The PAC architecture is shown in Figure 2-8. Board #1 in the PAC was the VUV driver and PAC power distribution board. Board #2 was the Reflectometer driver board. Board #3 was the AO, Carousel, and TQCM driver board while Board #4 was the TIS driver board. The PSC distributed power entered the PAC via the VUV board. The VUV PCA routed the necessary required distributed power to the remaining three PAC boards. Each of the four PAC board driver circuits were individually software controlled by the DACS to provide independent control for each instrument and subsystem. The signals from each of the instruments and subsystems were independently received by the DACS.

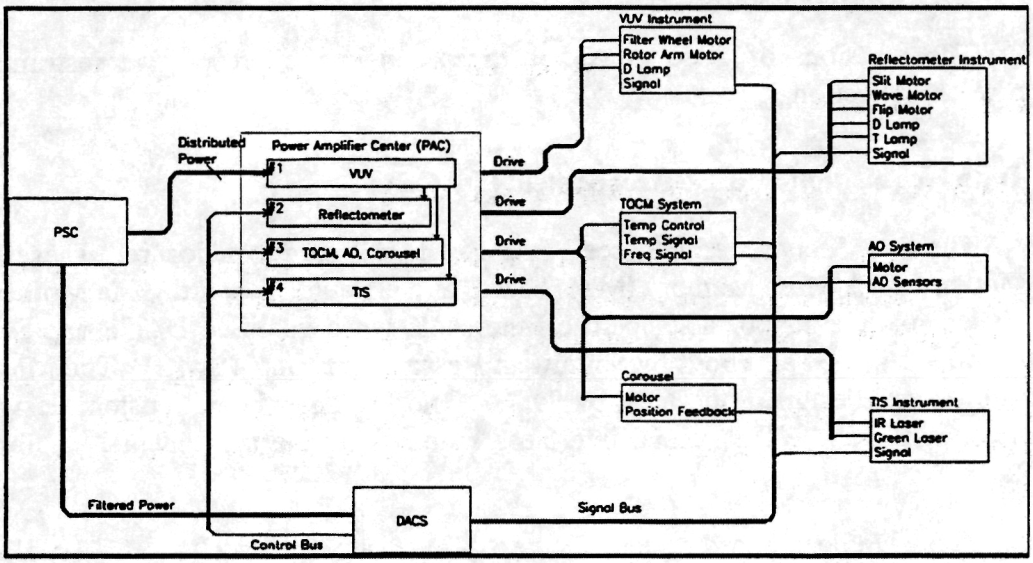


Figure 2-8. PAC Architecture.

The PAC was designed and built by the prime contractor, AZ Technology in Huntsville Alabama. These four PCAs and their functions are summarized as follows by board number:

1. VUV power controller
   - Deuterium Lamp Heater control circuit,
   - Deuterium Lamp Strike circuit,
   - Deuterium Lamp constant current source,
   - Motor drivers (Rotator Arm and filter wheel).
2. Reflectometer Power Controller
   - Deuterium Lamp Heater control circuit,
   - Deuterium Lamp Strike circuit,

- Deuterium Lamp constant current source,
- Tungsten Lamp programmable current source,
- Lead Sulfide (PbS) Thermo-Electric (TE) Cooler drive constant current source, and
- Motor drivers (Beam Deflector, Monochromator slit and wavelength drive motors).

3. TQCM Temperature controller
   - Two TQCM temperature controllers,
   - AO Motor driver circuits, and
   - Dual redundant carousel motor drivers.
4. TIS LASER power controller
   - Two Light Amplification by Stimulated Emission of Radiation (LASER) driver/controllers

The functions of these PCAs are discussed in their respective instrument/monitor description in Section 3.

2.3.3 Data Acquisition and Control System (DACS)

The DACS consisted of three PCAs inside a separate enclosure. These PCAs were the Mother board, Mass Memory (MM) board, and a Daughter board. The Mother board and the enclosure were part of a standard off-the-shelf space-qualified DACS, the SC-4A. This system was designed and built by Southwest Research Institute (SwRI). The MM board was a custom board designed and built by SwRI. The Daughter board, custom designed by AZ Technology to handle the special interfaces required by the instruments, was also built by SwRI.

The Mother board (see Figure 2-9) was an Intel-based 10MHz 80C186 microprocessor system complete with a math Co-Processor. The memory complement on this board was; 512K bytes Static Random Access Memory (SRAM), 256K bytes Electrically Erasable Programmable Read Only Memory (EEPROM), and 64K bytes of UV Erasable Programmable Read Only Memory (UV EPROM). All memory had double bit Error Detection and single bit error Correction (EDAC). The Mother board contained:

- 512K SRAM with EDAC,
- 256K EEPROM with EDAC,
- 64K UV EPROM with EDAC,
- 2 Channel Serial Input/Output (I/O), configured as RS-422
- 2 Software programmable timer modules (Intel 8254 type), each contained 3 programmable timer/counters,
- 4 Channel Digital-to-Analog (D2A) Converter,
- 32 Channel Analog-to-Digital (A2D) 10-bit Converter, and
- 16 channel discrete I/O port.

These interfaces were used as follows:

DACS Interface	Purpose
Serial I/O (RS-422)	Spacecraft communication (redundant)
Programmable Timer Modules	Software for timing events
D2A	Two (2) channels for TQCM temperature set-point, Two (2) channels were spare.
A2D	Health and status monitoring, Back-up to Daughter board A2D
Discrete I/O	PSC & PAC control and status

The DACS Daughter board, see Figure 2-10, contained all signal conditioning for each of OPM's three optical instruments as well as circuits for other OPM sub-systems not supported by the COTS CPU board. With the exception of the high voltage or high current drivers, all this signal conditioning was located on the DACS Daughter board. The Daughter board had the primary A2D converter which had 14-bit bi-polar resolution. There was a back-up A2D on the COTS CPU board with 12-bit resolution. The Daughter board had an external pin that connected the output of it's analog MUX to the COTS CPU's A2D. Each of the three optical instruments; reflectometer, TIS, and VUV, had it's own synchronous demodulator with a digital phase shift control. Although, they were all identical circuits, they were complete and separate in every way so that a component failure in one system would not effect another instrument. The Daughter board also contained:

- Two frequency counters for the TQCMs (1/2Hz resolution min.),
- Motor controllers for the instruments (6 Total controllers) and dual-redundant controllers for the carousel,
- Discrete I/O to augment the Mother board (used for the same functions),
- Separate 14-bit A2D,
- 8-bit D2As for excitation on thermistors and Platinum Resistance Thermistor (PRT)s, and
- Dual-redundant motor position encoder for the carousel.

The Daughter board also contained a Remote Acquisition Unit (RAU) and a 1553 communication interface for use on other carriers (not used on Mir).

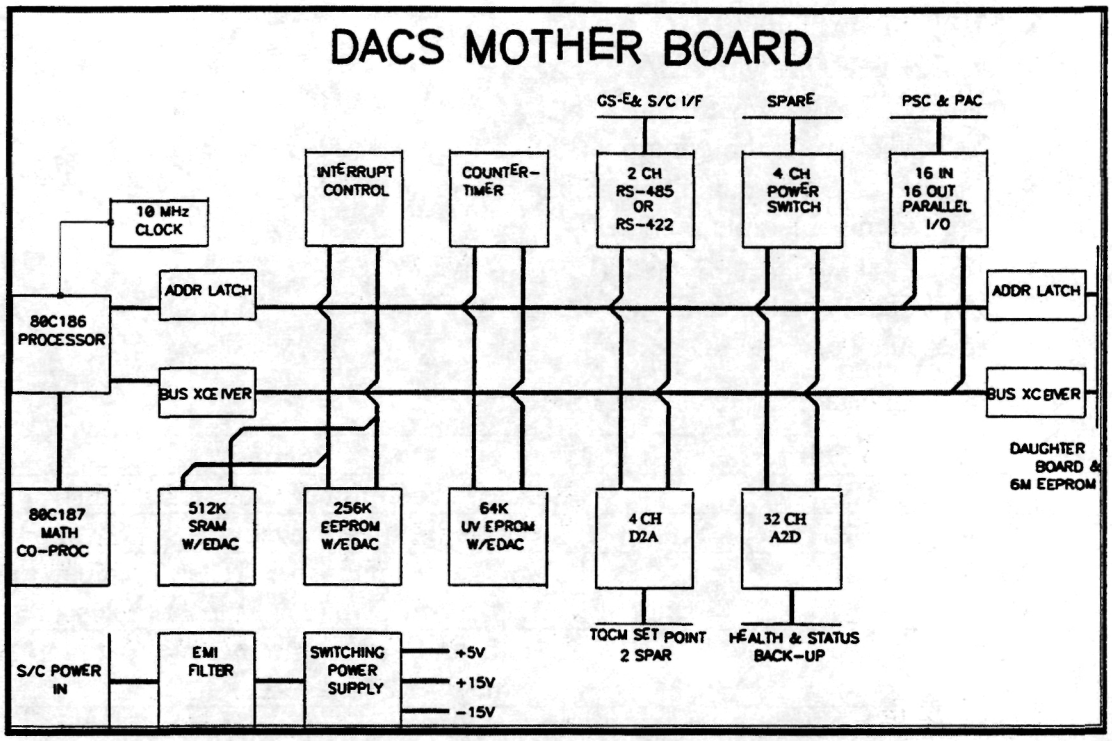


Figure 2-9. DACS Mother Board.

The SC-4A DACS was environmentally tested at SWRI's facilities at expected flight/mission levels. These tests included vibration, thermal cycle, and thermal vacuum. The vibration tests included, for each axis, sine sweep and random loads. These tests were at the same levels as those performed on the OPM System. The thermal cycle test was comprised of four cycles at -30°C and +60°C at ambient pressure where the DACS was stabilized at these extremes and then powered on and tested. The thermal cycle test included four cycles with a cold start at -20°C and hot start at +25°C, both at a pressure of 10^{-5} Torr (minimum). The temperatures in thermal vacuum were selected based on the OPM thermal model analyses. These tests were performed to gain confidence that the DACS could function in the environments anticipated for the OPM. A full series of system level environmental tests was performed at NASA/MSFC (refer to Section 1.3); however, the tests conducted at the vendor's facilities were performed to "Screen" the DACS to minimize problems during NASA/MSFC system testing.

2.3.4 Power Timeline

The OPM power profile, shown in Figure 2-11 for a one-week period, reflects a 149-hour quiescent mode and a 19-hour measurement mode. During the quiescent mode, the OPM was powered on, but was not actively making optical measurements. Rather, it was in a monitoring mode where the TQCMs, AO Sensors, radiometers, system thermistors, and the necessary core systems were powered to check the environmental conditions to which the

flight samples were exposed. Once a week, after 168-hours from the start of the previous measurement timeline, the OPM activated the optical instruments to take sample measurements during this 19-hour measurement mode. The optical instruments were powered on sequentially, not in parallel, to minimize instantaneous power requirements. As shown in Figure 2-12, the order of instrument operation was the TIS, VUV, reflectometer, followed by a four-hour period to make emittance calculations from the reflectometer samples. The time shown in Figure 2-12 is representative of the VUV instrument malfunction. The power levels (in watts) shown reflect the total power required to operate the OPM.

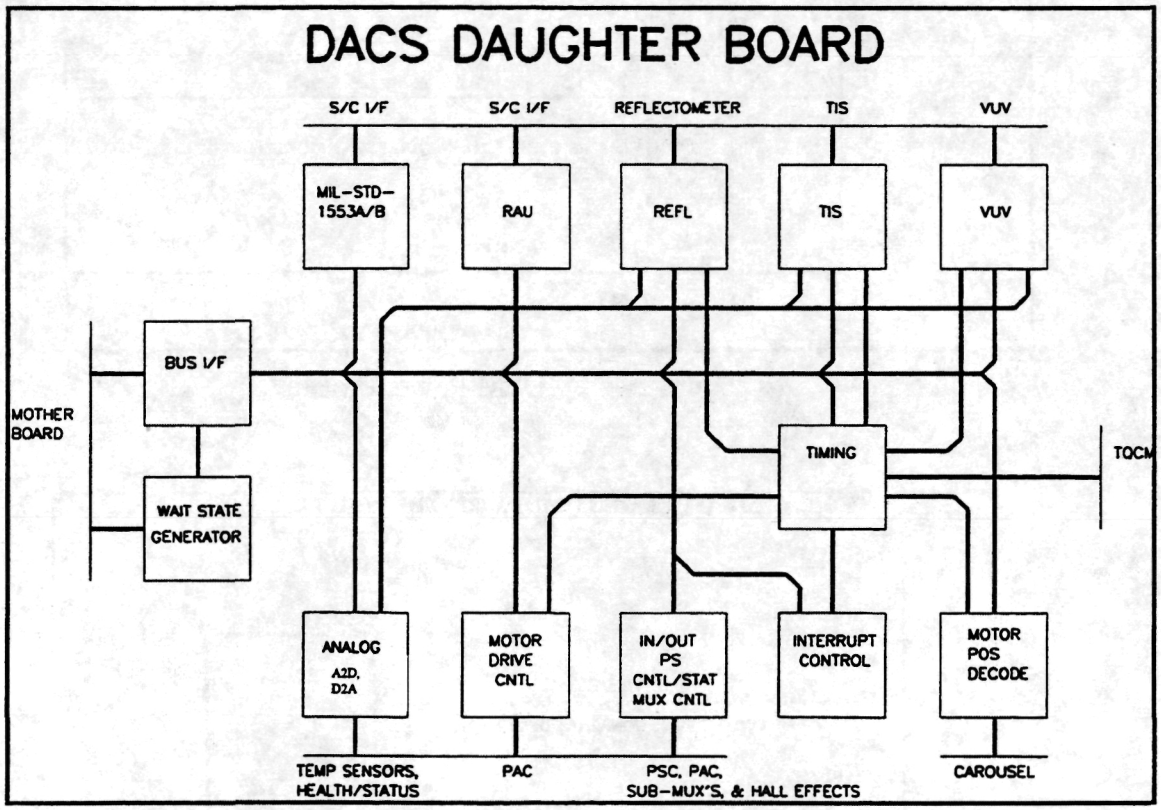


Figure 2-10. DACS Daughter Board.

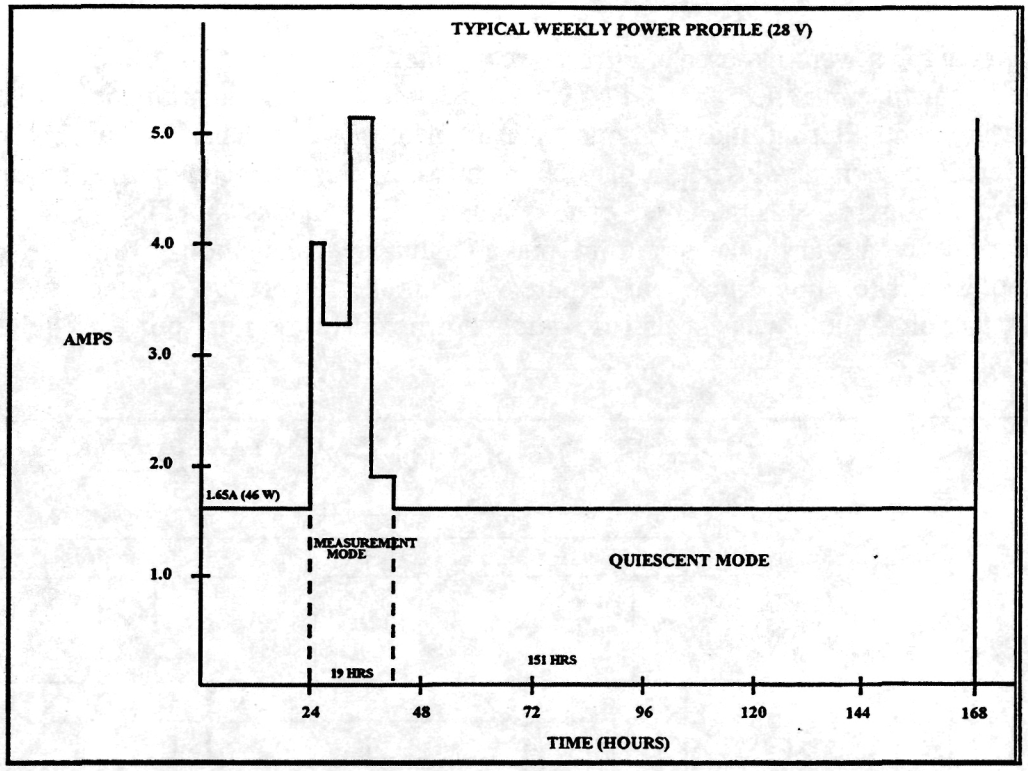


Figure 2-11. OPM Power Profile.

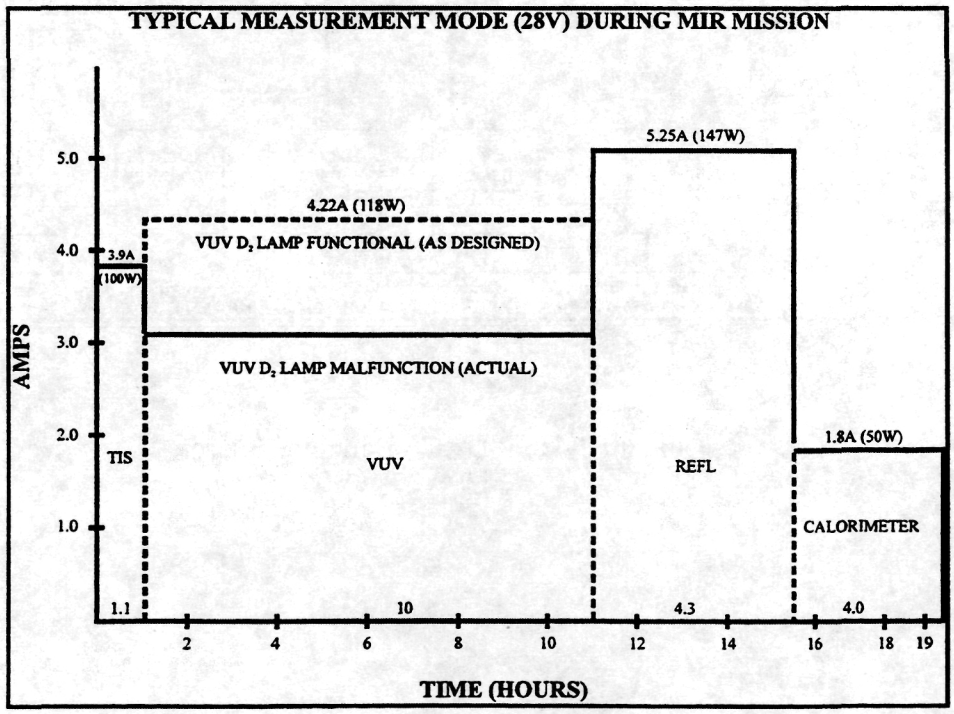


Figure 2-12. OPM Order of Instrument Operation.

2.3.5 Mission Performance

The PAC, PSC, and DACS performed well during the mission. No anomalies were observed nor reported. These subsystems performed to specifications from -20°C to 60°C. Several cold starts of the OPM successfully occurred at -20°C. Had any one of these subsystems failed during the mission, the OPM mission success would have been degraded.

The PSC was exposed to repeated power outages while on the Mir due to failed Mir attitude control systems, and probably encountered low voltage conditions due to the Mir switching to backup battery power. In September 1996, there were repeated power "on" and "off" cycles when the OPM was "on" at the power breaker, and Mir repeatedly went through the terminator each orbit. When this was observed by the Mir crew and reported to ground, AZ Technology requested the power breaker be powered off until OPM could be formally powered "on." However, there are no documented "brown outs" recorded by the Mir crew. None of these occurrences had any obvious effect on the PSC performance, but a visual inspection has not yet been performed on the PSC PCAs. Post-flight systems tests indicated the PSC was functioning to designed specifications. No failures were detected from the OPM data.

The PAC maintained good control of the instrument and monitoring subsystems. No anomalies or failures in operation were recorded, based on health/status data or instrument performance data.

The DACS maintained proper control of the OPM operation. There were no failures. Data aspects of the DACS memory are reported in Section 2.6.

The measurement timeline initially took approximately 14 hours to complete, but when the VUV Deuterium lamp malfunction occurred, followed by the VUV filter wheel anomaly, the measurement timeline stretched to approximately 19 hours.

2.4 Carousel Drive Assembly

The Carousel Drive Assembly (CDA) was comprised of the sample carousel, the drive motor, and the cable management system. The sample carousel contained the flight samples for in-situ measurements by the Reflectometer, VUV Spectrometer, and the TIS instruments, passive samples (not measured in flight), two radiometers (one solar and one infrared), the TIS calibration sample, and a carousel sub-multiplexer PCA. The drive motor was a dual-redundant stepper motor contained in a single housing. The cable management system was housed in a metal circular track around the carousel motor that enabled a total rotation of the carousel of 535°. The CDA featured hard stops at both ends of the rotation to prevent the destruction of the cable management system. The CDA was controlled by the DACS using a predefined timeline that operated autonomously.

2.4.1 Sample Carousel

The sample carousel housed all ninety-eight flight samples. There were seventy-two "active" samples; meaning these were measured in flight. There were twenty-six "passive" samples. Passive meant the samples were measured only by pre- and post-flight analyses. The active samples were further categorized by instrument: the reflectometer had twenty samples, the VUV had thirty-two samples (at forty-one sample positions), and the TIS had twenty samples. The VUV had nine calibration positions to permit an end-to-end calibration of the instrument during operation; one at every fifth VUV sample (refer to Figure 2-13).

The samples were spaced around the carousel in a polar configuration with the VUV samples on the outer row, followed by the reflectometer, TIS, and passive samples respectively on the inner rows. Figure 2-13 illustrates the placement of the samples on the sample carousel. The samples were spaced at 9° increments, except for the VUV samples, which were spaced at 4.5° increments because of the increased area available on the outer row.

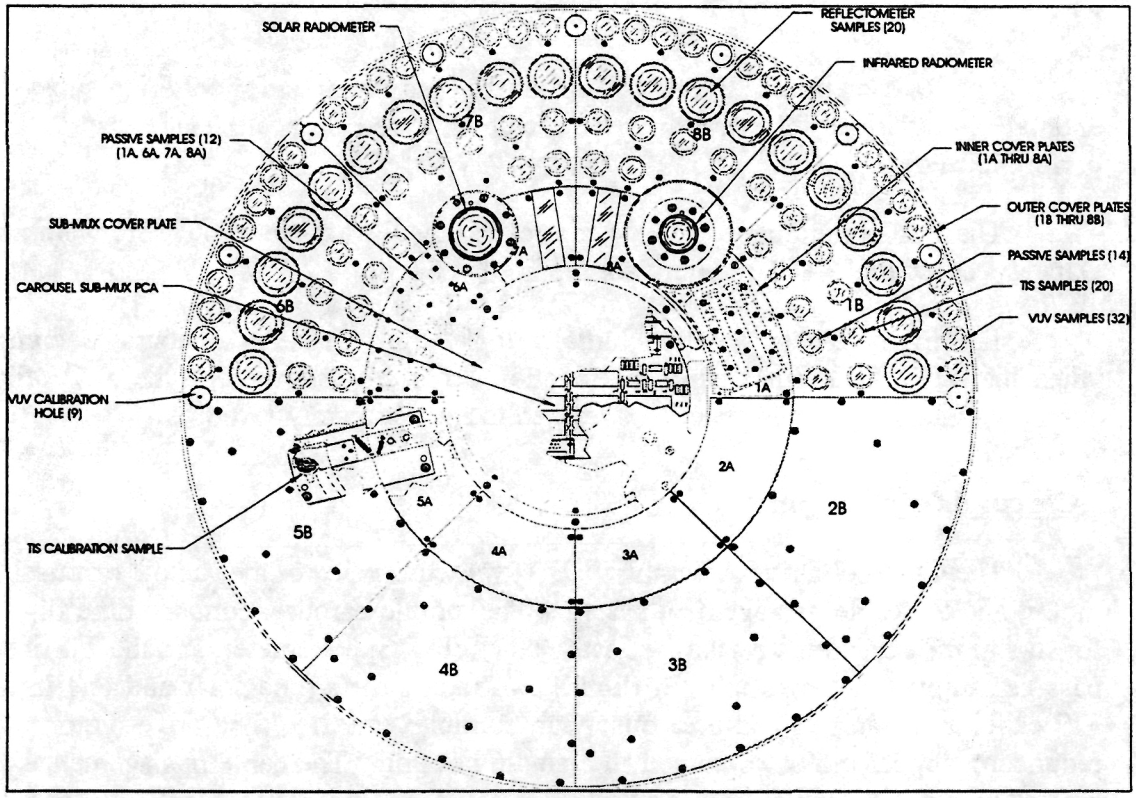


Figure 2-13. Sample Carousel.

The flight samples were installed in sample holders to accommodate the various thickness of flight samples, to mechanically hold them in place during the launch environment, and to enable ease of installation/removal in the Sample Carousel. These

sample holders were customized for the reflectometer, TIS, VUV and the passive samples. Figures 2-14 and 2-15 illustrate the three basic sample holders used in the Sample Carousel. The VUV and TIS/passive samples were identical except the outer circumference was machined to permit closer spacing around the carousel perimeter.

The reflectometer samples were calorimeters and provided a simple method to determine solar absorptance (α_s) and total emittance (ε_T) of test samples. The calorimetric technique measured the inputs to the heat balance equation and calculated solar absorptance and total emittance. To calculate emittance, in-space measurements of the test sample temperature and the external heat inputs, as measured by the irradiance monitors, were required. The design of the calorimeters isolated the test sample thermally from the OPM to minimize errors caused by radiative and conductive losses. The OPM calorimetric design was the same as that used on the TCSE and was developed originally by the GSFC and flown on the subsequent satellites.

The calorimetric measurement procedure was an improvement over past experiments for determining total emittance. Previous experiments could only determine total emittance when the calorimeter viewed deep space only (i.e., no view of the sun or earth). This orientation was difficult to insure, and the time spent in this orientation was, at times, too short to provide accurate measurements. The OPM procedure, however, rotated the samples inside the instrument, eliminating any view of the sun or earth.

The calorimeter consisted of three major parts: the sample disk, the inner cup, and the outer cup (see Figure 2-14). The concept for the three-part calorimeter was for the inner cup to act as a thermal guard for the sample disk. This design featured virtually zero conduction back through the sample holder, and low measurable radiative heat transfer to the sides. The inner cup, or "guard", had the same area and coating as the sample disk to maintain the inner cup temperature close to the temperature of the sample. The thermal capacitance of the inner cup was also as close as possible to that of the sample disk to ensure the guard was effective - even during transient thermal conditions. Kapton films, formed into two cylinders, were used to fasten the sample disk to the inner cup and to fasten the inner cup to the outer cup. Double-faced aluminized Mylar sheets with dacron netting were placed inside each cylinder to reduce the radiative heat losses. Vent holes were put in the cylinders and bases of the inner and outer cups, enabling the interior of these cups to vent to the vacuum environment. A solar absorber material was applied to the inner sides of both the inner cup and the outer cup to minimize errors caused by light leaks through the gaps between the sample, inner cup, and outer cup. A Platinum Resistance Thermister (PRT) was attached to the underside of each sample disk with thermally conducting silver epoxy to assure good thermal contact with the sample substrate. The DACS monitored the PRT to measure the temperature of the sample disk. The calorimeter was mechanically clamped into the carousel by the carousel mounting cover. The top of calorimeter was flush with the top of the carousel.

The sample carousel total rotation was fixed at 535°, (525° nominal) to enable the

samples to be rotated under the measurement instrument's aperture. From the nominally exposed position ("Home" position or 0 degrees), the carousel rotated 205° CCW and 330° CW. These rotation limits were devised for the singular operation of each instrument to optimize instantaneous power as well as the carousel motor operation time.

The sample FOV from the carousel plane was 123° minimum in one direction (towards the Top Cover), and 180° in the other directions (see Figure 2-16). The restricted view was towards the OPM cover that enclosed the three measurement instruments. Only those samples immediately adjacent to the Top Cover had the limited 123° FOV, all other samples had a FOV greater than 123° toward the Top Cover. This requirement maximized the samples' space exposure.

For thermal control, the sample carousel's external surfaces were hard anodized, except for the sub-multiplexer cover which was coated with Z93, and the samples themselves. The internal components of the carousel were alodined to ensure electrical continuity.

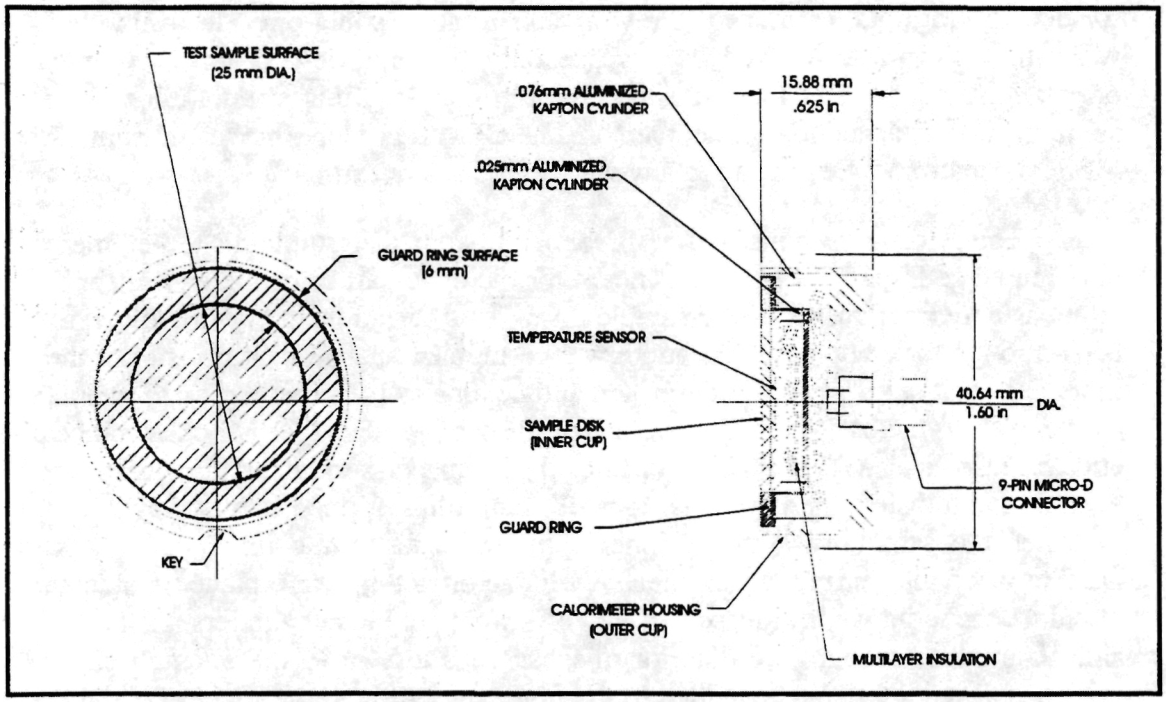


Figure 2-14. Calorimeter Sample Holder (Reflectometer Sample).

The carousel sub-multiplexer PCA was a dual 64 channel analog multiplexer (MUX). The electronics design utilized 16-channel analog MUX Integrated Circuits (IC). Each of these ICs had two fixed resistors that were used as a reference to allow some level of self-test. One of the fixed resistors was a high resistance to represent one extreme thermistor value. The other resistance was a low resistance to represent the other extreme thermistor value.

Not counting the reference resistors, the MUX PCA supported 56 thermistor inputs.

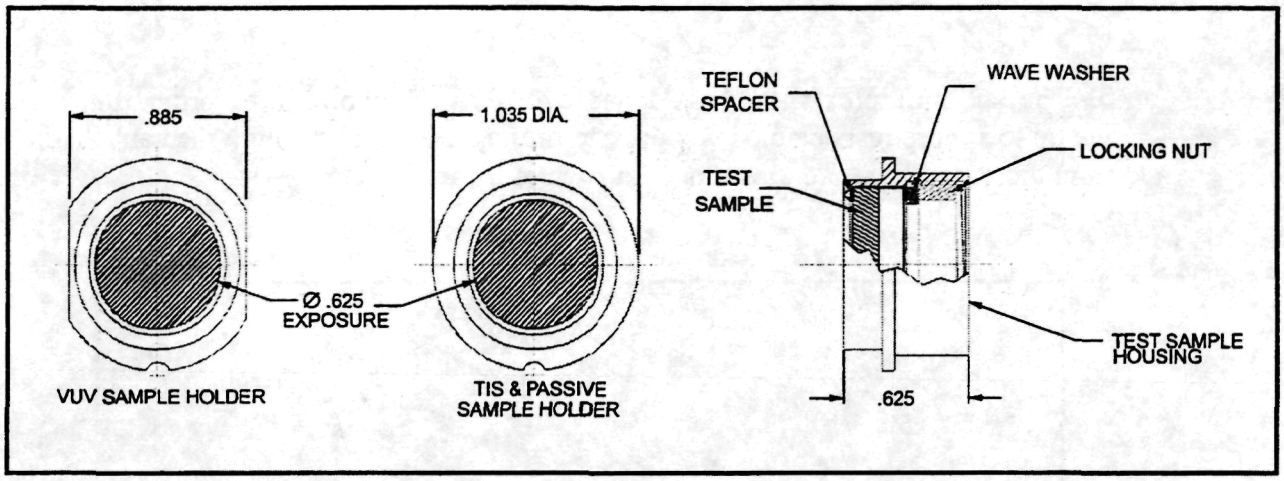


Figure 2-15. Test Sample Assembly VUV, TIS, and Passive Sample.

The dual MUX design supported a "pseudo" 4-wire Kelvin measurement. A software (S/W) programmable current source was used to provide excitation to the thermistors. One side of the dual MUX provided the excitation current to the thermistor to be measured. The other side of dual channel provided the thermistor voltage measurement to the system A2D converter. The measurement was made in the following manner: provide a known current through a unknown resistance (resistance varied with temperature) then measure the voltage and solve the equation (V=IR or R=V/I). The current source return and the A2D return were common with all thermistors. The Sub-multiplexer printed circuit layout as well as the wiring harness were carefully designed to keep all four wires separated until reaching a common point (for the current source return and A2D returns). This provided a true 4-wire resistance measurement while minimizing the number of wires through the cable management system to the DACS. Note that 56 four-wire measurements would require 224 wires! The use of the sub-multiplexer reduced the wire count to only nineteen; five for power, four for measurement, eight for address (ADDR) or channel selection, and two additional wires for the radiometer pre-amps.

The purpose of performing a 4-wire measurement is to reduce errors caused by Current times Resistance losses (IR). All wires have some finite resistance (R), and if current (I) passes through that wire, then there is a voltage (V) drop across the wire (V=IR). This voltage drop in the wire represents an error in the measurement. By using four wires, this error can be eliminated. One pair of wires carried a current from a constant current source through the resistor and back to the return of the source. A second pair of wires was connected ***at*** the two nodes of the resistor, one was the A2D measurement and the other was the A2D return. In this manner, the voltage drop in the wire from the current source to the resistor and the voltage drop from the resistor back to the current source were ***not*** measured. Thus this measurement error was eliminated.

The sub-multiplexer PCA also had a difference amplifier to bring the thermistor voltage up to a more respectable level prior to routing the signal through the cable harness. In addition, there were two pre-amps; one for each of the radiometers.

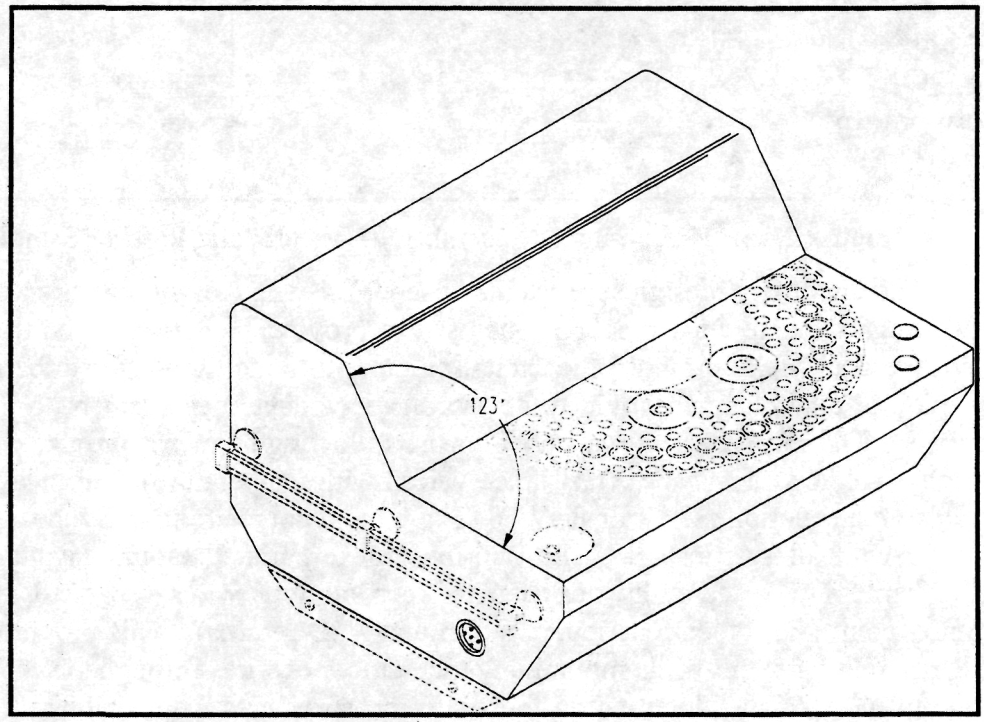


Figure 2-16. Sample FOV.

2.4.2 Carousel Drive Motor

The carousel drive stepper motor was a 1.5° per step, 160:1 harmonic drive gear reduction unit that operated at 28VDC. This drive motor was built by Schaeffer Magnetics (now Moog) of Chatsworth, CA. The rotation rate was software adjustable between 9 and 169° minute. The output torque was between 400 and 500 in-lb and required less than 15W of power. The reasons for selecting this unit were its robustness and successful space flight history, high output torque capability, wide range of rotational velocities, redundant stator, wide temperature ranges for operational and non-operational conditions, positional feedback capability using both potentiometers and incremental encoders, enhanced output load bearing capability, and its angular positional accuracy capability (0.56 Arc-minutes) exceeded the TIS requirement for microstepping across the TIS flight samples (5.4 Arc-minutes). This particular unit also was life tested, which it passed, for the expected number of rotational

cycles of the harmonic drive. Further, this unit was tested at the vendor's test facility at thermal vacuum levels between -20 and +50°C at 10^{-5} Torr and vibration levels expected for launch. A platter, that simulated the weight of the sample carousel, was attached to the carousel drive motor for the vibration test.

The TQCM PCA, in the PAC, had a dual redundant motor driver for the carousel motor. This driver converted the digital control signals from the DACS to the required voltage and current levels for the carousel motor. The redundant drive could be switched under S/W control. The carousel motor was a three-phase stepper motor with redundant windings. The carousel drive motor was designed also with dual redundant incremental position encoders and potentiometers. The incremental encoders indicated the angular position of the motor and actuator output with respect to a "home" position. This capability was provided by the use of one encoder to track the motor output (single steps) and home position as well as a second encoder for tracking the output actuator (carousel) corresponding to each sample position on the carousel. Each of these encoders was designed with a redundant encoder that could be software selected. Because the encoders were incremental and not absolute, redundant potentiometers were used to monitor the output actuator position relative to the "home" position. Each potentiometer spanned the 530° by using two-turns and had a resolution of better than 4.5°. Thus, if the power were ever lost to the OPM during a timeline, the potentiometers could resolve the carousel position - and not have to "home" the carousel to restart the measurement(s).

2.4.3 Cable Management System

The sample carousel contained two radiometers, twenty calorimeters, and thermistors to measure the carousel internal temperatures. These data were measured by the DACS to monitor mission environment and sample response to this environment. A cable management system was devised to connect these sensors and calorimeters to the DACS. Two designs were considered, a "slip ring" and a "cable wrap." The slip ring concept was not possible because the center of the stepper motor contained the harmonic drive mechanism. Therefore, the cable wrap design was selected for the cable management system. Another reason for selecting the cable wrap design was that the vendor had successfully designed and flown similar systems previously for space flight hardware. In the cable wrap design, the cable is wrapped or coiled inside a "donut" mounted around the perimeter of the stepper motor. The cable is rigidly attached at the entrance and exit of the donut. The length of the cable inside the cable management system is calculated based on the size of the donut and the amount of rotation required by the sample carousel. This design was further complicated by the requirement to have two cables in the cable management system, based on the amount of data to be measured by the DACS. Each cable (two total) was terminated by a space-rated connector for mating to the OPM main cable harness and the carousel sub-multiplexer PCA.

2.4.4 Mission Performance

The cable management system worked exceptionally well. There are no anomalies to report.

The carousel drive motor did exhibit one intermittent anomaly. After the OPM restart due to the Progress vehicle collision into the Spektr module, the carousel motor did not find the proper start position on six of sixteen timelines. Of those six timelines, four started with below 0°C thermistor readings. On two of those six timelines, the carousel position self-corrected during the timelines and successfully completed the timeline. This anomaly has not reoccurred in post-flight testing.

2.5 Software

This section describes the design and mission performance of the OPM software. Subsection 2.5.1 provides an overview of the design of each major component of the DACS flight software, ground software, and Mir Interface to Payload System (MIPS). Subsection 2.5.2 provides an assessment of the mission performance of the DACS flight software and MIPS software.

2.5.1 Design

The OPM software was developed using structured analysis and design techniques - data flow diagrams, data dictionaries, and structured English requirements. The embedded flight software followed guidelines specified in the *MSFC Software Management and Development Requirements Manual (MM8075.1)*.

2.5.1.1 Flight Software

2.5.1.1.1 Overview

The OPM flight software, the "Control Program" (CP), controlled all aspects of operation of the OPM instruments, monitors, and other subsystems. The flight software was stored in the DACS Mother board EEPROM. Upon power up, the flight software copied itself to DACS volatile memory, initialized all subsystems, and entered monitoring mode. Health and status were recorded, environment monitors were measured, and the internal clock was checked periodically for the occurrence of the next measurement run start time.

The DACS software CP operated in four states:

- Initialize
- Monitor
- Measure
- Shutdown/Deactivation

Figure 2-17 depicts these states and the events (e.g., spacecraft commands, power failure) that caused transitions among the states. The DACS operated primarily in the Monitor state, controlling and recording data from the OPM monitors (e.g., TQCM, AO Monitor, and Radiometers). Once per week for several hours, the DACS operated in the Measure state, controlling and recording data from the OPM instruments (Reflectometer, TIS, and VUV).

The flight software was designed to be as simple and reliable as possible. In general, more sophisticated operational approaches were avoided. The design goal was for the software to operate autonomously for up to 80 weeks in space without human intervention. There was concern about crew availability to support OPM operations, and these concerns proved true during the mission. The crew had very limited time to support OPM contingency/manual operations during the eight month mission.

The design approach is illustrated by how the carousel was rotated. The initial plan was to rotate the carousel to the "orbital" position (samples exposed) every time OPM was powered on. This would insure the samples were exposed upon initialization after a power failure. But there was also concern about the carousel being cold after a power failure and needing to warm up before being rotated. There were also concerns about the crew being close to OPM during deployment EVA when power-on occurred, broken glass, and not wanting the carousel to be rotating while the crew was still removing the OPM cover. There was a simple solution - don't rotate on power up. The carousel was only rotated during a measurement run. If power failed when samples were inside the OPM, they remained there until the next weekly measurement run.

The flight software was primarily written in the C programming language. A few startup routines were written in Intel 8086 assembler. The flight software was written as one program that performed all tasks sequentially in "a loop," rather than in parallel using a real-time kernel. A real-time kernel was not utilized for this task since there was no true parallel processing required. The only exceptions were several Interrupt Service Routines (ISRs) that processed external hardware events that could not wait for the normal processing loop. More detailed information on the software implementation can be found in the *OPM Software Reference Manual, AZ Technology Report No. 91-1-118-167.*

2.5.1.1.2 Functions

The flight software performed the following functions: AO Monitor, Calorimeters,

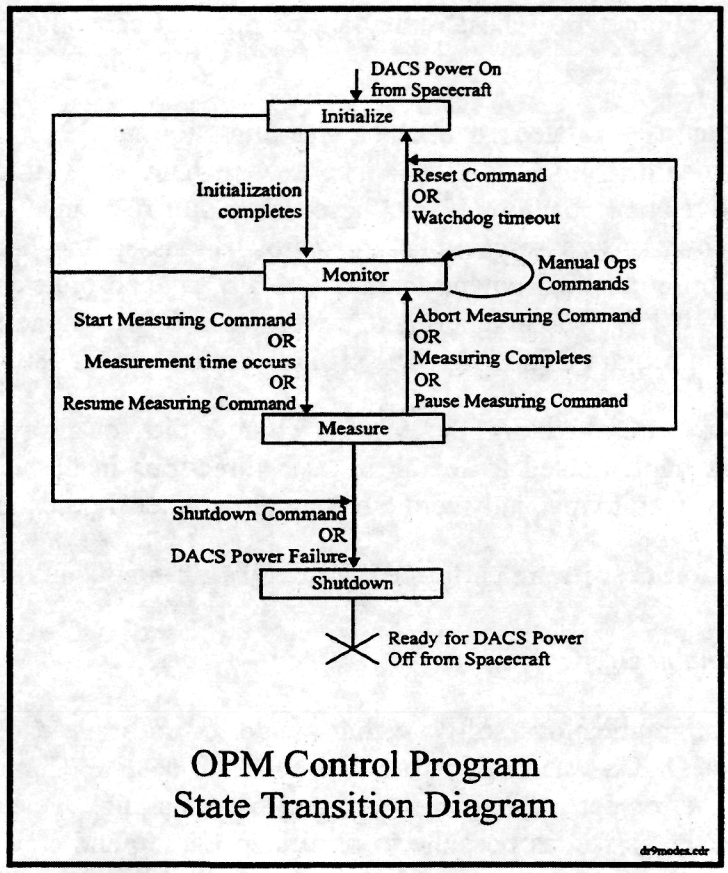
Carousel, Communications, Heater control, Measurement Sequence Control, Monitoring, System Initialization and Housekeeping, System Shutdown/Deactivation, Radiometer, Reflectometer, Data Collection and Storage, Temperature, TIS, TQCM and VUV. The instrument and monitor functions are described in their respective sections. Each remaining function is described below.

2.5.1.1.2.1 Calorimeters

There were twenty calorimeters, one per Reflectometer sample. These were measured weekly for several hours as a part of the measurement run. They were read for a timeline-specified time interval ("soak time") with the carousel in the exposed/orbital position, and then in the covered/launch position to measure the rate at which heat was emitted by the samples.

The calorimeter software performed nominally during the mission. To save storage space, the calorimeter readings were stored as 2 byte integers. In the future, they should be recorded as 4 byte floats to give better thermal resolution to the temperature measurements.

Figure 2-17. OPM Control Program State Transition Diagram.



2.5.1.1.2.2 Carousel

The carousel contained the samples exposed to the space environment, and rotated them under the OPM instruments for weekly measurements. Half the carousel contained samples; the other half was blank. The software rotated the carousel so that the samples were exposed to the space environment most of the time. This was called the *orbital position.* Prior to launch, the samples were rotated by manual software command so that they were inside the OPM to provide increased protection during launch and deployment EVA. This was called the *launch position.*

The carousel was not rotated upon power-up. The only time the software automatically rotated the carousel was during a measurement run. At the conclusion of a run, the carousel was rotated to the orbital position. As a part of the crew-initiated end of mission deactivation procedure, the carousel was rotated to the launch position.

Because the carousel was a critical component of the experiment, it contained several redundant subsystems: motor, motor output encoders, motor step encoders, and position potentiometers. While the encoders and motors were redundant, switching between primary and secondary subcomponents was enabled manually by IVA crew command. If potentiometers read out of range, the software would have automatically switched to the redundant potentiometers. These redundant component capabilities were not utilized during the mission.

The carousel rotated in a clockwise direction to +330° and decremented in the counterclockwise direction to –205°. There were hard stops at these positions. Encoder counters gave relative position (17-bit) based on motor movement since the counter was last reset. The counter was reset when the carousel passed the home or launch (0-degree) position. Carousel position potentiometers (14-bit) gave absolute carousel position. Position was linear: +/- 0.3%. The potentiometers were used to determine the direction to home the carousel and for rough positioning. The orbital position was at 180 degrees.

During carousel testing, the encoder counter did not always reset when homed. An algorithm was implemented to search in both directions in the vicinity of home using the potentiometers, then to manually zero the encoder counter if necessary.

The carousel software performed nominally during the mission.

2.5.1.1.2.3 Communications

The communications software that supported message exchange between the MIPS Laptop and the DACS was a key part of the software design. Communications must be very reliable, using error detection, correction, and handshaking. Telemetry data transfer to the Laptop should be as fast as possible to minimize Laptop and crew time. The implemented protocol had three layers: physical, file transfer, and application.

The physical layer included two RS-422 connections on the DACS end and RS-232 on the host end. Handshaking was done in software to prevent the sender from transmitting data more quickly than the receiver can process the data. The Universal Asynchronous Receiver/Transmitter (UART) for the RS-422 interface on the DACS was the 82510, downward compatible with the 8250. The OPM software used only the 8250 features. 9600 baud and higher rates were supported by the UART. For flight, 9600 baud was used to minimize potential transmission error rates. The time to transfer 300 Kbytes at 9600 baud was 6 minutes, assuming a worst case high noise rate with an effective throughput of 4800 baud. For testing, 34 Kbaud was used to speed download of test software from the PC to the DACS. This higher rate worked reliably in the lab.

The next layer used a common file transfer protocol, XMODEM with 16-bit cyclic redundancy check. The reliability rate is advertised as 99.997%. This protocol was selected

because it supported sending large "files", like the 300 Kbyte weekly telemetry data, as well as for sending 10-20 byte commands. Data were transferred in 128 byte packets. Unused bytes were padded with zeros. Software handshaking was used by this layer to control the rate of packet transfer. Packets were sent one at a time and numbered. Each packet had to be acknowledged before the next packet was sent. A fixed number of retries would be attempted (either no response from receiver or NAK from receiver) before the sender reported failure. The sender polled the receiver to start an exchange, asking to send the first packet. This was an additional initial step to the normal XMODEM protocol; it sped up the OPM DACS receiver routine. There should have been an 'S' in the receive buffer when the polling routine was called if the Laptop was ready to send.

The communications software kept control of the DACS processor when it was called until the file transfer was complete or canceled. For short files of one packet (e.g., commands), the exchange took less than 0.5 seconds. For long telemetry files of 300 Kbytes, the exchange took 6 minutes or more. During this time, only ISR processing occurred in addition to the file exchange. Thus, any DACS health & status processing (e.g., heater control) that could not wait 5-10 minutes was done in an ISR.

The application layer was unique to OPM. It defined a set of commands that could be sent from the host to the DACS, and a set of responses that could be sent from the DACS to the host. The DACS spoke only when spoken to, and then only if a status/telemetry request command was received:

Host		**DCAS**
Command file, no status request commands	--	Process commands (no response)
	--	
	-⟩	
Command file, status request commands	--	Process commands
	--	
	-⟩	
Process status/telemetry files	⟨-	Send requested status/telemetry
	--	
	--	

Each command had the format <cmd ID> {<parm>*} CR/LF. Commands were in ASCII. OPM commands were built and validated by the host application (e.g., MANUAL). When entering commands interactively via MANUAL, there was only one command per command file. Since commands were ASCII strings, one per line, batch files of commands could be entered with an editor, stored on the host disk drive, then transferred to the DACS.

Most commands did not initiate responses from the DACS. Only two commands, the status and telemetry request commands, resulted in binary "response files" being sent to the host using XMODEM. An invalid command would cause an error to be logged in the DACS,

but would not cause a response to be sent to the host. The host may request status or telemetry to track the results of command execution. The purpose of this was to simplify the MIPS-DACS interface. Typically, a crewmember issued a command such as START TIMELINE via the MANUAL program, unplugged the MIPS Laptop, and moved on to other tasks. The command completed several hours later, when there was no guarantee the Laptop was still attached to display command results automatically sent back to the Laptop.

To support flexible operations, the DACS software utilized a Parameter Table. The table contained fifty parameters most likely to require modification during pre-flight testing and during the mission. The DACS stored an array of these updateable parameters in high EEPROM. Each parameter was a 16-bit signed integer. The OPM Parameter Table could be modified interactively via the OPM MANUAL program. These parameters could be changed from the host using the "Set Parameter" command. The array of parameters could be displayed on the host for review using the "Get Parameter Status" command.

The "user module" for a parameter was required to read the EEPROM parameter table whenever its Initialize (Init) routine was called. For most modules, this occurred on power up only. Thus, the DACS had to be rebooted for these parameters to take effect. For measurement timeline related modules, this occurred at the beginning of a timeline execution. The Parameter Table was also used to store data, such as the MET, that had to persist across reboots.

Two redundant data cables connected the MIPS Laptop to OPM. An RS-422-to-232 converter was embedded in each IVA cable, which remained permanently connected to OPM through the Docking Module power panel bulkhead feed through connector. There was concern that connecting the MIPS Laptop to the Docking Module power connector while a measurement timeline was running would draw too much power and trip a Mir circuit breaker. So a light-emitting diode (LED) was inserted in the RS-422-to-232 converter that indicated the current status of the DACS. If the LED was:

- Always OFF: DACS was not operating - either no DACS power or DACS failure
- Always ON: DACS had power and was in monitoring mode
- One second blink: DACS was in measurement mode

The communications software performed nominally during the mission. During OPM restart after a shutdown period on Mir, a crewmember unintentionally queued START TIMELINE commands back-to-back, causing two timelines to run consecutively. Depending upon the user interface system for reflight, there should be a longer delay and a prominent message indicating the acceptance of each command after it is entered to prevent duplication of commands.

2.5.1.1.2.4 Heater Control

There were four heaters in the OPM instrument that operated in pairs. They were

located on the emissivity plate where the Reflectometer and TIS instruments were mounted. One pair of heaters was located below the TIS instrument; another, below the Reflectometer. Once-per-minute measurements on two emissivity plate thermistors determined when heaters were turned on or off.

The heater software performed nominally during the mission. The initial design called for a measurement run to be delayed until the OPM internal temperature reached a certain setpoint. But, there was concern about sensor failure that might cause no timeline to be made, so the final implementation did not test OPM internal temperature before starting a timeline. During the mission, several measurement timelines were started with below 0°C temperatures. However, no systems displayed any adverse effects.

2.5.1.1.2.5 Measurement Sequence Control

There were three basic approaches considered to define measurement timelines: "hardwired/coded," "table-driven," and "scripted." "Hardwired/coded" timelines require detailed reprogramming for changes and were too rigid. "Scripted" timelines were most flexible, but perhaps overkill for OPM. "Table-driven" timelines provided some flexibility without too much complexity, and were used in the OPM design.

The OPM CP had only one timeline table. A start time and frequency was stored in the OPM Parameter Table to predefine when measurement sequences started. By default, the first measurement run occurred one hour (elapsed time) after power on following OPM EVA deployment. Runs were repeated approximately every week (168 hours of DACS elapsed time). "OPM time" was measured by elapsed DACS operations time since OPM did not have a real-time clock or access to the carrier real-time clock. DACS elapsed time was maintained in the EEPROM Parameter Table. Mir power to OPM was intermittent for a few months, so little DACS time elapsed in this period. At the request of the OPM Team, the IVA crew interactively started some measurement runs in this period using the OPM MANUAL program.

As designed, an OPM measurement sequence took approximately 13 hours. Initial measurement runs during the mission typically took between 13 and 13.5 hours. Time varied due to use of "autogain" when reading instrument detectors; for example, if a Reflectometer detector read below a certain voltage, the software tried again after doubling the gain control on the channel. Other factors, such as difficulty striking a lamp, increased run duration. The longest runs took 19 hours. The nominal and extended measurement timeline times by measurement subsystem are presented in Table 2.1:

Relays were enabled and disabled prior to the initiation of each measurement system to minimize power consumption. After each systems execution, data were transferred from static memory to Primary and Backup EEPROM memory for safekeeping and storage.

Table 2-1. Normal and Extended Measurement Timeline Durations.

Measurement	Nominal Time (Hrs)	Extended Time (Hrs)
TIS	1.0	1.0
VUV	4.5	10.5
Reflectometer	3.5	3.5
Calorimeters	4.0	4.0
TOTAL	13.0	19.0

A measurement timeline included the following steps:

TIS

- Strike TIS red and green LASERs, let warm-up for 30 minutes.
- Carousel could be anywhere if power failed during the previous timeline, but was most likely in the orbital/180° position. Power on the carousel. Move carousel to the emissivity/launch position, which reset the encoder counters.
- Move the carousel to the TIS calibration sample, clockwise (CW) from 0° to 164°.
- Read the TIS calibration sample at seven sample "spots," rotating in the counter-clockwise (CCW) direction. Further, 30 additional readings were taken from the second specular spot.
- Read TIS samples 1.20, 3 sample spots per sample. Read CCW.
- Final TIS position is at -28.25° (traveled -192.75° CCW for TIS).
- Power off the TIS LASERs.
- Power off the internal system heaters and TQCM.

VUV

- Power on the VUV D2 lamp, motors, etc. Strike lamp and wait 20 minutes for lamp warm up. In case of lamp strike failure, repeat strike process after 5 minutes delay. Attempt 10 strike attempt cycles.
- Move 46.25° CW to VUV Cal hole 0 at 18° position. Move arm to down/reflectance position, take readings, move arm to up/transmission position, and take readings.
- Read VUV samples 1.40, read CCW to -162° position. Arm stays in up/transmission position, for sample readings. Arm is moved up and down for calibration holes at 5, 10,15,
- Power off VUV.

REFLECTOMETER

- Power on the Reflectometer D2 lamp/motors/TE cooler. Wait 10 minutes for warm up.
- Move 63° to the -99° position.
- Read Reflectometer samples CW to 72° position.
- Power off Reflectometer.

CALORIMETER

- Move 108° to orbital position, +180° position.
- Wait 2 hours for calorimeter temperatures to stabilize.
- Read calorimeter PRTs, radiometers, and a subset of the thermistors once per minute for 90 minutes.
- Move the carousel -180° to the emissivity/launch position and read calorimeter PRTs and emissivity plate thermistors once per minute for 30 minutes.
- Move 180° to orbital position, +180° position to expose the samples until next measurement run.
- Power off carousel motor.
- Power on the internal system heaters and TQCMs.

The measurement control software performed nominally during the mission. The original design called for multiple timeline tables that could be selected at run-time by the operator, as well as downloaded from the MIPS Laptop. The multiple table and download features were never implemented due to time constraints and concern for IVA crew operation. Implementation of the multiple table and download features should be considered for reflight where ground control is permitted. This would allow more flexibility during testing and mission operations. Also, the use of a battery back-up real-time clock would permit data to be time-tagged to important experiment of payload carrier events.

2.5.1.1.2.6 Monitoring

Monitoring referred to all data collection performed when a measurement run was not executing. Nominally this was 155 hours per week (168 hours in a week minus 13 hours for timeline). The monitoring sequence included:

- Read TQCM data (1 per minute)
- Read AO data (1 per minute)
- Read radiometer data (1 per minute)
- Read system voltage data (1 per 2 hours for 22 hours per day, 1 per 2 minutes, 2 hours per day)
- Read temperature data (1 per 2 hours for 22 hours per day, 1 per 2 minutes, 2 hours per day)

The monitoring software performed nominally during the mission.

2.5.1.1.2.7 System Initialization and Housekeeping

The OPM components were initialized upon power being applied to the DACS. ISRs were initiated to handle periodic functions such as watchdog timer refresh. Relays were enabled to power housekeeping components.

Memory "scrubbing" was performed periodically to correct and detect any memory upsets that may have occurred in temporary memory. Error Detection and Correction (EDAC) scrubbing was performed on the SRAM, as well as the Mother board program EEPROM. This scrubbing occurred upon initialization and every two hours during monitoring mode. Scrubbing occurred between system executions during the measurement run, so scrubbing may have occurred only every four hours or so during a measurement timeline. The Primary and Backup Memory did not contain EDAC circuitry in order to reduce the Daughter board size/cost. Only science data was stored on the Daughter board, and a few "hits" were not considered significant because of the quantity of data stored. In effect, a few "bad" points could be discarded and recovered during data reduction/analyses.

The DACS contained a watchdog timer which was reset periodically by the software to prevent the DACS from rebooting. Initial reset after power-on occurred within 1.6 seconds, then within every 100 milliseconds thereafter. This allowed automatic recovery from a "hang" condition, such as a hardware failure or software infinite loop. An interrupt routine was used to refresh the watchdog timer. This alone was not adequate to prevent infinite loops in the main program from hanging the system, so the main program tasks reset the interrupt routine periodically. If the interrupt routine ran without being reset for more than 30 minutes, it allowed the watchdog timer to expire and caused a DACS reboot. No DACS reboots occurred during the mission.

Heaters were controlled via interrupt routines to insure timely control.

Upon completion of initialization, the DACS main program went into a software loop, waiting for an event (such as):

- a monitoring event time to occur (minute, hour, day, ...)
- the next scheduled measurement run time, stored in OPM Parameter Table (nominally 168 hours from start of last measurement run time), or
- a crew command on either serial port from the MIPS Laptop

Upon completion of the event, the main program returned to its software loop.

2.5.1.1.2.8 System Shutdown/Deactivation

The OPM system could be powered off at any time by the IVA crew. There was a special function called Deactivation, which was executed by the crew running the MIPS Laptop OPMDEAC program at the conclusion of the mission and just prior to EVA retrieval

of OPM. The JSC/NASA Safety Panel had required the OPM to perform a self-test prior to the retrieval EVA to check for the potential of frangible material. This self-test looked at the status of the three instrument's optical components. The procedure was simple: demonstrate the optical systems were still functional, and the conclusion must be they are still intact. For this test, the OPM would have been powered on with the carousel most likely in the orbital position. The samples would have been exposed to the space environment. Therefore, to perform this procedure as quickly as possible, the samples were not to be rotated to the measurement position. At the conclusion of the optical systems tests, the carousel was commanded to go to "home" position, to protect the flight samples. The deactivation procedure included the following tests:

- Tungsten Lamp test: set Tungsten lamp at maximum intensity, warm up 5 secs, wavelength set at 2500, slit width set to 0.7, take reference reading for PbS. Reading less than 1V was failure.
- Ref D2 lamp test: turn D2 lamp on, warm up 5 minutes, wavelength set at 400, slit width set to 0.8, take reference reading for Si. Reading less than 1V was failure.
- VUV D2 lamp test: turn D2 lamp on, warm up 5 minutes, filter wheel to calibration hole, rotate carousel to cal hole 0 (+18 degree), take transmission reading. Reading less than 1V was failure.
- Carousel test: carousel home routine reports other than success (1) was failure.

The OPMDEAC program was not performed by the IVA crew prior to EVA retrieval. Mir was having control system problems at this time, and OPM was often without power. The crew reported the OPM LED's were blinking (indicating the OPM was in Measurement Mode) when the procedure was to be performed, and could not communicate with the OPM via the MIPS Laptop. Power was removed and OPM retrieved without incident.

2.5.1.1.2.9 Data Collection and Storage

A permanent MM data storage capability was required to hold data between weekly downloads of OPM data to the MIPS system. The storage provided protection against data loss in case of power failure or permanent loss of communications with the MIPS system. OPM was designed to store health and science data internally for a maximum 80-week mission.

The standard SC-4A design used a MM with a battery pack the size of the DACS and 3 month lifespan, which was unsuitable for OPM. Options included:

1. Populate only one-fourth of MM with 6 Mbytes of Dynamic Random-Access Memory (DRAM). The NiCad battery pack should last proportionally longer (up to 1 year instead of 3 months). The 4 Mbit DRAM chips need 12 mA, 5 V constant supply. But the NiCad battery pack was as large as SC-4A. The Lithium battery was smaller and lighter but harder to get approved by NASA due to explosion hazard.
2. Use 6 Mbytes SRAM on Daughter board or modified Mother board. One Mbit

SRAM chips available. Much smaller battery required.

3. Use 6 Mbytes EEPROM on Daughter board. One Mbit EEPROM chips available. No battery required.

The third option was chosen to save space and insure the data in MM would be viable for more than one year. Due to Daughter board space constraints, error detection and correction circuitry was omitted. Only data, not code, was stored on the Daughter board, and a few memory upsets were not considered significant. The memory was divided into two sections:

Primary Memory - a cache held up to three weeks of detailed data (approximately 1-MB space available) between downloads of OPM data to the MIPS system. The crew was to perform downloads at least every week, but two weeks were added for crew contingency. The primary memory was treated as a circular queue. After three weeks of caching without crew downloads, the queue wrapped around and start overwriting the oldest data.

Backup Memory - storage of the essential data (approximately 5 MB space available) for the entire mission, up to 77 weeks. Not all detail data were stored, in order to save space. For example, monitor data were recorded for 2 hours per day, rather than the primary memory rate of 24 hours per day. The backup memory was treated like a "tape drive." Data were written sequentially from low to high memory as records of various types: TIS, standard monitor data, etc. The records were created in OPM Random-Access Memory (RAM), then transferred to MM after they had been "filled" with data. Records were written approximately every two hours, so, at most two hours of data were lost when a power failure occurred. The MM layout is depicted in Figure 2-18.

The OPM MIPS software included crew commands to download the primary and backup memories to the MIPS laptop. All data, or just new data, could be selected for downloading. Normal procedure during the mission was for the crew to download new, primary data. On one occasion the crew went over three weeks between downloads, resulting in perhaps a day of monitor data not being recorded.

The data collection and storage software performed nominally during the mission. Approximately 25 weeks of data was collected over the 8 month period OPM was mounted outside Mir, utilizing one-third or 1.7 MB of backup memory. After the mission, at the SpaceHab Payload Processing Facility, the MM data download was attempted to archive the data and to see status of the memory (in terms of single event upsets, etc.). During this OPM functional post-test, the OPMMAN GSE "Download All Backup Data to PC" function failed to complete at approximately 60% through the download. The problem reoccurred at the same MM location during the functional post-ship test at AZ Technology. Download was successfully completed later using a copy of the OPM CP downloaded into OPM RAM from the OPM GSE computer. This discrepancy was caused by operator error in attempting to download the data. The download was redundant, since all data were successfully retrieved from Primary Memory during the mission.

2.5.1.1.2.10 Temperature

Temperature data was taken from 31 thermistors placed throughout OPM. Temperature data was stored in raw 16-bit format. The OPM GSE reduction software reported temperatures in degrees C.

The temperature monitoring software performed nominally during the mission.

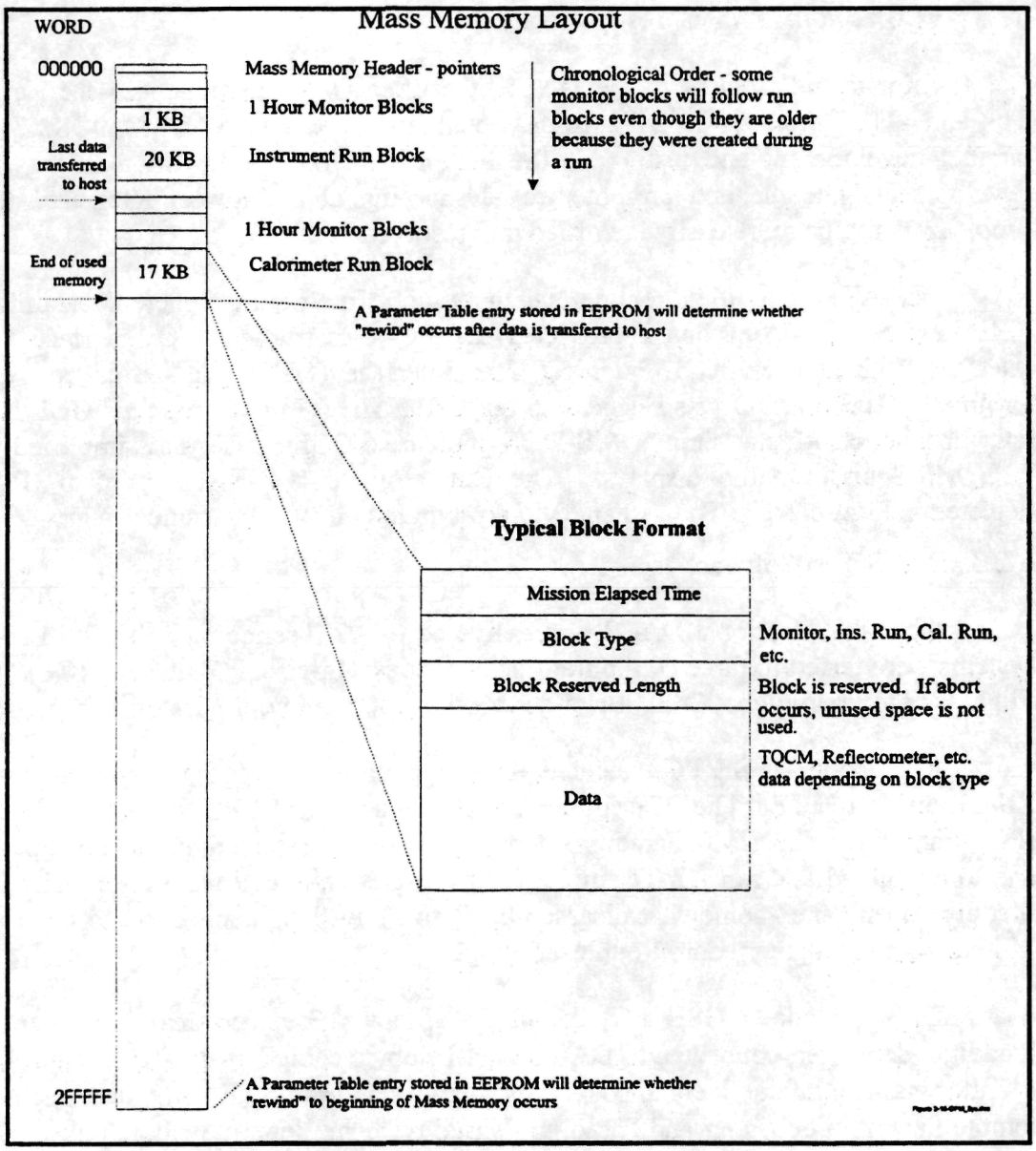


Figure 2.18. Mass Memory Layout

2.5.1.2 Ground Software

2.5.1.2.1 Overview

The OPM ground software includes PC-based Instrument Test Software, DACS Test Software, OPM Electrical Simulation Unit (ESU) software, and Data Reduction Software.

2.5.1.2.2 PC-Based Instrument Test Software

Prior to the delivery of the DACS, the three OPM instruments - the Reflectometer, TIS, and VUV - were tested utilizing IBM-compatible PC's running MS-DOS. This allowed parallel development and testing of the instrument and the DACS to mitigate the tight development schedule and promote troubleshooting at the lowest integrated level where problems could be more easily identified and resolved.

The AZ Technology commercial instrument Integrating Sphere Transmitometer and Reflectometer (ISTAR) board provided the PC-to-instrument I/O interface. The user interface utilized a Borland Graphical-User Interface (GUI) package called TurboVision. Originally, TurboVision was selected as the OPM MIPS Flight Programs GUI, but this was later abandoned for the simpler MS-DOS standard I/O interface that simplified integration with MIPS and Cyrillic displays. The Reflectometer PC-based program (REFCTL) is depicted in Figure 2-19. The TIS and VUV programs utilized the same design.

2.5.1.2.3 DACS Test Software

Once the functional DACS was delivered to AZ Technology, the OPM software and systems were tested in three configurations or modes: In-circuit Emulator (ICE), Debug, and Flight, as shown in Figure 2-20. Brief descriptions of these configurations are presented.

ICE Mode - GSE PC executed AMC/Paradigm debugger, connected to DACS via RS-232 cable to ICE. The ICE connected to Mother board CPU socket by Pin Grid Array (PGA) adapter. The AMC/Paradigm debugger was run interactively to poke/peek memory and to download and ran AZ Technology diagnostics and subsystem tests. The DACS was literally "open" (i.e., somewhat disassembled) to allow ICE connection to CPU socket and Mother board/Daughter board troubleshooting.

Debug Mode - GSE PC executed Windows 3.1 Terminal Emulator or remote Paradigm debugger, connected to DACS via "Telebyte cable" or RS-422 (Laptop). The SC4 Monitor was run interactively to poke/peek memory and ran SwRI-provided diagnostics. The remote Paradigm debugger and Paradigm kernel were run interactively to poke/peek memory and to download and run AZ Technology diagnostics and subsystem tests. For this mode, the DACS was "closed" (assembled).

Flight Mode - GSE PC ran OPM MIPS programs, connected to DACS via "Telebyte

cable." XMODEM 1024CRC protocol was utilized. OPM CP (full flight version) or CPSHORT (modified version for test, shorter timeline) was run. For this mode, the DACS was "closed".

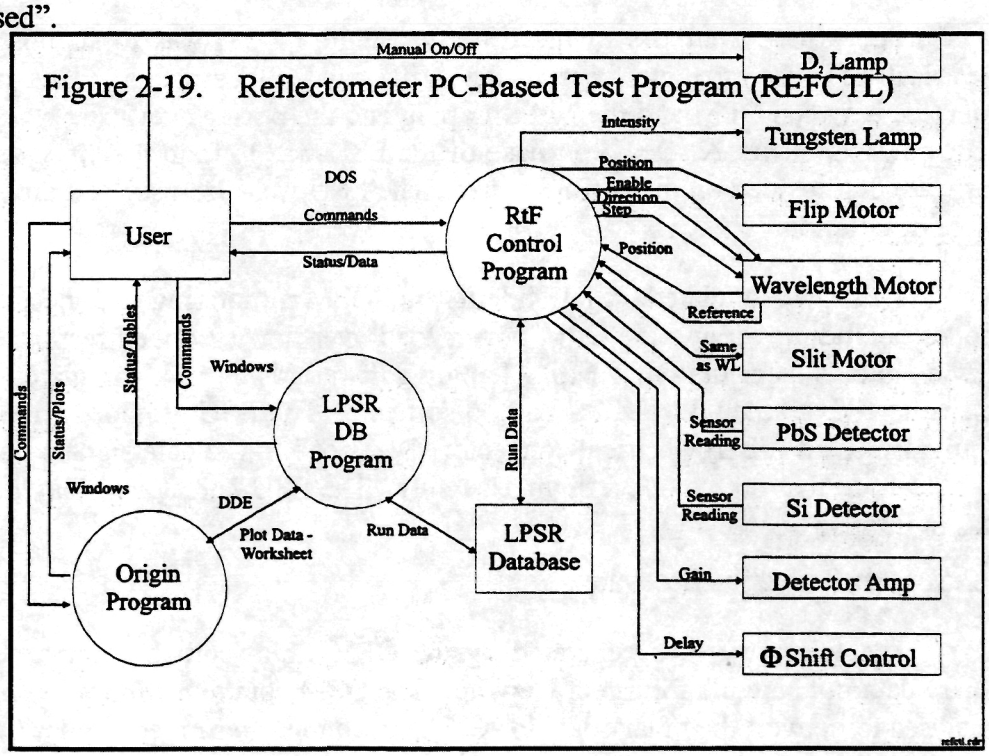


Figure 2-19. Reflectometer PC-Based Test Program (REFCTL)

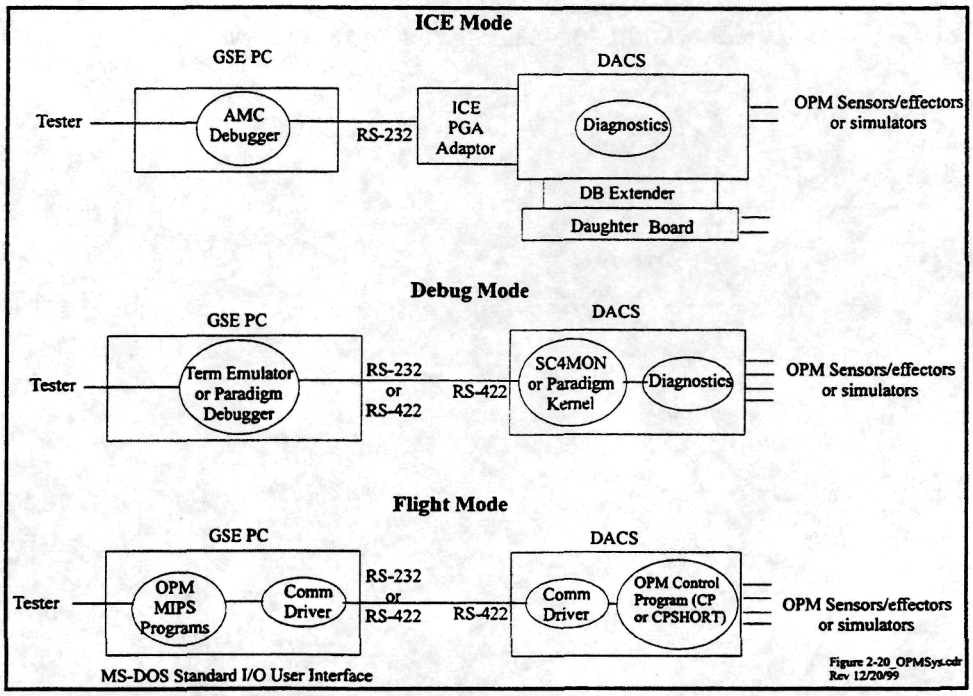


Figure 2-20. OPM/DACS Test Configurations

2.5.1.2.4 OPM Electrical Simulation Unit

The primary purpose of the ESU (see Figure 2-21) was to support testing of OPM electrical and software interfaces to the MIR and MIPS systems. This included the data interface between OPM and the MIPS Laptop and the power interface between OPM and the MIR power system. A second purpose of the ESU was to train the crew in use of the OPM software that resided on the MIPS Laptop. The ESU was also used to train the crew in OPM cable installation.

The ESU simulated, at low fidelity, the OPM monitoring and measurement sequence modes, including varying the OPM power load over time. Canned responses were provided for commands from the OPM MIPS Laptop software. The ESU simulated the download of telemetry files to the OPM MIPS Laptop software. The ESU provided an OPM Functionally Equivalent Unit (FEU) electrical connector (2 sets of RS-422 data signals plus power signals) equivalent to that on the OPM flight assembly. The ESU operator display/keyboard interface was in English.

2.5.1.2.5 Data Reduction Software

The telemetry files generated by the OPM flight software contained tightly-packed binary data not suitable for direct viewing. The OPM data reduction program (REDUCETV) was used to convert the binary data to ASCII or Comma-Separated Value (CSV) format. The

processed files could then be viewed directly with text editors or Excel. The entire telemetry file could be reduced or subsets could be chosen based on selected OPM subsystems or DACS elapsed timestamps. The user interface is shown in Figure 2-22.

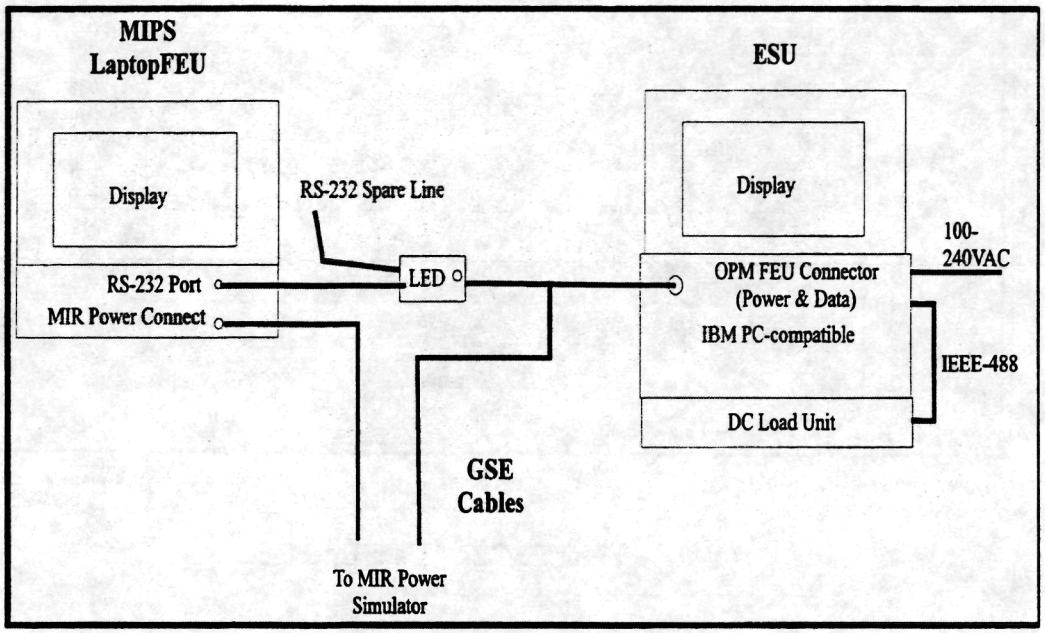


Figure 2-21. ESU Configuration

2.5.1.3 MIPS Software

2.5.1.3.1 Overview

The initial checkout and the weekly data collection required by the OPM were conducted by the Mir crew using the JSC-developed MIPS system. The MIPS system was already in use on Mir for U.S. payload experiment control and data acquisition. Data were transferred to the MIPS optical disk and to the ground by means of the Mir telemetry system (Figure 2-23).

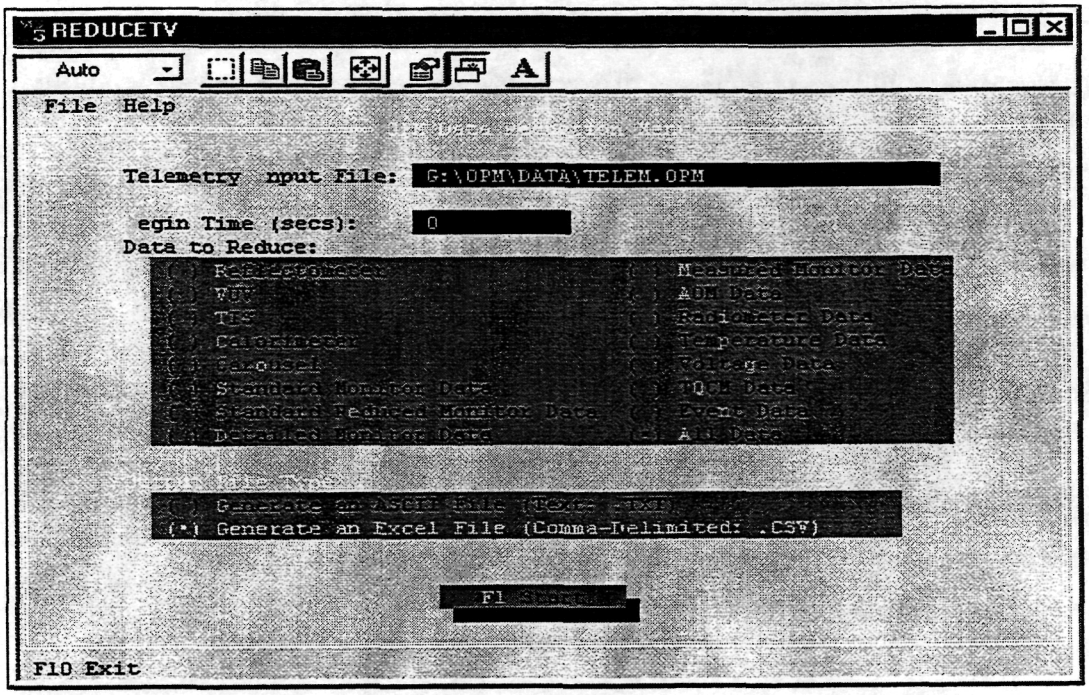


Figure 2-22. User Interface

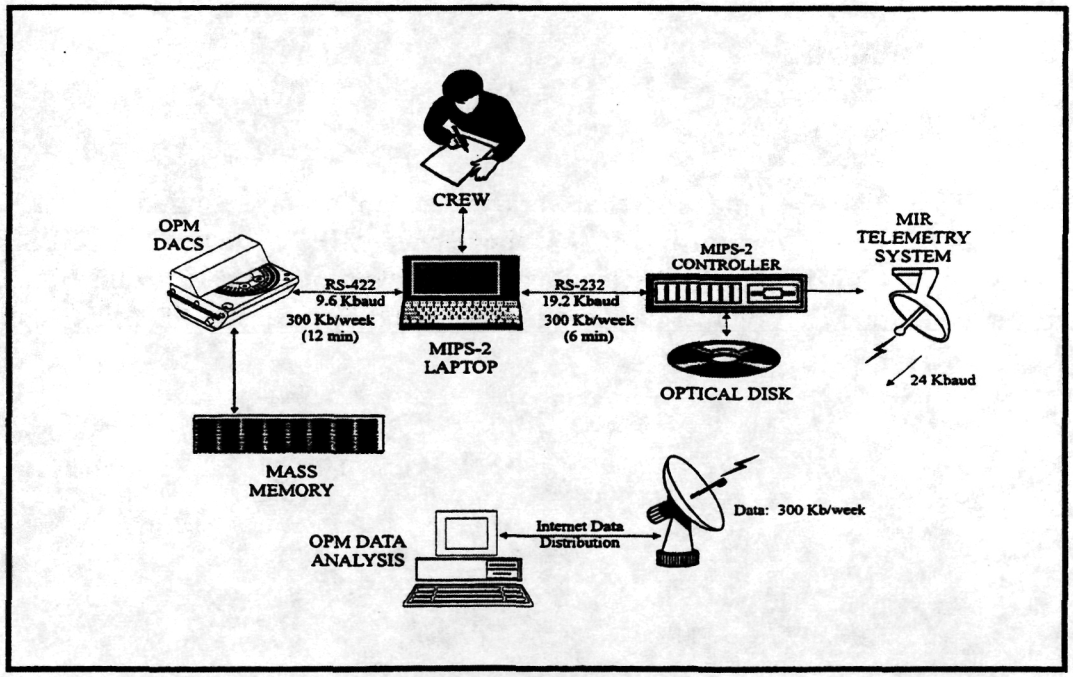


Figure 2-23. OPM-MIPS-Mir Data Transfer

Typical weekly payload operations were as follows. The crew carried a MIPS Laptop (IBM ThinkPad computer) to the OPM experiment cables located in the Docking Module, connected the Laptop by serial port to the experiment computer, then used it to operate the payload using experimenter-provided software. The OPM DACS had two RS-422 serial interfaces (refer to Figure 2-5). Both interfaces were wired in the OPM cable and passed to the MIPS Laptop computer inside the Docking Module. Only one serial port was required, but a redundant cable was implemented to increase reliability.

Acquired data was temporarily stored on the MIPS laptop. The laptop was then carried to the MIPS system controller where the data were transferred via serial port to the MIPS controller. The MIPS controller then interfaced to the Mir downlink telemetry system to schedule payload data for downlink to a Mir ground station.

The data files were transmitted to the ground embedded in the downlink video during 10-minute orbital passes over Moscow-area ground stations. The data files were then e-mailed to the experimenter in the next few days via JSC. Since the data were part of a video stream, no error checking was provided. It was up to the experimenter to verify the data and request retransmit of corrupted data. Whenever Mir lost contact with ground stations, the last file being downlinked was susceptible to truncation. Therefore, the MIPS staff recommended the OPM telemetry data be subdivided into multiple smaller files to reduce the potential for "lost" data. A file size of 25 Kbytes was used, requiring approximately 12 files for a typical weekly data set.

There were two options considered for connecting the RS-422 interface from the DACS to the MIPS Laptop:

1. PCMCIA ("PC") RS-422 card inserted in MIPS Laptop. Data cable from DACS connected to PC card in Laptop.
2. RS-422-to-RS-232 converter built into the data cable from DACS to Laptop. Data cable from DACS connected to standard RS-232 port in Laptop. Converter drew power from DACS transmit data or Request to Send (RTS) line.

The second option were chosen because it had no impact on the MIPS Laptop (see Figure 2-23) that would require requalification. A commercial RS422 to RS232 converter was procured with a stainless steel housing for use on Mir. The converter was qualified for flight using a vendor supplied schematic and after passing the OPM System Environmental testing.

The purpose of the MIPS displays was to adjust the operation of the OPM flight program during final verification testing and during the mission. Crew procedures in English and Russian gave detailed instructions to the crew on OPM operation. OPM was designed to be able to operate autonomously without the MIPS laptop. In case of a MIPS communication failure, OPM would run its predefined timelines and store data for up to 80 weeks.

The Mir Crew Timelines scheduled roughly one hour for the nominal weekly OPM Data Collection procedure. The procedure included the Laptop setup and tear down, the data collection (data transfer) from the OPM to the Laptop, and the time to transfer data from the Laptop to the MIPS controller. For nominal operations, one hour was sufficient. The MIPS OPM software was loaded and on the MIPS laptop hard disk and ferried to Mir each Shuttle mission. Several copies were taken as SEV/DEV were occurring often.

2.5.1.3.2 Functions

A GUI user interface was initially desired for the OPM MIPS laptop software. Since the MIPS laptop operating system was PC-DOS, a Borland TurboVision GUI package was selected for the OPM user interface. The Borland interface was used for the stand-alone instrument tests. However, this interface was abandoned and a simpler DOS command line interface was used when it was learned that the PC-DOS interface was required for use by all MIPS laptop software. Three DOS programs were delivered to the MIPS project:

- OPMUP
- OPMMAN
- OPMDEACT

The OPMUP display was developed in both Cyrillic and English. Contingency displays were in English, with a Russian translation in the printed crew procedures.

2.5.1.3.2.1 OPMUP - Upload Data to MIPS Laptop

OPMUP uploaded data in one large file to the MIPS Laptop. Upon completion, it divided the large file into small files to improve chances of success of download via Mir telemetry system, which could lose individual files as ground stations went out of range of Mir orbit.

2.5.1.3.2.2 OPMMAN - Manually Operate OPM

The top-level OPMMAN menus are shown in Table 2-2. OPMMAN was provided to the Mir crew for contingencies. Each subsystem had parameters that could be adjusted and commands that could be issued manually. The detailed screens of OPMMAN can be found in the Mir Crew Procedures, available upon request from AZ Technology.

OPMMAN was used on a few occasions by the crew; i.e., after the long power outage to initiate timelines and collect primary data a second time.

Table 2-2. Crew Manual Control Program Menus

OPM Crew Manual Control Program, Version 1.1 Copyright (c) 1996
AZ Technology, Inc. Parameter modifications update EEPROM. The DACS must be rebooted for EEPROM parameter modifications to take effect. Press ESC to abort input.

OPM Main Menu F1 Get OPM Status F2 Telemetry Menu... F3 Timeline Menu... F4 Carousel Menu... F5 DACS/PSC Menu... F6 Reflectometer Menu... F7 TIS Menu... F8 VUV Menu... F9 Monitors Menu... F10 Exit Enter Choice:

2.5.1.3.2.3 OPMDEACT - Test OPM Status Prior to Deactivation

The OPMDEACT program was added upon request of the JSC Safety Panel to provide the crew information about OPM components prior to EVA retrieval at end of mission.

The procedure did not really shut down OPM. OPM stayed in monitoring mode, with heaters operational. The time the crew waited for the success/fail message from OPM was approximately 30 minutes. The status returned by OPM indicated if any components had failed, possibly indicating a safety concern, such as broken glass. The carousel was rotated to the launch position.

2.5.2 Software Test and Verification

Both the OPM flight software and the OPM MIPS software were subjected to rigid test and verification procedures.

2.5.2.1 Flight Software

2.5.2.1.1 Thermal Vacuum Testing

Flight software formal testing and configuration management began at the OPM System Environmental tests when operational tests of the OPM were required. Two versions of the program were created: Control Program (CP), and Control Program Short (CPSHORT). They were loaded via desktop PC and Paradigm debugger. CP was run at the minimum and maximum operational environmental temperatures (tests 3.7 through 3.14) of the OPM Thermal Vacuum Test Procedure.

CPSHORT, which executed for approximately one hour, was run at ambient environmental temperatures (tests 3.2, 3.3, 3.6, and 3.16). In addition, CPSHORT was run at the minimum non-operational temperature (test 3.4) for 10 minutes to insure the heaters began warming OPM at the minimum temperature.

CP Details

- Ran full instrument timeline plus monitors
- Brief calorimeter soak/read
- Relevant data was displayed on laptop as it was collected, as well as stored in MM
- Monitors displayed power/heater/thermistor data as it was collected. The "detail monitor data", that was normally collected on 2 minute intervals one 2 hour block per day, was displayed so that heater operation on power up and during monitoring mode could be verified during first 10 minutes. Thermistor data was displayed in degrees C. The instrument timeline started 10 minutes after power on.

CPSHORT Details

- Ran only 2-3 samples for each instrument plus monitors
- Prompted user on startup for vacuum info: TQCMs could not be driven to –30°C in air
- Identical to CP in all other functions

During thermal vacuum, it was determined that there was a large amount of noise in the Reflectometer PbS sensor at vacuum. Therefore, the number of readings taken per sample position were increased to integrate out this noise.

2.5.2.1.2 Post-Flight Configuration and Operation

The OPM raw data files have been stored on Compact Disk (CD). The raw data subdirectories and data files are currently stored on the AZ Technology file server. The files in each subdirectory have been put into a Zip file to further conserve space. A .TXT file is also in each subdirectory with the file directory for each Zip file.

Several formal tests have been run to troubleshoot anomalies and determine post-flight status since return of OPM to AZ Technology in March, 1998. The AZ Technology

post-ship test ran nominally, with one exception. The MET was inadvertently zeroed after the KSC post-test, but prior to the AZ Technology post-ship test. Other OPM Parameter Table entries remained unchanged (except pointers). The cause of this was operator error. Apart from the area of program EEPROM that was zeroed, the non-zeroed portion showed no changes due to radiation, etc. Also, the 6 MB MM file ran through the data reduction program without error, indicating that no header fields were changed.

2.5.2.2 MIPS Software

The OPM MIPS software was verified during the Russian OPM Acceptance Test at AZ Technology. A MIPS laptop FEU was brought to AZ Technology by MIPS personnel. The previously delivered OPM MIPS software had already been installed on the MIPS laptop by MIPS personnel. MIPS personnel had created an OPM Menu for use by the crew to initiate the three OPM programs: OPMUP, OPMMAN, or OPMDEACT. The three programs were executed and the results verified by MIPS personnel.

2.5.3 Mission Performance

2.5.3.1 Flight Software Anomalies

1. DACS elapsed time counter reset between the SPPF post-landing functional test and the AZ Technology post-landing functional test.
2. OPMMAN GSE "Download All Backup Data to PC" function failed to complete during ground processing at SPPF.
3. Two timelines were performed back-to-back. This occurred upon the OPM restart after being without power caused by the Progress collision into the Spektr Module. The crew was performing manual data operations during this time. It is possible for two "Start Timeline" commands to be queued in the DACS. For reflight, a "sanity check" should be performed on repeated commands.
4. On TIS, some of the gain factors were recorded incorrectly. One of the 1064nm specular readings from the calibration mirror was 3.798 V with a gain factor of 4. All other calibration mirror readings were about 3.8 V with a gain factor of 0. The gain factor of 4 was incorrect. For this same timeline, the specular gain factors on sample #3 were both significantly different than any before. Lastly, a gain factor of 5 was recorded on one reading. The software should limit the gain factor to 4, not 5.

2.5.3.2 MIPS Software Anomalies

The OPM MIPS software performed nominally with this one minor exception. A software change was made to improve the timestamping of the telemetry data. The change sent MIPS Laptop time to the DACS when an OPM data upload was requested. The change was only put in the OPMMAN program, not the OPMUP program, which reduced the number of MIPS Laptop timestamps inserted into the DACS status data. The MIPS Laptop

time was often incorrect, so this feature did not prove helpful.

2.6 Data Acquisition and Analysis

2.6.1 Overview

Section 2.6 contains general information on the types of data acquired by the DACS for all OPM systems during the mission and detailed information on DACS system health and status data, such as single-event upsets.

The OPM data collection timeline is depicted in Figure 2-24, based on a planned measurement timeline of 13 hours.

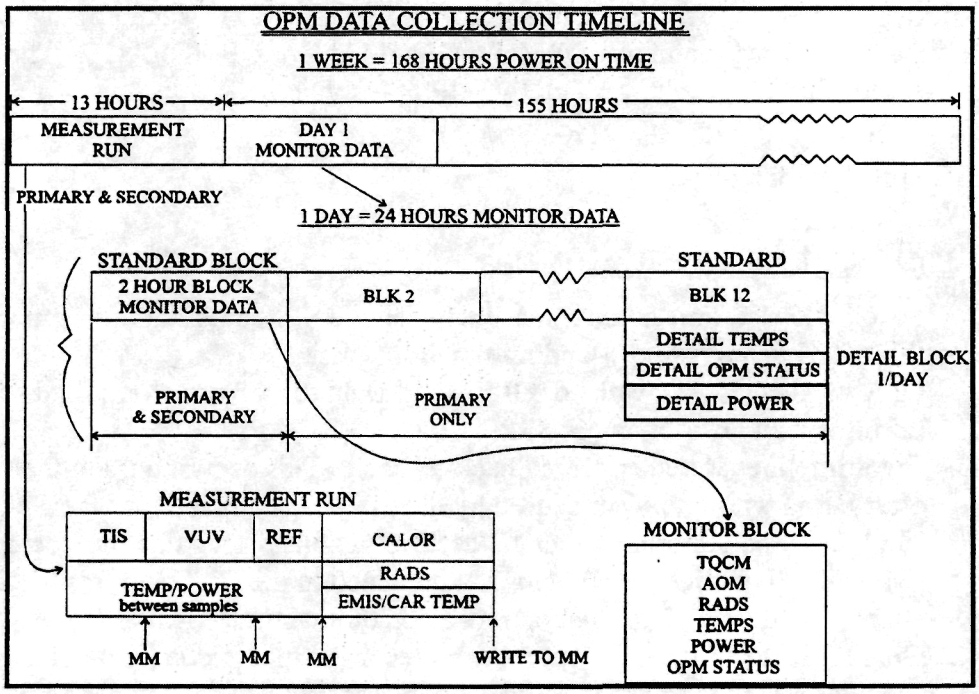


Figure 2-24. OPM Data Collection Timeline

Tables 2-3 and 2-4 show the types, sizes, and collection rates for the OPM telemetry data. The left half of Table 2-3 describes the "Backup Data" stored permanently in MM for retrieval after the mission, if necessary. These data were a subset of the "Primary Data", shown on the right side of Table 2-3. The Primary Data were collected continuously for up to three weeks in a temporary area of MM (see Table 2-4). The Mir crew downloaded the Primary Data to the MIPS laptop for transmission to the ground.

Table 2-3. Telemetry Data Types, Sizes, and Rates

Data Type	Backup Data (76 weeks of Backup Data) Bytes Per Block	Bytes Per Week	Mass Memory Log Rate	Primary Data (last 4 weeks of Telemetry Data) Bytes Per Block	Bytes Per Week	OPM MIPS-2 Log Rate
Measurement/Run Data (once a week)						
Reflectometer	18810	18,810	3.5 hours	18810	18,810	3.5 hours
TIS	1398	1,398	1 hour	1398	1,398	1 hour
VUV	2594	2,594	4.5 hour	2594	2,594	4.5 hour
Calorimeters	6728	6,728	1/min;2 hours; plus 2 hour soak	6728	6,728	1/min;2 hours; plus 2 hour soak
Temp/Power	5798	5,798	between samp VUV/TIS/REF	5798	5,798	between samp VUV/TIS/REF
Standard Monitor Data						
			2 hours per day:			24 hours per day:
Header	4	28	1 per 2 hours	4	308	1 per 2 hours
TQCM	960	6,720	1/min	960	73,920	1/min
AO Monitor	720	5,040	1/min	720	55,440	1/min
Radiometers	960	6,720	1/min	960	73,920	1/min
Power	176	1,232	1 per 15 min for 120 min	22	1,694	1 per 2 hours
Temperature	496	3,472	1 per 15 min for 120 min	62	4,774	1 per 2 hours
OPM Status	408	2,856	day summary	408	31,416	day summary
Detail Monitor Data						
						2 hours per day:
Header				4	28	1 per 2 hours
Power/heaters detail				1,500	10500	1 per 2min for 120 min
Temperature detail				3,720	26040	1 per 2min for 120 min
OPM Status detail				226	1582	day summary
Total/Week:		61,396	Bytes/week		314,950	Bytes/week
# of Weeks:		76			80	
Total/Mission:		4,666,096			25,196,000	Total Telemetry

Table 2-4. Mass Memory Usage

Mass Memory Totals - Bytes	
Backup Memory	4,666,096
Primary * 4 weeks	1,259,800
Total Memory Used	5,925,896
MM Size	6,000,000
MM Not Used	74,104

2.6.1.1 Single Event Upsets, Double Event Upsets

Memory "scrubbing" was performed periodically to correct and detect any memory upsets that may have occurred in memory. Error Detection and Correction (EDAC) scrubbing was performed on the SRAM, as well as the Mother board program EEPROM. This scrubbing occurred upon initialization and every two hours during monitoring mode. If a memory word was read by the software, the EDAC circuitry performed a checksum test to see if the contents of the word had changed since the last time it was written. A 1-bit change was corrected by the circuitry. A multiple-bit change could not be corrected. Both events caused interrupts which service routines recorded. However, the circuitry did not indicate the memory location of the upset. Table 2-5 shows the rate of memory upsets detected during the mission. The one double-event upset recorded was due to a software error in the Software Status Report code that read memory which had not been initialized.

Table 2-5. OPM Memory Upset Frequency

Timeline	Date	Single-event Upsets (SEU)	Double-event Upsets (DEU)
1	4/29/97	1	1*
2	5/6/97	0	0
3	5/13/97	0	0
4	5/20/97	0	0
5	5/27/97	3	0
6	6/3/97	0	0
7	6/10/97	0	0
8	6/17/97	3	0
9	6/24/97	0	0
10	9/12/97	7#	0
11	9/13/97	0	0
12	9/14/97	1	0
13	9/22/97	2	0
14	10/1/97	0	0
15	10/8/97	2	0
16	10/10/97	3	0
17	10/17/97	0	0
18	10/26/97	0	0
19	11/2/97	0	0
20	11/9/97	0	0
21	11/16/97	1	0
22	11/21/97	1	0
23	11/28/97	0	0
24	12/5/97	4	0
25	12/12/97	1	0
26	12/19/97	2	0
27	12/26/97	1 @	0
28	2/25/98	0	0
29	3/5/98	0	0
30	3/16/98	0	0
31	3/19/98	0	0
Totals		32	1

\# Large number of SEU's after OPM had been turned off for several weeks, which prevented periodic memory scrubbing

* DEU caused by error in Software Status Report that reads memory that had not been initialized

@ Last flight timeline

There were a large number (32) of single-event upsets recorded, but no real double-event upsets occurred. This indicated the EDAC scheme performed well. Since OPM was without power frequently during the mission, the EEPROM memory was exposed to radiation for long periods without being scrubbed. This may explain why 7 upsets were recorded after OPM had been off for nearly three months.

2.6.2 Data Log Formats

2.6.2.1 Instrument Sample Numbering

Refer to Figure 2-13 for sample orientation in the carousel.

Samples/holes are numbered clockwise:
TIS 0 (cal),1..20
TIS samples are measured CCW, 1 to 20.
VUV 0..40, cal holes are at 0,5,10,15,20,25,30,35,40.
VUV is measured CCW, 0 to 40.
REF 1..20 (same for CAL)
REF is measured CW, 20 to 1.

2.6.2.2 AO Monitor Data

The AO monitor consisted of 4 sensor positions and a blank position. The AO sensors were exposed for only 2 hours per day. At each AO position there were two sensors (one exposed, one covered) and a thermistor. While exposed, AO sensor and temperature data were taken at a rate of once per minute.

Table 2-6 below describes the AO data that was listed in the OPM telemetry data files.

There were five AO sensor positions (positions 1 - 4 plus a blank position). There were also five position sensors (P5,P4,P3,P2,P1) and a Geneva drive sensor (G). By reading the sensor values in the telemetry data, the present position of the AO monitor was determined. For example, when the AO monitor was recording data in the first sensor position, the position bit pattern in the telemetry stream should have read 1 0 0 0 0 1 or (decimal 33).

The "exposed" column in the table below lists the initial resistance, in ohms, of the exposed sensor in the OPM telemetry data. The "covered" column in the Table 2-6 below lists the initial resistance, in ohms, of the covered sensor in the OPM telemetry data. The thermistor column lists the resistance of the AO thermistor measured, in ohms, at clean room temperature (approximately 70 C) in the OPM telemetry data. During the mission, the resistance values for the AO Sensor (exposed, covered, and thermistor) were recorded by the DACS.

Table 2-6. AO data listed in the OPM Telemetry Data Files

Sensor	P5	P4	P3	P2	P1	G	Decimal	Exposed	Covered	Thermistor
1	1	0	0	0	0	1	33	54	70	483
2	0	1	0	0	0	1	17	242	471	513
3	0	0	1	0	0	1	9	111	382	456
4	0	0	0	1	0	1	5	280	535	548
blank	0	0	0	0	1	1	3	-	-	-

Additional information on the AO Monitor System is found in Section 3.5

2.6.2.3 Radiometer Data

There are two radiometers in the OPM system. In the OPM data files, one radiometer was referred to as an "earth" radiometer. The other was referred to as a "solar" radiometer. There were two operational amplifiers in between the radiometers and the A2D converters in the DACS to increase the output signal to acceptable levels. Additional information on the Radiometers if found in Section 3.6.

2.6.3 DACS Health and Status Data

2.6.3.1 Overview

First Hour of Monitor Collection

Upon initial power up after the EVA deployment, the OPM DACS ran for approximately 1 hour before starting the first measurement timeline. At boot time, the monitoring process was started. When monitoring, data were written to MM every 2 hours, unless a measurement sequence began. If a measurement sequence began in the middle of a 2-hour monitoring period, the monitoring period was completed after the measurement run and the monitor data were written to MM.

2.6.3.2 Reduced OPM Data File Types

The OPM data reduction program, REDUCETV.EXE, generated several files. These files and their contents are described below in Table 2-7.

Table 2-7. REDUCETV.EXE generated files

Filename	Description
TELEM.ALL	Reduced ASCII file containing msmt and monitor data
TELEM.CSV	Comma Separated Value file containing msmt and monitor data
TELEM.REF	ASCII file containing reflectometer data
TELEM.VUV	ASCII file containing VUV data

Filename	Description
TELEM.TIS	ASCII file containing TIS data
TELEM.CAL	ASCII file containing calorimeter data
TELEM.CAR	ASCII file containing carousel data
TELEM.MON	ASCII file containing standard monitor data
TELEM.RED	ASCII file containing standard reduced monitor data
TELEM.DET	ASCII file containing detailed monitor data
TELEM.MEA	ASCII file containing monitor data taken during msmt sequence
TELEM.EVT	ASCII file containing OPM event data
TELEM.AOM	ASCII file containing AO monitor data
TELEM.RAD	ASCII file containing radiometer data
TELEM.TEM	ASCII file containing temperature data
TELEM.VOL	ASCII file containing system voltage data
TELEM.TQC	ASCII file containing TQCM data
TELEM.@2@	LPSR format database file
TELEM.@3@	LPSR format database file
TELEM.OPD	WIN 95 format database file

2.6.3.3 OPM Voltage Measurements

Voltage data was sampled from various points throughout OPM. Various points were possible, but only four were enabled. These points were represented by the P0, P1, ..., P10 labels in the OPM data files. Table 2-8 describes each voltage sample in the OPM instrument.

2.6.3.4 System Time

MET was the amount of time that OPM had been operating from a preset time. For software reasons, the MET was initially set to 158387. MET was updated in RAM every second and updated in EEPROM every two hours. Note, if power to the OPM instrument was lost, up to two hours of the operating system time could have been lost. MET was written in the OPM telemetry data files in two forms. The first form was an integer that represented the number of seconds the system had been running. The second form had the following format: hours/minutes/seconds. It also represented the amount of time that the system had been running.

Table 2-8. Voltage Samples in OPM

Voltage label	DACS Channel	Voltage description
P0	MB A2D 1	+5V monitor
P1	MB A2D 22	+5V aux monitor

Voltage label	DACS Channel	Voltage description
P2	MB A2D 23	Not Used
P3	MB A2D 24	-5V pot reference
P4	MB A2D 25	+5V pot reference
P5	MB A2D 26	Not Used
P6	MB A2D 27	Not Used
P7	MB A2D 28	Not Used
P8	MB A2D 29	Not Used
P9	MB A2D 30	Not Used
P10	MB A2D 31	Not Used

2.6.3.5 Events

Many important events occurred during an OPM timeline. An event may be thought of as a system occurrence that was worth recording. This occurrence may have been a measurement sequence starting, a measurement sequence ending, a system error, etc. These events were stored in an event buffer and placed in the OPM telemetry data stream. The format of an event is described below.

Length of an event: 32-bits

Bits 0 - 7: Event Id byte (described the type of event, see table below)

Bits 8 - 15: Event data byte (a byte of data that gave additional information about the event)

Bits 16 - 31: Lower 16-bits of the MET (gave the time that the event occurred)

Table 2-9 shows a list of the event identifications and a brief description.

Table 2-9. Event Id and Description

Event	No.	Brief description
EVT_BUF_FULL	1	input buffer full
EVT_INVALID_CMD	2	invalid command id OBSOLETE
EVT_SCI_NO_CTS	3	can't output, no CTS
EVT_SCI_OR	4	receiver overrun
EVT_DACS_RESET	5	DACS power on or reset
EVT_OUT_FULL	6	serial output buffer full
EVT_PWR	7	invalid relay, on fail
EVT_A2D_INVALID_INPUT	8	invalid channel id
EVT_A2D_DB_FAIL	9	DB A2D fail
EVT_VUV_ARM_FAIL	A	VUV Arm component failed
EVT_VUV_FILTER_FAIL	B	VUV wheel component failed
EVT_VUVRUN	C	VUV run error

Event	No.	Brief description
EVT_TISRUN	D	TIS run error
EVT_MEM_ERR	E	memory EDAC error detected
EVT_D2A_INVALID_INPUT	F	invalid input
EVT_DIS_ERR	10	invalid input
EVT_REF_WAVE_FAIL	11	wave/slit motor fail
EVT_REF_ERR	12	invalid input
EVT_TEMPER_ERR	13	invalid input
EVT_CMD_ERR	14	command module error
EVT_COMM_1_ERR	15	comm port #1 error
EVT_COMM_2_ERR	16	comm port #2 error
EVT_MEAS_STEP_ERR	17	bad step
EVT_VUV_D2_FAIL	18	VUV error
EVT_EEP_8_CHECKSUM	19	EEPROM 8-Bit Checksum
EVT_AOM_AOMFAIL	1A	AOM sensor failure
EVT_AOM_PSNFAIL	1B	AOM position sensor failure
EVT_AOM_GENFAIL	1C	AOM Geneva sensor failure
EVT_AOM_SENFAIL	1D	AOM Geneva and position sensor failure
EVT_AOM_NOIPSN	1E	(all position sensor failed)
EVT_AOM_SEN_ERR	1F	AOM sensor error in monitor routine
EVT_TQCM_CARFFAIL	20	TQCM carousel frequency out of range
EVT_TQCM_CARTFAIL	21	TQCM carousel temperature out of range
EVT_TQCM_CONFFAIL	22	TQCM contamination frequency out of range
EVT_TQCM_CONTFAIL	23	TQCM contamination temperature out of range
EVT_WATCHDOG	24	Watchdog counter tripped
EVT_COMM_TX_BUF_FULL	25	
EVT_PRI_MM_WRITE	26	Attempt write outside primary mass memory
EVT_BCK_MM_WRITE	27	Attempt write outside backup mass memory
EVT_AOM_EXPOSED	28	AO monitor exposed
EVT_AOM_COVERED	29	AO monitor covered
EVT_MSR_START	2A	start measurement timeline
EVT_TIS_START	2B	start TIS
EVT_VUV_START	2C	start VUV
EVT_REF_START	2D	start REF
EVT_CAL_START	2E	start CAL
EVT_MSR_END	2F	start CAL
EVT_MSR_CANCEL	30	start CAL
EVT_STDDATA_PMM	31	write standard reduced data to pri mass memory
EVT_DETDATA_PMM	32	write detailed data to primary mass memory
EVT_DETDATA_PMM	33	write standard data to backup mass memory
EVT_24HOUR	34	24 hour time event

2.6.4 Temperature Data

2.6.4.1 OPM Thermistor Placement

Temperature data was taken from 31 thermistor placed throughout OPM. These sensors were represented by the T00, T01, ..., T30 labels in the OPM data files. Temperatures were listed in °C. Table 2-10 describes each thermistor's placement in the OPM instrument. The *Mission Thermal Data Book, AZ Technology Report No. 91-1-118-166* contains more detailed information on the placement locations for these thermistors.

Table 2-10. Thermistor Placement in OPM

Thermistor label	Thermistor location
T00	Thermistor located on Tray 6
T01	Thermistor located at Sample 6
T02	Thermistor located at Wheel 7
T03	Thermistor located on Tray 7
T04	Thermistor located on Tray 8
T05	Thermistor located at Wheel 8
T06	Thermistor located on Tray 1
T07	Thermistor located at Sample 1
T08	Emiss Plate Thermistor #1 (near heaters 3,4)
T09	Emiss Plate Thermistor #2 (near heaters 1,2)
T10	Emiss Plate Thermistor #3 near TIS on far edge
T11	Emiss Plate Thermistor #4 near TIS sphere
T12	Car Mtr Thermistor #1
T13	Car Mtr Thermistor #2
T14	Enc Top Cover Thermistor #1
T15	Enc Top Cover Thermistor #2
T16	Enc Top Panel Thermistor #1 top panel TQCM
T17	Enc Top Cover Thermistor #2 top panel AOM
T18	Flip Motor Thermistor
T19	Wave Motor Thermistor
T20	Filter Motor Thermistor
T21	G LASER Thermistor
T22	IR LASER Thermistor
T23	AO motor Thermistor
T24	DACS Housing Thermistor
T25	PSC Housing Thermistor
T26	PAC Housing Thermistor

Thermistor label	Thermistor location
T27	TQCM Mounting Plate Thermistor
T28	Enclosure Base Plate Thermistor
T29	Enclosure Side Panel Left Thermistor
T30	Enclosure Side Panel Right Thermistor

2.7 Harness/Cabling

The OPM main assembly harness was designed and built as a single unit. A dimensional mockup of the OPM assembly was fabricated to permit the three-dimensional cable to be fabricated more easily. Since the OPM was a protoflight unit, only one harness was manufactured and flown. Therefore, the harness, once installed in the OPM, was not removed unless absolutely necessary.

The main harness connected the OPM subsystems with each other. There were subsystem harnesses fabricated for each instrument/monitor to enable its easy removal from the OPM assembly as required. The approach permitted the main assembly harness to be checked prior to installation.

The connecting cabling between the OPM and the Mir space station was divided between one EVA cable set and one IVA cable set (see Figure 2-5). The design for the power, data, and ground was negotiated with the Russian engineers. The cables were to connect to existing cables launched on the Mir Docking Module, and the interfaces between the cables had to be modified to work with these cables.

2.7.1 OPM Harness

The OPM wiring harness was built to NHB-5300 series documents. Each instrument and sub-assembly has its own connectors to the harness to enable an individual sub-assembly or instrument to be independently removed from OPM for test, checkout, or repair. The main harness was tested for continuity, insulation resistance, and dielectric withstanding voltage prior to installation in the OPM assembly. After a fit check, the harness was attached to the assembly using cable clamps and tie wrapped in place.

2.7.2 EVA Cable

The EVA cable was built as two separate cables (see Figure 2-5). Cable lengths were dictated by Russian engineers based on the OPM location on the Docking Module exterior and the power panel inside it. Cable 42, launched with the OPM, was 2.5M in length, and was built by both AZ Technology and the Russians. The Russians added their EVA mating connector to this cable after fabrication in the US. Cable 42 attached to an EVA compatible connector on OPM while the other end of the cable mated with a Russian EVA connector on Cable 43. Cable 43, built by the Russians and launched with the Mir Docking Module, was mated to a Mir bulkhead connector. In preparation for the EVA deployment, the US cable

was unpacked and attached to OPM prior to the EVA. During the EVA deployment, the Russian and US cables were mated by the EVA crew. This cable contained the OPM power and redundant RS-422 data/command communication lines.

The EVA cable was fitted with an Aluminized Beta Cloth sleeve to protect the cable against AO and mechanical damage. Moveable Beta Cloth cable straps were added to allow the crew to restrain the cable, using Velcro, where necessary to prevent cable entanglement with subsequent crew missions or the Space Station Mir.

2.7.3 IVA Cable

Cable 45 carried both power and a redundant RS-422 communication interface to OPM via the internal Docking Module bulkhead connector. The cable looked like a "Y," with two redundant RS-422 serial connectors at one end, a power connector, and the "tail" mating to the bulkhead. One of the RS-422 connectors was mated to a MIPS Laptop during crew command or data collection. Cable 45 was partially assembled in the US then shipped to Russia to assemble the mating Russian Bulkhead connector to the cable. Cable 45 lengths for the various segments were specified by Russian engineers. This cable was wrapped in Nomex and protected from flammability by a Teflon wrap. Cable 44, a Russian built cable, was launched with the Docking Module.

2.7.4 Mission Performance

The OPM main wiring harness did not have any anomalies or failures.

The EVA cable performed as expected. There were no problems. During the EVA, the cable mated as expected, and the cable length was adequate. There were some observed discolorations on the Beta Cloth Sleeve and cable straps, similar to the OPM MLI discoloration. However, this had no adverse effect on the EVA cable's performance. The cable straps worked well to restrain the cables, and the crew reported the straps were easy to use. A post-flight inspection revealed the Velcro is still functional. There is no visible AO damage to the EVA Teflon cable, so the Aluminized Beta Cloth is thought to have worked as intended.

The IVA cable also fit well to the Docking Module power panel and bulkhead fitting. The Teflon wrap successfully protected the Nomex and was found to be intact upon ground inspection at the SPPF.

3.0 OPM INSTRUMENT/MONITORING SUBSYSTEM DESCRIPTIONS AND MISSION PERFORMANCE

The measurements of the space environmental effects performed by OPM were made using several optical instruments and monitoring subsystems. This section describes each of the three optical instruments: the Reflectometer, VUV spectrometer, and the TIS. In addition, the irradiance (solar and infrared) radiometers, AO monitor, and the contamination monitor are described. The engineering attributes of these instruments and monitors are detailed in this report along with a brief science synopsis of each instrument/monitor that define the significance of the measurements. More detailed science data are presented in the *OPM Science Data Report, AZ Technology Report No. 91-1-118-169.*

3.1 Reflectometer

The OPM Reflectometer provided a measurement of the solar absorptance properties of materials which are commonly exposed to the space environment. The solar absorptance of a material is the main phenomena by which the outer surface of the spacecraft (i.e. satellite, Space Shuttle, Space Station, etc.) absorbs solar energy, thus heating the spacecraft. By tailoring the amount of energy the spacecraft absorbs in relation to how much energy the spacecraft radiates, the temperature of the spacecraft can be controlled.

Past experience has shown that many materials optically degrade in the space environment. This degradation mechanism often involves the loss of atmospheric gasses, such as oxygen, that are rapidly reabsorbed when the materials are re-exposed to atmospheric gases. Some of the damage to these materials is "bleached" out. This proved true for most of the reflectometer samples flown on OPM. This, and other factors, made it advantageous to perform in-situ testing of the materials in the space environment. Simulating the space environment in a vacuum chamber cannot take into account all of the combined and "induced" space environment which is caused by nearby man-made objects such as the spacecraft itself. This is just one more reason why in-situ testing in the actual space environment is desired.

The main purpose of this measurement is to provide thermal spacecraft designers with realistic Beginning-of-Life (BOL) and End-of-Life (EOL) data for solar absorptance and spectral reflectance data. Spectral reflectance data enables material/coating developers to begin to understand why the material changes occur. These changes are due to the natural space environment, such as AO, solar UV, and high energetic particulate radiation exposure, as well as the induced space environment such as contamination from material outgassing. Furthermore, the natural and induced space environments can interact and cause reactions between various constituents that are not well understood, even today.

The reflectometer measured total hemispherical spectral reflectance from 250nm to 2500nm (effectively 97 percent of the solar energy spectrum), and provided spectral data at 100 wavelengths over this span. The data were integrated over this span to derive solar absorptance. The design and verification specifications for this instrument were:

- Spectral Range: 250nm to 2500nm
- Accuracy: ± 3%
- Repeatability: ± 1%
- Spectral Resolution: ± 5% of wavelength

Essentially, this reflectometer provided laboratory grade measurements on exposed materials while in the space environment. The great advantage of this experiment was that materials could be measured prior to space exposure, after space exposure, and most importantly *during* the space exposure.

The OPM reflectometer was designed and built by the prime contractor, AZ Technology in Huntsville, Alabama. This instrument was patterned after AZ Technology's commercial instrument, the Laboratory Portable SpectroReflectometer (LPSR).

3.1.1 Instrument Description

3.1.1.1 Operation

Please refer to Figure 3-1 as the basic operation is described. Light from one of two light sources was focused through a prism monochromator. The monochromator selected each of the 100 wavelengths during the optical scan (250nm through 2500nm). The output wavelength of the monochromator was chopped or modulated by a 150Hz Tuning Fork Light Chopper (TFLC). The TFLC was used to increase signal to noise ratio. The light energy was then directed into a 115 mm diameter integrating sphere. A beam director directed the energy onto either the sphere wall or the sample being measured. Photodetectors converted the reflected light energy into electrical signals and passed this information on to the signal conditioning electronics. The reflectance at each of the 100 sample points was equal to the ratio of the energy collected by the sphere wall from the sample to the sphere wall itself (remember the beam director directs the energy onto either the sphere wall or the sample). Thus:

$$\text{Reflectance} = \frac{\text{Energy reflected from sample}}{\text{Energy reflected from sphere wall}}$$

The solar absorptance was calculated from the reflectometer spectral data using the selected ordinates method from ASTM-E903 standard test method.

3.1.2 Instrument Design

The following three sections (optical, electronics, and mechanical) describe the OPM Reflectometer design.

3.1.2.1 Optical Design

The optical schematic, given in Figure 3-1, illustrates the reflectometer optical system design. Two lamp sources were used to span the spectral range of the instrument. The instrument measurement scan was from 2500nm (starting point) to 250nm (ending point). This scan order was chosen to allow the deuterium lamp to stabilize prior to the scan entering the region where this lamp was used. The first light source was a Tungsten halogen filament source, similar to a flash light bulb, and was used from 2500nm to 420nm. The Tungsten lamp was powered by a programmable constant current source. This current source allowed the lamp intensity to be varied during the scan to provide sufficient energy while not saturating the detector. The deuterium arc lamp was used to cover the 410nm to 250nm portion of the wavelength scan. The deuterium source intensity was not varied during the scan. The collection optics (see Figure 3-1) included a 400nm to 2500nm high pass dichroic filter. The dichroic filter, which transmitted the Tungsten lamp energy but reflected the deuterium lamp energy, allowed the two sources to be physically located at two different points and passively combined.

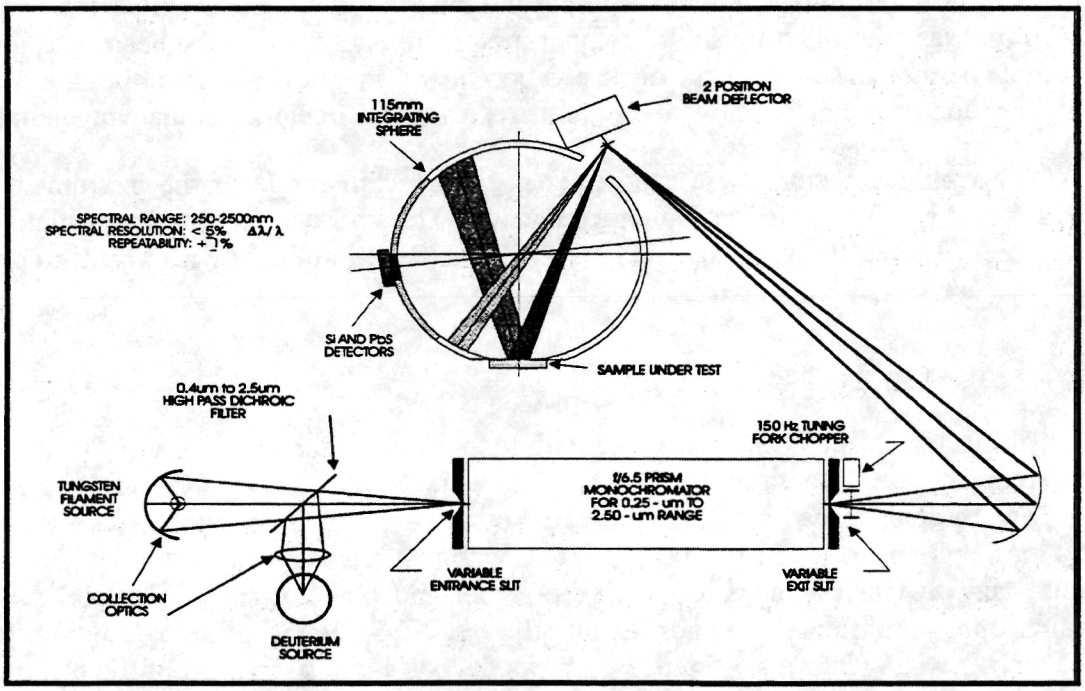


Figure 3-1. Reflectometer Optical Schematic.

Next in the optical path was a f/6.5 prism monochromator for the 250nm to 2500nm wavelength range. This monochromator used two space qualified stepper motors to control wavelength and slit width. The wavelength motor drove a worm gear which moved a cam. A cam follower moved a mirror behind a prism inside the monochromator to select the wavelength. The second motor drove a worm gear which also moved a cam, but this cam opened and closed the entrance and exit slits of the monochromator. The variable entrance and exit slits allowed the output intensity of the monochromator to be controlled to optimize the signal level and to control

spectral resolution. Both motors also drove potentiometers which gave positional feed back information to the OPM Data Acquisition and Control System (DACS).

The output of the monochromator was then chopped or modulated by a 150Hz TFLC. A TFLC looks just like a tuning fork. It is a mechanically resonant device which has a very stable frequency. The TFLC used on OPM had four electro-magnets, two on each vane or tine of the tuning fork. In order to keep the tuning fork vibrating, one pair of coils was electrically energized by a closed loop oscillator. The other pair of coils acted as a pick-up and closed the loop on the electrical oscillator. This kept the oscillator operating at the mechanically resonate frequency of the TFLC. The purpose of modulating the light source was to provide an alternating current (AC) signal riding on top of a background direct current (DC) signal. The DC signal includes drift, thermal noise, offset voltage, and is difficult to stabilize. Modulation of the source light permits separation of its signal from the DC component for signal conditioning to enhance the signal to noise performance of the instrument. This is further explained in Section 3.1.2.2.

The last fold mirror prior to entering the integrating sphere is called the beam director. This mirror was controlled by a third stepper motor. In one position the beam was directed onto the sample being measured. In the other position the beam was directed to the integrating sphere wall. The ratio between these two measurements was the reflectance at that wavelength.

Two photodetectors were used to span the spectral range of the instrument. The first photodetector is a TE cooled PbS photoconductor. The PbS was used from 2500nm to 1100nm in the scan. The second photodetector was a Silicon (Si) photodiode with a built-in pre-amplifier which was used from 1067nm to 250nm.

3.1.2.2 Electronics Design

There were four PCAs associated with the reflectometer. Two of the PCAs were located on the reflectometer integrating sphere; they were the Si photodiode PCA and the PbS pre-amp PCA. The Si detector had a built-in pre-amp but no simple way to mechanically mount it to the integrating sphere. The Si photodiode PCA was just a mounting fixture which held the Si detector and provided a place to attach the signal and power wires. The PbS pre-amp PCA contained pre-amplifier electronics to amplify the PbS signal prior to routing through the reflectometer wiring harness. Figure 3-2 shows the basic block diagram of the electronics signal conditioning for the reflectometer.

A third PCA was located in the PAC. The PAC was a separate modular enclosure which contained four PCAs. The reflectometer PCA contained power control circuits for the following functions:

- Deuterium Lamp Heater control circuit,
- Deuterium Lamp Strike circuit,
- Deuterium Lamp constant current source,
- Tungsten Lamp programmable current source,
- PbS TE Cooler drive constant current source, and
- Motor drivers (Beam Deflector, Monochromator slit and wavelength drive motors).

The Deuterium lamp heater control circuit provided a constant 10V to the deuterium lamp during warm-up. The heater filament inside the lamp heated the lamp's cathode. After the lamp struck, the heater voltage dropped to 7V during operation. The heater was turned off when the lamp was not in operation.

The deuterium lamp required a large discharge voltage in order to initialize the arc. The strike circuit discharged a capacitor into an auto transformer in order to generate the 600 to 800V required to strike the lamp.

Once the deuterium lamp struck, it required a constant 300mA current flow through the arc in order to maintain stability. The PAC contained a 300mA constant current source which powered the lamp after the lamp struck. This circuit also provided the OPM DACS with a feedback signal so the software would know the lamp had struck. Sometimes these lamps require multiple attempts to strike. All strike attempts were under software control.

The Tungsten lamp current source was used to drive and control the intensity of the Tungsten lamp. It was controlled by a D2A converter inside the DACS under software control.

The PbS TE Cooler drive was a constant current source which powered the TE cooler mounted inside the PbS detector. This constant current source was operated open-loop, that is, the temperature was not controlled. It simply provided a current which operated the cooler at maximum cooling without damaging the TE device. The TE Cooler was turned off when the reflectometer was not in use.

There were three motor drivers on this PAC PCA; one for each of the two monochromator motors and the beam deflector. These drivers converted the digital control signals from the DACS to the required voltage and current levels for the motors.

The signal conditioning electronics for the detector signal began with a CMOS switch which selected between the two photodetectors, depending on the point in the scan. Refer to Figure 3-3 for a more detailed block diagram of the electronics. After the switch was a 150Hz band-pass filter. Remember, the light was chopped at 150Hz by the TFLC. The purpose of the band-pass was to eliminate any noise outside this frequency. The band-pass filter was followed by a software Programmable Gain Amplifier (PGA). This amplifier was used to boost the signal to increase the signal strength to take advantage of the maximum resolution of the A2D. The high-pass filter following the PGA further aided in removing low frequency noise.

Prior to the A2D was a lock-in amplifier, sometimes called a phase or synchronous

demodulator. The lock-in amplifier was basically two closely matched amplifiers one with positive gain (in OPM +2) and one with negative gain (in OPM -2). A "switch" was used to select which amplifier's output was the lock-in's output. This demodulated the input signal with respect to a synchronous input, which in the reflectometer's case was the TFLC (the original modulation source). This increased the signal to noise ratio, see Figures 3-4 and 3-5.

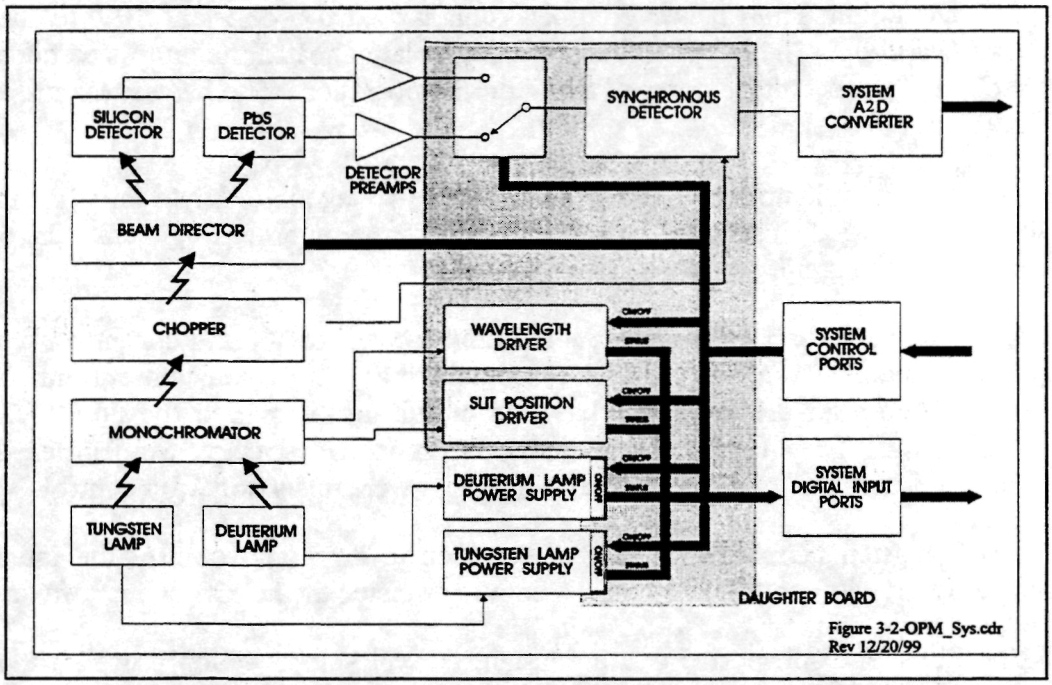


Figure 3-2. Integrating Sphere Reflectometer Subsystem

As noted in Figure 3-4, most of the noise in an optical system is at low frequency. The noise is primarily due to dark currents and temperature shifts in the photodetectors. By modulating the light source, in the case of OPM with a TFLC, the signal is effectively moved up in the (electrical) frequency spectrum above the noise. Now, in order to make sense of the signal, it must be moved back down to (electrical) DC (see Figure 3-5). This was done with the synchronous demodulator or lock-in amp. The lock-in amplifier behaved somewhat like a high precision bridge rectifier, i.e. it converted an AC electrical signal to a DC signal. The lock-in amplifier had the additional benefit of being phase sensitive. This meant the "rectification" of the input was done with respect to some other signal (normally the original modulation source); hence the name lock-in, synchronous, or phase demodulator. Any noise that was the same frequency as the signal was greatly reduced in magnitude if it was not exactly in phase with the input. The more the noise was out of phase, the greater it's magnitude was reduced. In OPM the TFLC pick-up signal was digitally phase shifted and used as the sync signal for the lock-in amp. The low-pass filter shown in Figure 3-3 on the output of the lock-in amp was used to "smooth" the bumps (ripple) from the lock-in amp's output. Mathematically, it acted as an integrator.

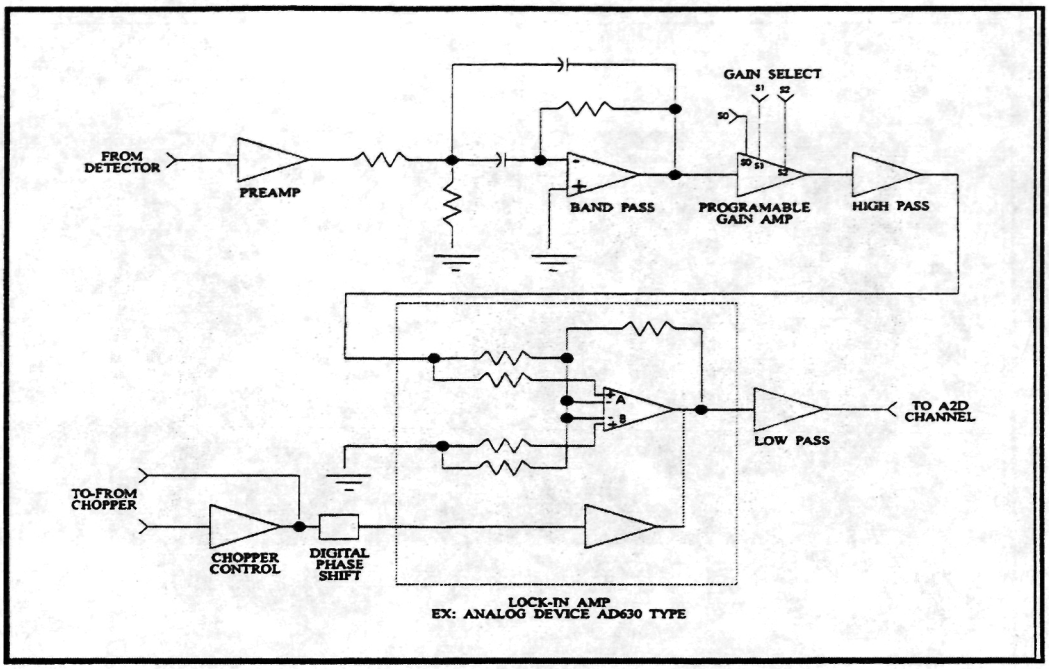


Figure 3-3. Synchronous Detector Block Diagram

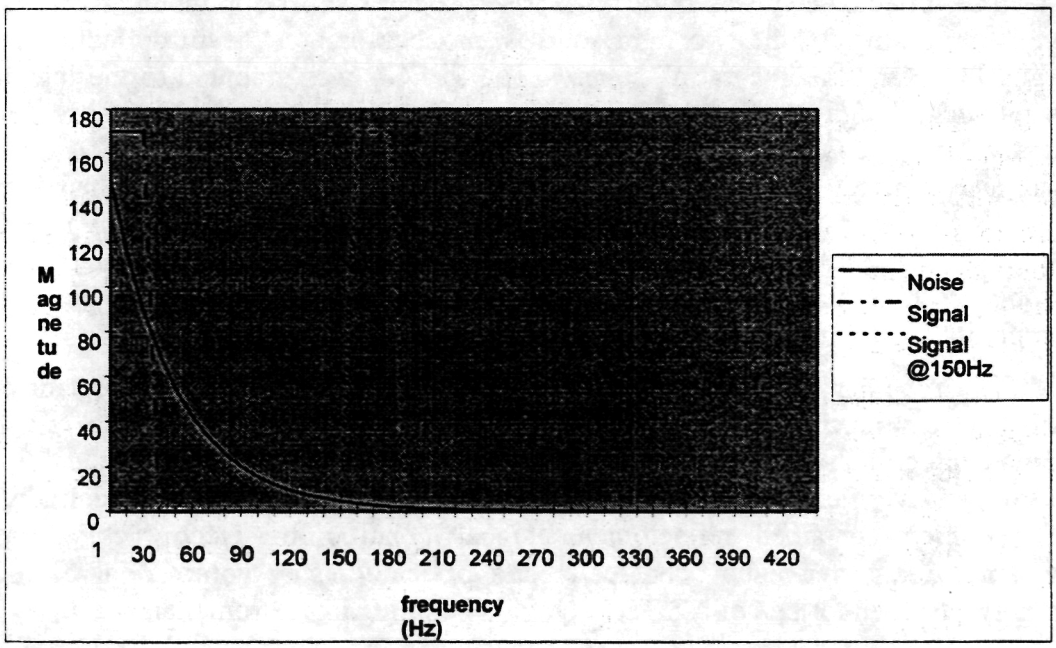


Figure 3-4. Signal and Noise versus Frequency.

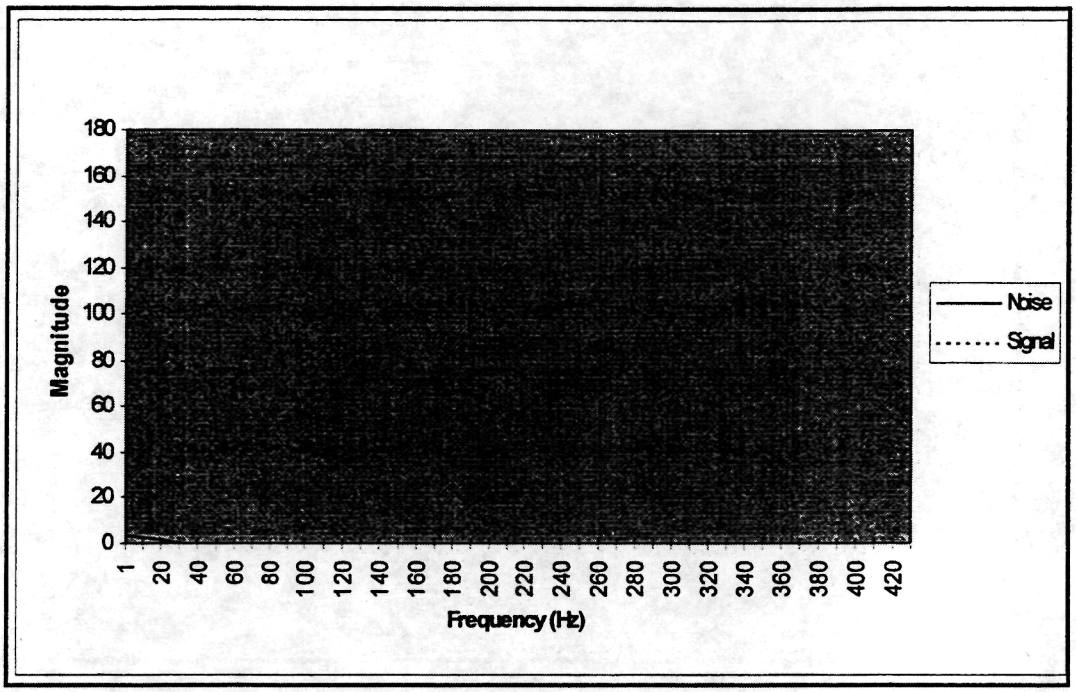


Figure 3-5. Demodulated Signal and Noise.

3.1.2.3 Mechanical Design

The reflectometer was built on a base-plate assembly for modularity. The base-plate provided mounting for the two light sources, monochromator, beam deflector, all optics, PbS pre-amp PCA, and the integrating sphere. The Si PCA was mounted to the integrating sphere. This modular design allowed the base-plate to be placed on a bench during testing prior to integration into the OPM assembly. During OPM integration, this assembly was placed "upside down" and mounted to the OPM emissivity plate. The emissivity plate had a cutout for the sphere to fit down into for measuring the samples on the carousel. Figure 3-6 shows a photograph of the reflectometer assembly. Figure 3-7 is a drawing showing the reflectometer assembly, both plan and elevation views. Figure 3-8 shows a photograph of the (background) assembly integrated into OPM. The TIS assembly is in the foreground.

The modular mechanical design of the reflectometer was an important consideration. Obviously, it is much easier to operate the reflectometer on the bench as a "stand alone" unit than after integration into OPM. This allowed for ease in optical alignment, calibration, as well as testing and verification of the independent reflectometer unit. Prior to delivery of the OPM DACS (which contained reflectometer signal conditioning electronics) from SwRI, the reflectometer was verified mechanically and optically using commercial electronics boards originally designed for one of AZ Technology's commercial instruments.

Another important mechanical innovation was the monochromator body. Prior to OPM, AZ Technology's commercial monochromators had multi-piece bodies; top, bottom, and four sides. The OPM monochromator had a "solid" body; that is, the top and four sides were machined out of one piece of aluminum. The solid-body monochromator had a separate bolt-on

bottom plate. This new monochromator had several advantages over the old style monochromator. The solid-body monochromator had less flexing when bolted down to the base plate - this meant less movement of the optical components as well as less change in the calibration. Additionally, the solid body monochromators have less thermal-gradient - providing increased wavelength stability. Since OPM, all of AZ Technology's commercial instruments have used this new solid-body monochromator design.

Dimensions of the reflectometer assembly were 8.1-inches at the widest point, 14.3-inches long, and 6.4-inches high. The approximate weight of the reflectometer assembly was 12.2 pounds. The reflectometer's mechanical pieces were alodined for electrical conductivity, and all mechanical parts were electrically conductive to prevent charging. Specified components of the reflectometer were painted with an optically black space stable ceramic coating, RM550, developed by AZ Technology to minimize stray light.

3.1.2.4 Software Design

Certain initialization processing, similar for all instruments, was to be performed at power up. The instrument relays were enabled, a "zero offset" reading was made of the detectors, and the light source (lamp) was struck and allowed to warm up/stabilize. (The zero offset was later subtracted from the detector readings by the OPM Ground Support Equipment (GSE) data reduction software.)

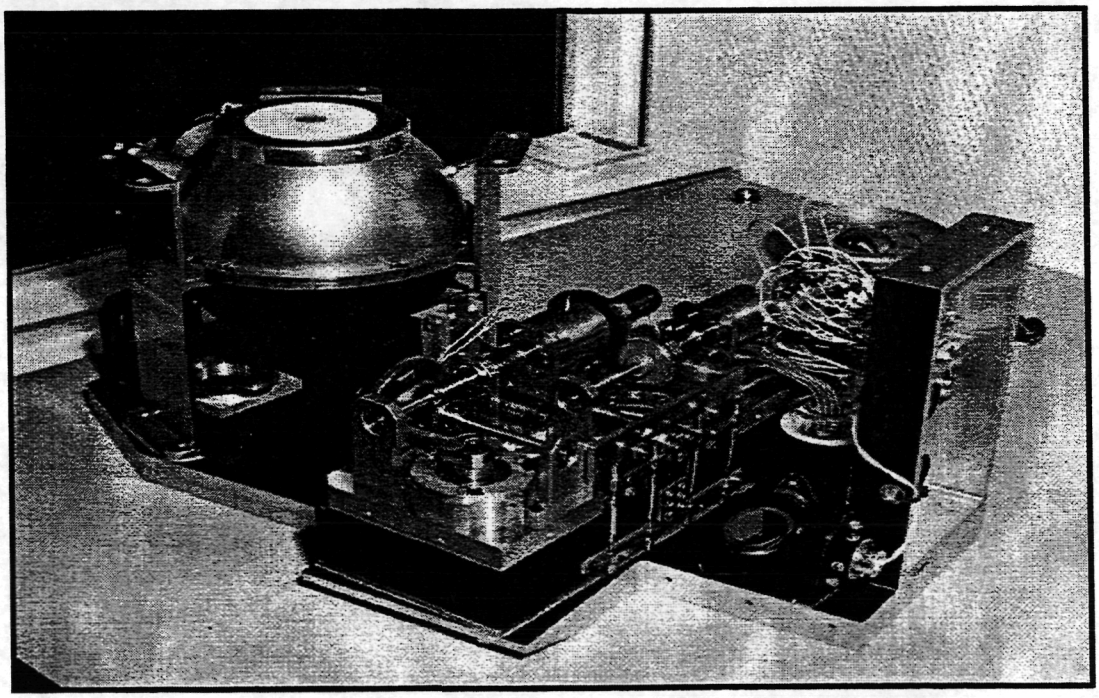


Figure 3-6 Photograph of the Reflectometer Assembly.

Each of the twenty Reflectometer samples were then measured. The reflectance of the sample was measured at one hundred different wavelength positions, using calibration values

determined during testing. The calibration table contained the wavelength target potentiometer reading, slit width target potentiometer reading, Tungsten lamp intensity, detector selection (PbS or Si), and starting detector gain setting for each wavelength position. The reference reading was first established. Measurements used the following algorithm for each wavelength position:

- Seek to the next prism wavelength using stored step counts, then fine-tune the position using the potentiometer.
- Seek to required slit width using stored step counts, then fine-tune the position using the potentiometer.
- Adjust the Tungsten lamp intensity, as required
- Allow the light source to settle for up to two seconds
- Take a reference reading with light source, adjusting the detector gain as necessary to be in the desired range of 2V to 4.5V.
- Adjust the slit width if necessary to attain the desired range. This was done by closing the slit by 10% up to four times.
- A sample reading (light source directly on sample) was then taken with the same settings as used for the reference reading. The ratio of the sample-to-reference readings gives the reflectance ratio.
- All readings and settings were saved for ground processing.

The Reflectometer software performed 27 runs during the mission.

3.1.3 Testing

The reflectometer was assembled and tested as a functional unit to verify its operation to specifications before integration in the OPM Assembly. PCAs that were electronically equivalent to the OPM Assembly were used to supply the power, simulate the data interface, and control the reflectometer functions. Measurements were performed to ensure performance objectives were obtained independent of the OPM core systems. When the performance objectives were met, the reflectometer subassembly was integrated into the OPM Assembly.

The reflectometer was not tested outside the OPM Assembly for environmental tests. However, some optical components were vibration tested to gain confidence in their surviving flight loads at launch. All components were tested after vibration and found to be operational. Therefore, they were qualified for use in this subsystem.

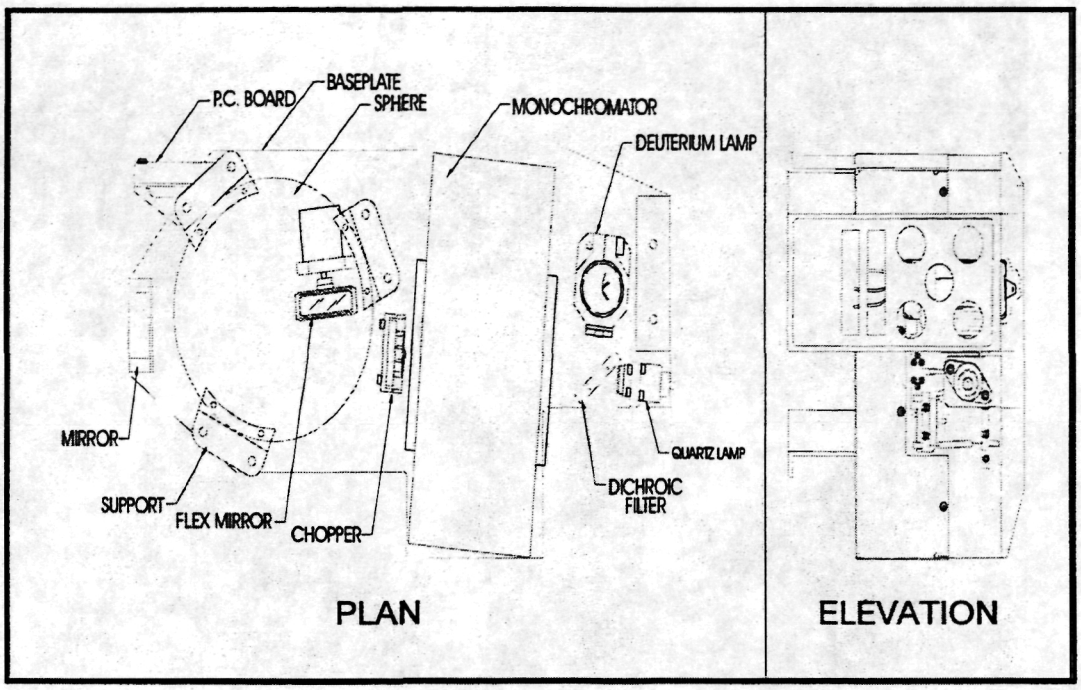


Figure 3-7. Drawing of the Reflectometer Assembly.

3.1.4 Mission Status

3.1.4.1 Flight Performance

The reflectometer performed well during the eight and half month mission. Measurement and health/status data were collected and analyzed. Preliminary results of the data reveal the instrument performed to specification. Figure 3-9 illustrates this pre-flight and post-flight data for one of the flight test materials. Other data are reported in the Science Data Report.

The reflectometer operation on-time was approximately 108 hours for 27 measurements. The power consumption was approximately 150W (5.25A @ 28V) during the measurement.

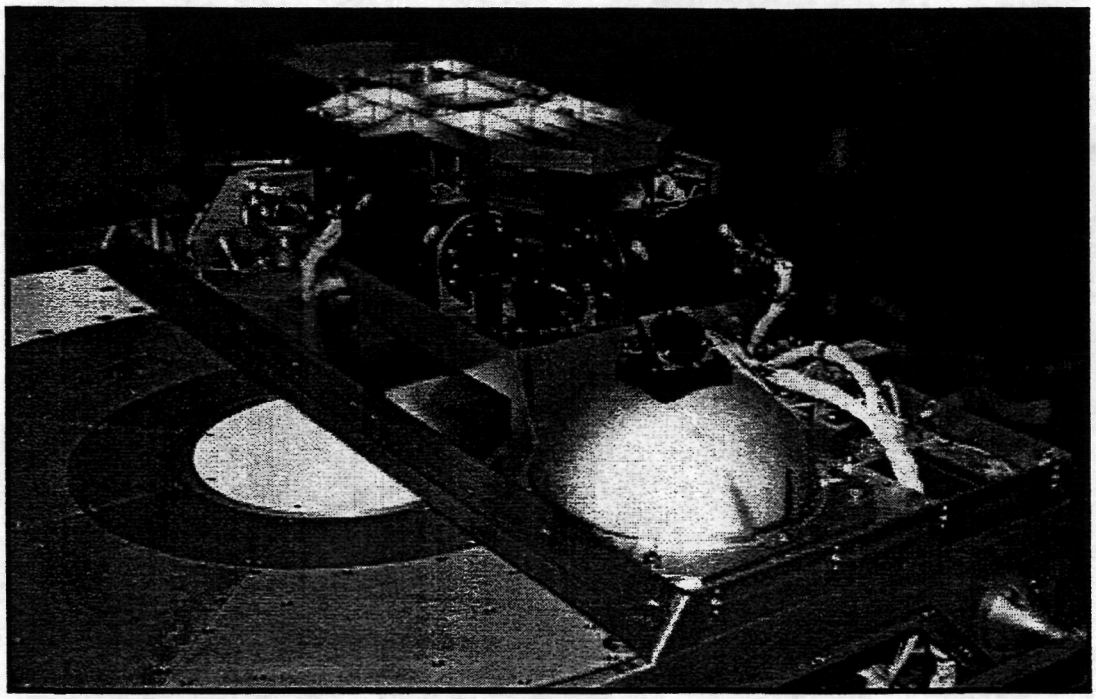


Figure 3-8. Instrument Assembly Integrated into OPM

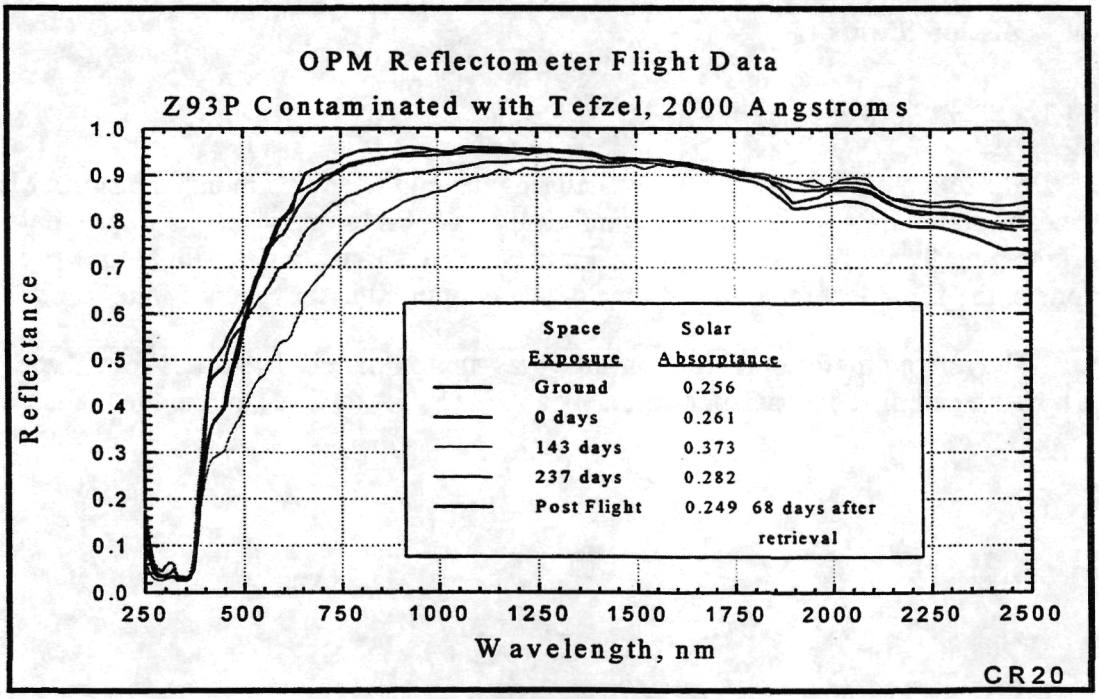


Figure 3-9. Pre- and Post-flight Data for Precontaminated Z93

3.1.4.2 Flight Anomalies

During the last measurement sequence (Timeline 27) made on Mir, and prior to the OPM/EVA retrieval; the Tungsten lamp failed. This was the only anomaly for the reflectometer. Post-flight microscopic inspection revealed the lamp filament had opened (or separated). Discussions with the lamp vendor indicate the probable cause of failure was the bulb reached EOL. No problems were identified with the lamp drive electronics. When the lamp was replaced, the reflectometer was able to perform again within specifications. This lamp was the same lamp used throughout the reflectometer integration and pre-flight testing.

3.2 Vacuum Ultraviolet (VUV) Spectrometer

The VUV spectrometer measured the specular reflectance and transmittance of test samples in the vacuum UV spectrum from 121.6nm (Lyman α) to 250nm. The VUV instrument was to characterize the change in specular reflectance and transmittances over time. This ruggedized instrument was to provide laboratory-grade data in a space environment. The design and verification specifications for this instrument were:

Accuracy:	± 5%
Repeatability:	± 2 %
Measurement wavelengths:	121.6nm
	140.0nm
	160.0nm
	170.0nm
	180.0nm
	200.0nm
	250.0nm

The main purpose of this instrument was to provide optical designers with realistic data of the space environmental effects on exposed optical surfaces.

3.2.1 Instrument Description

3.2.1.1 Operation

Please refer to the VUV Optical Schematic (Figure 3-10) as the basic operation is described. A ruggedized deuterium lamp with a magnesium fluoride window provided the energy for the VUV. An off-axis ellipsoidal mirror converged the light energy through an eight-position filter wheel monochromator to a fold mirror, a collimating mirror, and to the test sample. The light was either reflected or transmitted through the sample to identical detectors above and below the sample. At the filter wheel, seven narrow band pass UV filters selected the desired wavelength. One position in the filter wheel was a "hole" (i.e. no filter) used for end-to-end system calibration. A small stepper motor, controlled by the DACS, rotated the filter wheel for individual filter selection. The monochromatic beam was chopped using a 150Hz tuning fork light chopper to increase the signal-to-noise ratio. The fold mirror was mounted to a rotator arm

that rotated at pre-defined intervals for detector calibration. Several sample locations were left vacant to allow calibration of the two detectors. The detector reading through a calibration hole provided a 100% (incident energy) reading for determining reflectance and transmittance. By rotating the rotator arm, the second detector was calibrated. The detectors were commercial Si photodiode detectors with the UV quartz window removed. A Lexan cylinder coated with VDA along its axial length ("light pipe") and sodium salicylate coating of the exposed end converted the UV energy to a visible energy the detector could sense. The detector outputs were read by a phase-sensitive detection circuit and processed by the DACS.

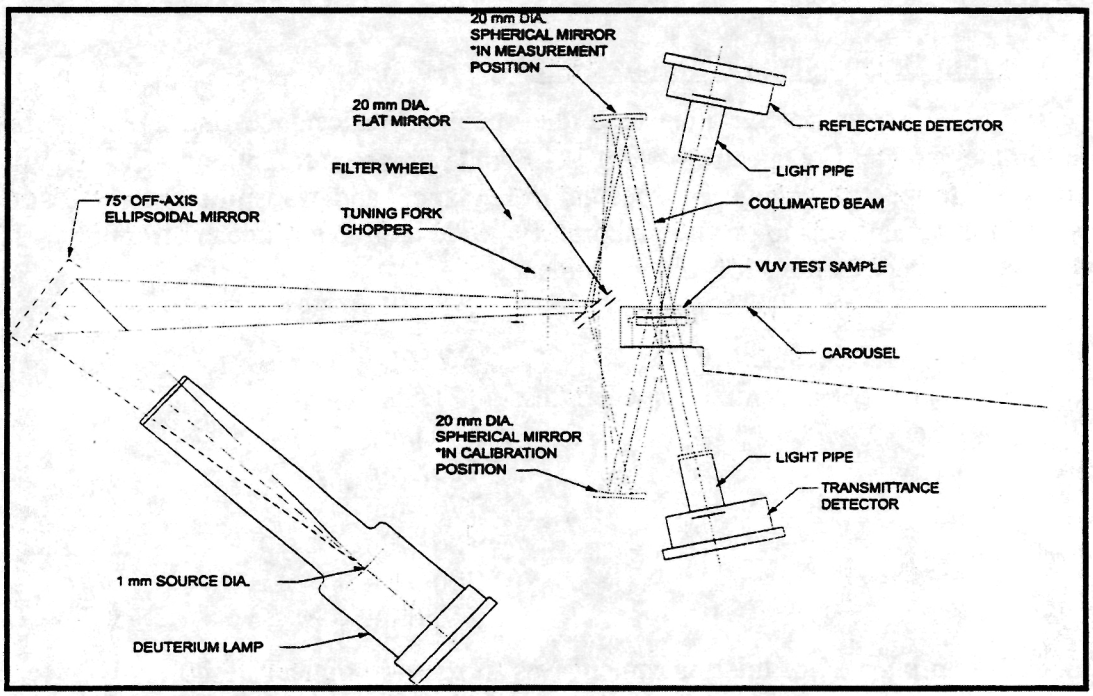


Figure 3-10. VUV Spectrometer Optical Schematic.

3.2.2 Instrument Design

The following sections (optical, electrical, and mechanical) describe the VUV Spectrometer design. Figure 3-11 shows the assembled VUV instrument in a fixture that simulates the sample placement in the carousel.

3.2.2.1 Optical Design

The light source used for the VUV instrument was the V05 Deuterium Lamp manufactured by Catheodeon, LTD. This lamp was an arc lamp complete with an anode, cathode, and heater. The lamp heater was used to warm up the cathode prior to the anode being struck. Once the cathode was warm, the anode required a high voltage strike to turn the lamp on.

The lamp produced UV light in the wavelength range of 121.6 - 250.0nm.

A custom precision tuning fork chopper used in the instrument was manufactured by TFR Laboratories, Inc. The chopper ran at a frequency of 150Hz with Type S shutters for sine wave modulations. The shutters were coated with an optical flat black coating. The chopper electrically shaped the light beam into a sinusoidal beam as it passed through a filter assembly. The filter assembly consisted of a filter wheel with eight holes. Seven of the eight holes contained UV filters in the wavelengths of 121.6nm, 140nm, 160nm, 170nm, 180nm, 200nm, and 250nm. The eighth position was a small aperture hole used for calibration.

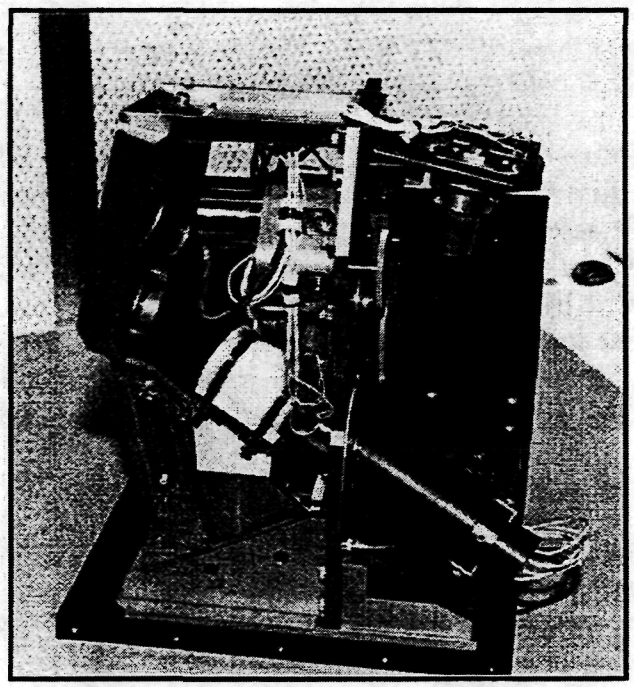


Figure 3-11. Assembled VUV Instrument.

The VUV instrument utilized two identical detector assemblies for the reflectance and transmission data collection. Each detector assembly consisted of a detector and PCB. Both detectors were the HUV4000B Si PIN Photodiode Preamplifier Module manufactured by EG&G Optoelectronics, Canada. The detectors utilized an UV-enhanced PIN photodiode with a hybrid pre-amp with an internal feedback resistor and a fixed bandwidth. The standard detector was a self-contained device in a hermetic TO package with an UV quartz window. The PCB utilized in the assemblies provided the source power to the detector and received the data signal from the detector.

The VUV instrument's objective was to detect UV wavelength as low as 121.6nm. The detector, with the quartz window, only allowed transmission down to 185nm. To achieve the stated objective, a light pipe assembly was designed to improve the detectors responsivity to low energy wavelengths. The light pipe assembly consisted of the detector assembly, the light pipe, baffle, base, and clamps. A detector was custom manufactured by EG&G Optoelectronics with

the UV quartz window removed to allow for optimum transmission. The light pipe was a custom cut cylindrical piece of Lexan. All surfaces of the piece were polished to remove all scratches, burrs, and sharp edges. The exterior cylindrical face of the Lexan piece was coated with aluminum by vacuum deposition. One end was coated with sodium salicylate. The other end of the Lexan piece was placed flush against the opening of the detector housing. The detector and light pipe were mounted on a base and clamped within a baffle housing assembly to form the light pipe assembly.

The light pipe assembly altered the VUV wavelengths into a usable wavelength to allow the detector to respond. The sodium salicylate coating fluoresced at ~500nm when exposed to the VUV wavelengths down to 121.6nm. The fluorescent light reflected off of the internal aluminum coating of the light pipe and was measured by the detector.

Three different types of custom mirrors were used in the VUV instrument to shape and direct the light. The first mirror that shaped the UV light was the ellipsoidal mirror contained in the ellipsoidal mirror assembly. The UV directed light then passed through a filter and was chopped by the tuning fork chopper. The filtered chopped light was shaped and directed further by two mirrors housed by the Rotator Arm assembly. The first mirror in the Rotator Arm assembly was the flat mirror called the base mirror. The base mirror reflected the filtered chopped light onto the arm mirror. The light traveled off of the arm mirror onto the VUV sample and was detected by either the reflectance or transmission detectors.

The Ellipsoidal mirror was a custom 1.5-inch diameter 75° Off-Axis ellipsoidal mirror manufactured by Aero Research Associates, Inc. The mirror was manufactured of nickel plated Brass with an overcoat of OPCO Lab "X-hard" coating for the UV applications. The base mirror was a custom 20mm flat mirror manufactured by Optics for Research. The substrate material was made from Pyrex with vacuum deposited aluminum with an overcoat of magnesium fluoride to provide a wavelength range of 100nm through 300nm. The arm mirror was a custom 20mm spherical mirror with a 1.5-inch focal length manufactured by Optics for Research. The arm mirror was made from Pyrex with vacuum deposited aluminum with an overcoat of magnesium fluoride to provide a wavelength range of 100nm through 300nm.

3.2.2.2 Electrical Design

The VUV subsystem was controlled by the three OPM electrical subsystems: PSC, PAC, and DACS. The PSC was the central power provider for the PAC, DACS and the VUV instrument. The PAC provided motor control, lamp control, lamp power source, etc. The DACS was the processing control unit for the VUV instrument and provided the control on the PAC and PSC. The VUV detector signals were routed and decoded by the DACS. Data storage was performed by the DACS. Figure 3-12 shows the basic block diagram of the electronics signal conditioning for the VIV.

3.2.2.2.1 PAC

The OPM PAC contained the power control circuits for the following VUV functions:

- Deuterium Lamp Heater control circuit
- Deuterium Lamp strike circuit
- Deuterium Lamp constant current source
- Motor Drivers (Filter wheel and Arm)

The deuterium lamp circuit descriptions were discussed in the Reflectometer's Electronics Design, Section 3.1.2.2, and were also used for the VUV lamp.

The VUV PAC PCB contained the stepper motor driver circuits for the filter wheel and rotator arm. These drivers converted the digital control signals from the DACS to the required voltage and current levels for the motors. Each motor drive circuit was independently software controlled by the DACS.

The VUV instrument had two detectors, each producing the data signal. The DACS contained the conditioning circuits for the detector signals. A software control switch selected between the reflectance and transmission signals. After the switch, the signal traveled through a 150Hz second order band-pass filter, the same frequency as the tuning fork chopper. The filter eliminated any noise outside the frequency of interest. Immediately following the band-pass filter, the signal traveled through a software PGA to boost the signal the necessary amount for maximum resolution of the A2D converter. A high pass filter following the PGA further aided in removing low frequency noise. The VUV employed the same type of phase or synchronous detection as described in the Reflectometer Electronics Design, Section 3.1.2.2.

The VUV DC integrated signal from the low-pass filter was the input to a software controlled CMOS mux. Once the channel was selected for the VUV DC integrated signal, the signal traveled to a 14-bit resolution A2D converter. The A2D converted the signal into a 14-bit word that was read by the microprocessor for data calculation. Once the signal was calculated, the DACS stored the data in non-volatile memory.

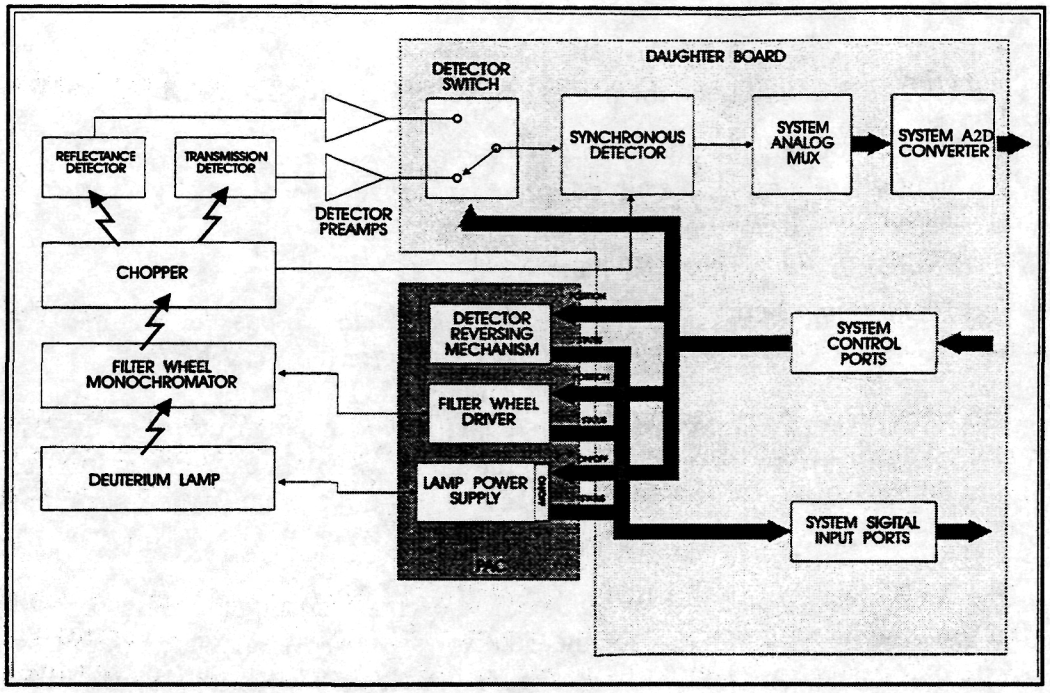


Figure 3-12. VUV Spectrometer Subsystem

3.2.2.2.2 DACS

The DACS controlled the operations of the VUV instrument. The VUV filter wheel and rotator arm was controlled by VUV DACS utilizing feedback from Hall Effect Sensor PCAs. The filter wheel contained seven unique filters and a calibration hole. A unique Hall Effect PCA contained sensors that detected a magnetic source. A small magnet was placed in the filter wheel to provide positional feedback to the DACS for proper filter selection. Similarly, a magnet was placed in the back of the rotator arm for rotator arm position feedback. Two small PCBs, each equipped with a hall effect sensor, were placed in the rotator drive assembly main support frame of the VUV. One was placed in the top portion of the frame, and the other was placed in the bottom portion of the frame. The rotator arm assembly motor moved the assembly until the Hall Effect Sensor picked up the magnet. When the magnet was sensed, the motor was stopped with the rotator arm in its proper place for measurement.

3.2.2.2.3 PSC

The PSC was the power source for the PAC, DACS, and the instrument systems. The PSC contained individual DC/DC converters and SSRs that were software controlled by the DACS for individual subsystem operations. When the VUV was not in use, all power required for the VUV instrument was turned off to conserve power.

The Deuterium lamp used in the VUV instrument required 105VDC. The PSC supplied

the 105VDC by stacking three ± 15V dual 30 Watt DC/DC converters in series. A SSR was used to switch input power on or off to the converters by the DACS software. The heater of the Deuterium lamp required an isolated supply. The isolated supply was provided by utilizing an optocoupler in the ground supplied to a 12V DC/DC converter. The optocoupler allowed the ground reference to move when the lamp was struck.

The PSC supplied the required 12V and 24V to the driver circuits of the filter wheel and rotator arm motor. The required voltage was achieved by the use of a ± 12V dual 30 Watt DC/DC converter. A SSR switched power on or off under DACS software control.

3.2.2.3 Mechanical Design

The mechanical design incorporated concepts to keep the optical path simple, minimize moving parts, and minimize volume. The VUV instrument was designed as an upright assembly that utilized a single light source with a simple optical path. This engineering design for the VUV instrument included support brackets, main support frame, mirror supports, rotator arm assembly, and a lamp holder assembly. Additionally, thermal analysis and structural stress analysis was performed on the design to ensure environment conditions could be met.

The VUV instrument was designed as an independent modular instrument. The VUV assembly design used its baseplate as the main support structure. The VUV assembly was mounted near the top of the OPM, and under the Top Cover. Its two detectors were placed on either side of the sample carousel (see Figures 3-10 and 3-11). The instrument was designed as a modular unit for easy removal and re-assembly in the OPM.

The use of the deuterium lamp required special attention in the mechanical design. A custom lamp holder had to be designed because the deuterium lamp was very fragile and it had to withstand the vibration and acoustics environment induced by the Shuttle launch. Likewise, the deuterium lamp holder was designed to protect and hold the lamp in the launch environment. The holder was made of Teflon material to protect the lamp. An electrical connector, made of Vespel, was custom designed to clamp to the electrodes protruding from the end of the lamp. When the lamp was struck, the lamp electrode differential voltage ranged from 600V to 900V. Vespel was selected because it could accommodate the lamp operating temperature and had a high dielectric voltage that accommodated the high voltage differential between the lamp electrodes.

The VUV instrument had two motors for the two movable assemblies: rotator arm assembly and the filter wheel assembly. The rotator arm assembly was designed to direct the light source to the top and bottom of the sample for calibration of the single beam system. For calibration of each detector, the rotator arm assembly would rotate up and down 180°. A custom Geneva drive system with a stepper motor drove the rotator arm assembly.

The filter wheel assembly was designed to hold seven different wavelength filters for the VUV instruments. The wheel had eight holes: seven holes for the filters, and one aperture hole

for instrument calibration. A custom Geneva drive system with a stepper motor drove the filter wheel assembly.

The VUV dimensions were approximately 4.8-inches wide, 9.3-inches deep, and 10.1-inches high. The approximate weight of the VUV Assembly was 6.5 lbs.

3.2.2.4 Software Design

VUV was the second instrument operated during the weekly measurement run. During initialization processing, the instrument relays were enabled, a "zero offset" reading was made of the detectors, and the Deuterium lamp was struck and allowed to warm up/stabilize.

The carousel contained 41 positions for VUV measurements. VUV was measured counter-clockwise, for positions 0 to 40 with calibration holes set at positions 0,5,10,15,20,25,30,35,40. Thirty-two samples were at all remaining positions. The VUV rotator arm remained in the up/transmission position for sample readings. The VUV rotator arm was moved up and down for calibration holes. Each sample was measured using seven filters plus a calibration hole on a rotating filter wheel. Two detectors, transmission and reflectance, recorded the reflected light. Using the same technique as for the Reflectometer and TIS instruments, "autogain" was used to adjust measurements. The software averaged 30,000 readings of each detector for each measurement sample.

3.2.3 Testing

The VUV was assembled and tested as a functional unit before integration in the OPM Assembly to verify its operation to specifications. PCAs that were electronically equivalent to the OPM Assembly were used to supply the power, simulate the data interface, and control the VUV functions. Measurements were performed to ensure performance objectives were obtained independent of the OPM core systems. When the performance objectives were met, the VUV subassembly was integrated into the OPM Assembly.

Additional tests were performed to gain confidence in new or unproven components. The VUV deuterium lamp was vibration tested to expected launch loads in the VUV assembly. The lamp was successfully operated after vibration. In addition, the VUV assembly was tested in a vacuum chamber to ensure operation in a space environment. The vacuum test was the only way to check the system performance at the VUV wavelengths of 121.6nm through 180nm. This test was also successful.

3.2.4 Mission Status

3.2.4.1 Flight Performance

The VUV assembly did not perform to specifications. The deuterium lamp never struck

during the space mission, and while the other parts of the VUV assembly performed well, no data could be collected.

The VUV Software performed 27 measurement timelines during the mission, and performed nominally. The VUV operational on-time was approximately 270 hours for 27 measurements. The power consumption was approximately 90W (3.2 A @ 28V) during the measurement timelines.

3.2.4.2 Flight Anomalies

The VUV lamp never struck on orbit. Preliminary thermal data indicated the heater was not working, which would prevent the lamp from striking. After the OPM return to AZ Technology and upon ground inspection and troubleshooting, the heater circuit in the lamp has been verified to be "open." The VUV deuterium lamp was visually inspected and x-rayed at NASA/MSFC. No cause of failure could be determined from these efforts. Next, the lamp was returned to the manufacturer in England for analysis. The vendor performed a visual inspection, continuity test, and helium leak test. The first visual observation was the "green" color evident on the heater filament material that is characteristic of oxygen invasion of the deuterium gas environment. Operation of the lamp while exposed to "air" will turn the filament material green. Their second visual observation revealed two possible leaks in the glass envelope: One near the end of the lamp where the energy is emitted, and the second at a glass to metal seal of one of the pins (anode). Both were subsequently tested for leaks with helium while the lamp was under partial vacuum. Both areas were indeed confirmed to be breaks in the glass envelope. The leak rates were measured to be at least 10^{-9} mb litre/sec.

The continuity test indicated the heater filament was indeed "open," and confirmed tests performed by AZ Technology.

The conclusion of the lamp manufacturer is as follows: The lamp seal was broken, in at least two areas, that permitted the lamp to operated in an oxidizing environment (in air). Over time, this embrittled the heater filament. Since the lamp operated on the ground during a pre-flight test at KSC, it is believed the brittle filament broke during the Shuttle launch – creating an "open circuit" failure of the lamp.

The VUV filter wheel rotation became intermittent after the Spektr collision. The filter wheel began "sticking" on the tenth timeline, which was the first timeline after the two and one-half month power down period. The filter wheel had intermittent problems rotating on approximately half of the subsequent timelines. Ground testing did not reveal the specific cause of this anomaly, but two areas are suspected. The first is increased drag of the filter wheel, and the second is a degraded drive system output torque. Post-flight testing revealed the motor torque had degraded by some 20 to 25 percent. Other causes have been eliminated by post-flight ground testing.

3.3 Total Integrated Scatter [1,2] (TIS)

The TIS Scatterometer measurements augment the data taken by the reflectometer and VUV. Each of these instruments measured transmittance and/or reflectance of selected samples, but cannot identify other effects that can impact surface scatter, such as, surface roughening and surface contamination. Roughening and/or oxidation of various materials by LEO AO can have significant effects on material performance. Further, particulate contamination from the natural or spacecraft induced environment can adversely impact material properties. The most common surface inspection methods used in ground laboratories include stylus profilometers and interference microscopes - both difficult to accomplish on-orbit. An alternative technology, the TIS can be used to monitor both effects. The design and verification specifications for this instrument were:

Measurement wavelengths:	532nm and 1064nm
Minimum angular extend of scatter collection:	2.5° to 80° from specular
TIS measurement range:	1 x 10^{-4} to .35 (0.5nm to 50nm rms roughness
Accuracy:	±10%
Repeatability:	±2%

The TIS provided laboratory grade measurements on exposed materials while exposed to the space environment. This was the first time this type of instrument had been flown.

The significance of the TIS measurement was in-situ monitoring of surface damage (roughness) and/or contamination of optical and thermal control surfaces caused by the space environment. A two color system, at 1064nm and 532nm, differentiated the changes in TIS values between surface damage and/or contamination. These data are desired by spacecraft designers wanting to select materials that exhibit minimal changes in the surface properties of materials due to the space environment.

3.3.1 Instrument Description

3.3.1.1 Operation

The TIS of a surface (in reflectance) is defined as the ratio of the scattered power to the total reflected power of a light beam incident on the surface, or

$$TIS = scatter/(scatter + specular) \quad (1)$$

A schematic representation of an instrument to measure TIS is shown in Figure 3-13. A narrow beam of light (usually from a LASER) is incident on the sample at a slight angle to the normal. The specularly reflected beam travels back to one detector while the scattered light is collected by a hemispherical mirror (called a Coblentz sphere) onto another detector. The optical powers measured by these two detectors are then used to calculate the TIS of the sample. The beam is usually chopped and synchronous detection employed to improve the signal-to-noise ratio. Since the hemispherical mirror can not collect all of the scattered light, a correction factor

is determined by measuring a highly-Lambertian surface. The TIS of a perfectly Lambertian surface is equal to 1, which leads to a correction factor of

$$C = V_{INC} * R_{LAMB} / V_{SCATT} \quad (2)$$

where V_{INC} is the power incident on the Lambertian sample (measured by moving the scatter detector into the incident beam), R_{LAMB} is the certified total hemispherical reflectance value of the Lambertian surface, and V_{SCATT} is the measured scattered power from the Lambertian reference surface. All subsequent scatter readings are then multiplied by the correction factor which is usually in the range of 1.3 to 1.5.

For randomly rough surfaces, the rms roughness (within a certain band of spatial frequencies defined by the angular extent of the collected scattered light) can be calculated using the following equation:

$$\delta_{RMS} = \lambda/4\pi[-\ln(1 - TIS)]^{1/2}. \quad (3)$$

This equation assumes that all of the reflected light comes from the first surface and that the rms roughness is much less than the wavelength of the light. These assumptions are valid for many of the optical surfaces of interest in this experiment.

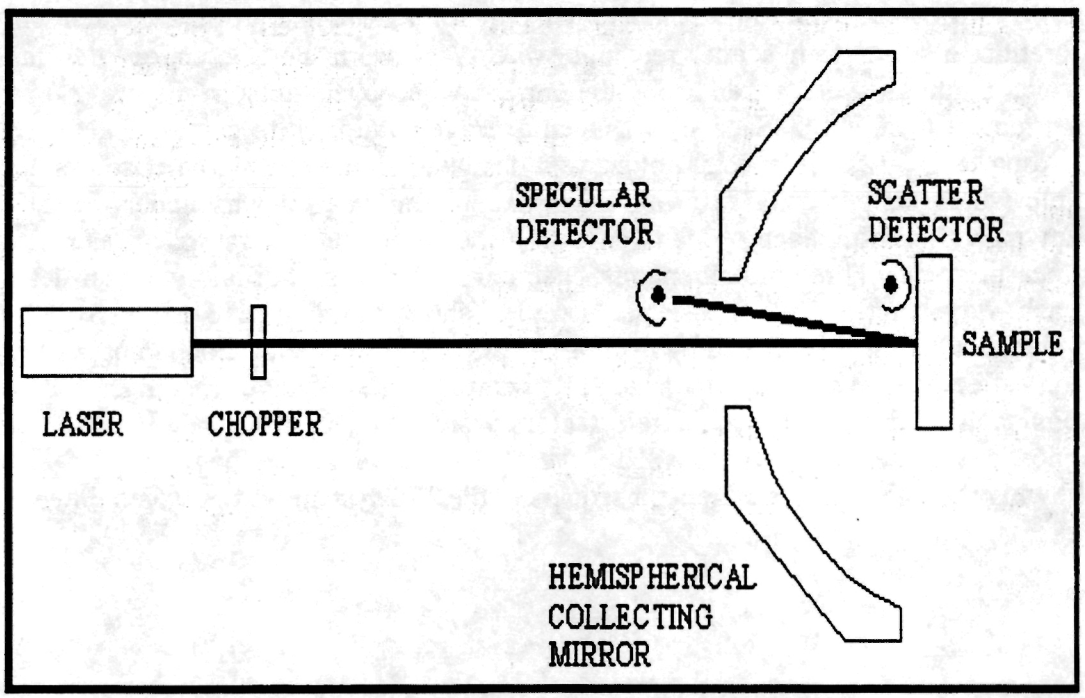


Figure 3-13. Schematic of a TIS Instrument.

Figure 3-14 shows the TIS of a sample (rms roughness of 2.95nm) as function of wavelength. Theory predicts a linear relation on a log-log scale. Actual measurements obey this relation out to about 2μm. At this point, the contribution from particulate scatter begins to dominate. The particulate scatter is roughly constant for all wavelengths, except at wavelengths

close to the particle size (notice the slight peak at 1μm). Thus, if one uses two wavelengths, one short and one long, then the effects of surface roughening and particulate contamination can be distinguished. As a surface gets rougher, the two TIS readings will increase together as predicted by Eq. (3). As particulate contamination increases, the ratio of the short-to-long TIS readings will decrease. Laboratory experiments on a breadboard TIS instrument have proven the validity of this method.

Thus, a two-wavelength measurement of the TIS from the exposed samples can provide both the surface roughness and the particulate contamination in a relatively simple instrument.

The design measurement sequence description follows. Following turn-on of the TIS instrument, the LASERs were allowed to warm up for 30 minutes. Next a calibration was performed prior to test sample measurement to account for any changes in the system, such as a change in Coblentz sphere reflectance. A special calibration sample was developed consisting of a Lambertian material surrounding a high-quality mirror (Figure 3-15). The Lambertian material was a space-grade Spectralon™ (PTFE) which has been shown to be, with proper handling, a clean, stable sensor calibration material for LEO. The total hemispherical reflectance of the Spectralon™ at both TIS wavelengths is 0.99. The mirror was required since the scatter detector can not be moved into the incident beam to measure the power. The mirror directed each beam, with very little loss, back to the specular detector for measurement of the incident power. During calibration, a set of four scatter readings were taken from the Spectralon™ surface, and three specular readings were taken from the mirror (the seven dots in Figure 3-15 indicate the measurement locations). Each set was then averaged and used to calculate the correction factor according to Eq. (2). A special holder was designed in the sample carousel for the calibration sample which kept it covered at all times except for when it was under the TIS instrument. Following calibration, each of the twenty 0.75-inch diameter test samples was rotated into place for measurement. Three measurements, each consisting of scatter and specular detector voltages at each wavelength, were made per sample (shown in Figure 3-15). Switching between wavelengths was accomplished by cycling power to the choppers. Each chopper, when powered down, effectively shuttered the LASER beam. The voltage readings, along with their automatically adjusted electronic gain factors were saved in OPM permanent memory. Some diagnostic voltages from the LASERs were also saved at the beginning of each sequence. Following the one hour measurement sequence, the TIS system was powered down.

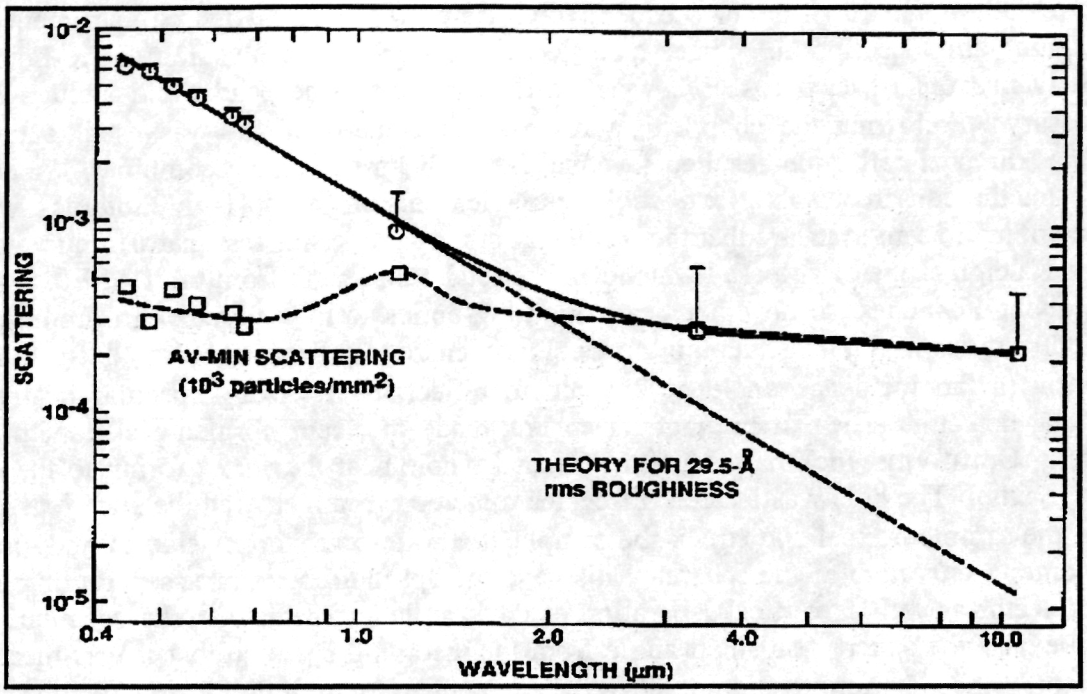


Figure 3-14. Relationship between TIS and Wavelength.

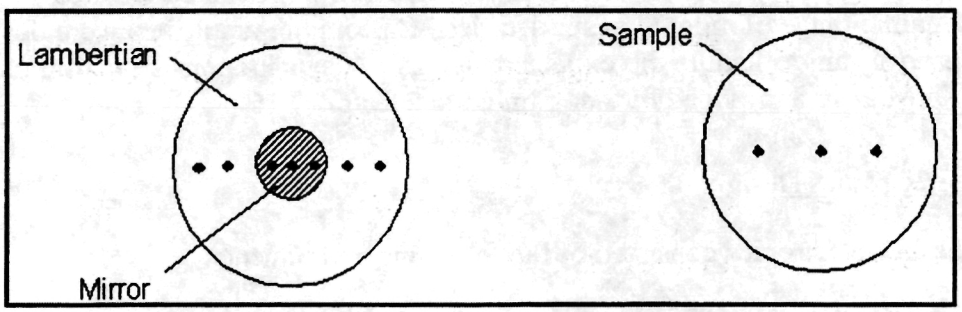


Figure 3-15. Calibration (left) and Test Sample (right) Layout.

3.3.2 Instrument Design

The following three sections (optical, electronics, and mechanical) describe the OPM TIS design.

3.3.2.1 Optical Design

Two diode-pumped Nd:YAG LASERs, manufactured by McHugh Photonics[3] and modified by AZ Technology for flight, were used to provide the two color wavelengths of 532nm and 1064nm. Both LASERs produced vertically-polarized, Continuous Wave (CW) output within the stability requirement of ±2%. The output powers were nominally 5 and 50mW

for the 532nm and 1064nm units respectively. Refer to Figure 3-16, TIS instrument layout, for the flight unit description. Space-qualified tuning-fork choppers (from TFR Labs), located directly in front of each LASER, were used to modulate the beams and shutter them when necessary. Following the choppers, a fused silica window at 45° was used to combine the beams. Fresnel reflection resulted in equal power beams after the combiner. A beam dump collected the unused beams. Next, a collimating lens, also from McHugh Photonics, was used on the combined beam to insure that the beam size at the sample was less than 1mm in diameter and had a Raleigh range of at least 13-inches. The total path length from the LASER to the sample was about 12-inches, so no other beam focusing optics were required. An aluminum/MgF_2 - coated, zerodur fold mirror sat atop the Coblentz sphere to reflect the beams down to the sample location (at an incidence angle of 2°) and to reflect the returning specular beams onto the specular detector. The 7-inch diameter sphere, made of electro-formed nickel with a rhodium coating (Opti-forms, Inc), had a 0.4-inch diameter hole near the vertex (5mm to the side of the optical axis). The hole was located off center so that the beam entered the sphere at an angle of 2° to the sample normal and struck the sample at a point 5mm to one side of and 4mm outside the center a curvature of the sphere. This gave the optimum horizontal separation of the beam and detector as well as vertical separation of the sample and detector. The specularly reflected beam exited the sphere at a small angle from the incoming beam so that it was measured by a detector. Since aberrations did not allow efficient collection of light beyond 80°, the sphere was made to collect from 2.5° to 80° from the specular direction. The detectors were off-the-shelf Si photodiodes from Hamamatsu (S2386-45K) with 3.9mm x 4.6mm active areas. They possessed a linear dynamic range of more than six decades. Custom pre-amplifiers were designed and built with the proper gain to handle the expected signals. A synchronous detection circuit located in the main OPM DACS provided further gain up to a factor of 16.

3.3.2.2 Electronics Design

The TIS electronics consisted of the following components:

- LASER Driver and Controller,
- Photodetector Pre-Amp, and
- Signal Condition Electronics.

Each unit's LASER Driver and Controller PCB was located in the PAC and contained drive circuits to control the two TIS LASERs. Each of the two circuits was independent. Basically, each LASER controller was made up of several second order analog closed loop control circuits and a constant current source for the LASER diode. The closed loop control circuits operated TE heaters and coolers inside the LASER cavity. That is, certain areas of the cavity, as well as the diodes were maintained to a constant temperature. The design of this PCB was based on a schematic provided to AZ Technology by the LASER manufacturer, McHugh Photonics. Commercial parts were replaced with military specification equivalent parts. After assembly and testing of the LASER drivers, this PCA was carried to the LASER manufacturer where the PCA was "tuned" or optimized for the flight LASERs. Further testing was performed by placing the boards and LASERs in a thermal chamber and testing performance over the

expected temperature range.

The photodetector pre-amp provided amplification of the signal prior to routing through the wiring harness. Each detector was physically located near the pre-amp board. The final PCA, called the DACS Daughter board that contained all the signal conditioning for TIS, was located in the DACS. The Daughter board contained all signal conditioning for each of OPM's three optical instruments as well as circuits for other OPM subsystems not supported by the Commercial-off-the-Shelf (COTS) CPU board (refer to Figure 3-17). With the exception of the high voltage or high current drivers, all this signal conditioning was located on the DACS Daughter board. The Daughter board had the primary A2D converter which had 14-bit bi-polar resolution. There was a back-up A2D on the COTS CPU board with 12-bit resolution. The Daughter board had a external pin which wrapped the output of its analog MUX to the COTS CPU's A2D.

The signal conditioning electronics began with a CMOS switch which selected between the two photodetectors, specular and scatter. Refer to Figure 3-17 for a more detailed block diagram of the electronics. After the switch was a 150Hz band-pass filter. Remember, the light was chopped at 150Hz by the TFLC. The purpose of the band-pass was to eliminate any noise outside this frequency of interest. The band-pass filter was followed by a software PGA.. This amplifier increased the signal strength to take advantage of the maximum resolution of the A2D. The high-pass filter following the PGA further aided in removing low frequency noise. A lock-in amplifier increased the signal-to-noise ratio.

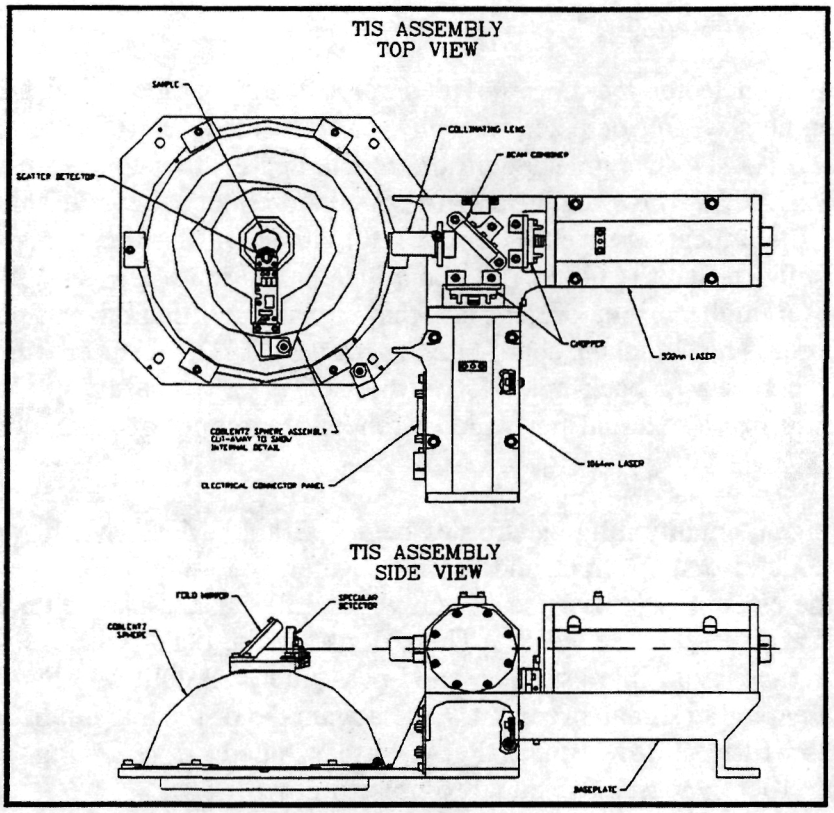


Figure 3-16. TIS Flight Assembly.

3.3.2.3 Mechanical Design

The TIS was designed for mounting all components to a solid, single-piece, aluminum baseplate for structural integrity. The LASERS and Coblentz sphere were accurately located using dowel pins. The other components were attached in ways that allowed for rotation, tilt (with shims), and lateral adjustment for alignment. A boss on the underside of the baseplate was designed to fit very closely into a pilot hole in the OPM emissivity plate to accurately place the TIS instrument relative to the samples in the carousel. In this configuration, the illuminated spot on the sample was located 5mm to one side and 4mm outside the center of curvature of the Coblentz sphere. The center of the scatter detector was then located at the conjugate point 5mm to the other side and 4mm inside the center of curvature. The aluminum surfaces of the instrument were either alodined (for corrosion resistance) or painted with a low-reflectance black coating developed by AZ Technology (for stray light control). Eight easily-accessed bolts were used to fasten the TIS to the OPM. Two power cables connected the LASERS to the OPM PSC. Two other connectors interfaced the choppers, detectors, and thermistors (one on each LASER) to the OPM DACS.

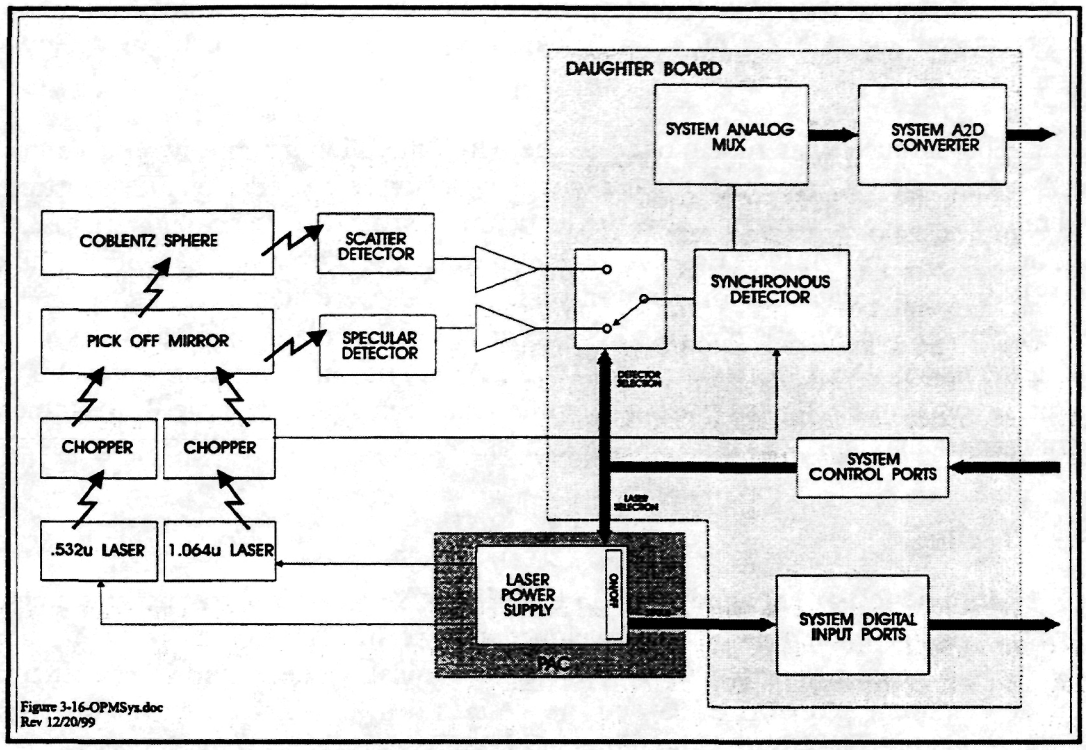


Figure 3-17. TIS Subsystem

The most challenging components for the flight instrument were the LASERS. No space-qualified LASERs were found that were suitably compact, low power, nor of the desired wavelengths for the TIS. The only space-qualified LASERs identified at the time were extremely expensive, bulky, and designed as one-of-a-kind components for specific flight programs. Small diode-pumped Nd:YAG LASERs made by McHugh Photonics were used in the conceptual breadboard TIS instrument. With their small size and ruggedness (developed for field use in the telecommunications industry), these LASERs seemed to be the best choice for flight. A sealed, aluminum housing was designed to make the LASERs vacuum-compatible. The standard McHugh Photonics diode assemblies (one 532nm and one at 1064nm) were put into the housings and sealed with Viton o-rings. The resulting LASERs were roughly 5.5-inches long x 2.5-inches wide x 2.5-inches tall and weighed about 1.2kg (2.7lbs) each (the 532nm LASER is slightly bigger than the 1064nm LASER). Hermetic connectors were mounted to the housing for power/feedback control cabling.

The final configuration of the TIS envelope was 18-inches wide x 11-inches deep x 6-inches high. The TIS flight weight was approximately 14lbs.

3.3.2.4 Software Design

TIS was the first instrument operated during the weekly measurement run. During

initialization processing, the instrument relays were enabled, a "zero offset" reading was made on the detectors, and the 532nm and 1064nm LASERs were struck and allowed to warm up/stabilize.

The carousel was first moved to the TIS calibration sample, whose cover was "pulled back" when the sample was rotated counter-clockwise under the TIS aperture. The TIS calibration sample was measured at seven sample "spots." One reading was taken from each spot on the sample. In addition, 30 readings were taken from the second specular spot. For LASER diagnostic data each of the twenty TIS samples were then measured, with 3 sample spots per sample The sample was measured with each LASER, utilizing software-controlled oscillating "shutters" that blocked the light path of the LASER not in use. Two detectors, specular and scatter, recorded the reflected light. Using the same technique as for the Reflectometer and VUV instruments, "autogain" was used to adjust measurements.

3.3.3 Testing

Multiple tests were conducted on the TIS LASERs. Initial testing was conducted on the "environmentally hardened" units, developed by McHugh Photonics for the communications industry (for commercial, not laboratory, applications). These initial tests included thermal cycling, vibration, and EMI/EMC and are described in the *Development Tests for the Amoco LASER Company Solid-State Diode Pumped LASERs, AZ Technology Report No. 91-1-118-129.* The test results indicated these units would be able to survive the launch environment, could operate within the thermal design extremes anticipated on-orbit, and could comply with EMI/EMC requirements. Vacuum testing was not possible on these commercial units because they were not sealed.

A new sealed housing design was initiated with the technical assistance of McHugh Photonics to develop a flight-qualified LASER. New housings were designed for sealing with indium and O-rings, and subsequently leak-tested to vacuum pressure levels. Both designs indicated good sealing, so the O-ring was selected for ease of use and repeated sealing capability. The O-ring sealed housing was then retro-fitted with the LASER electronics at McHugh Photonics, recalibrated for output power, stability, etc. and retested in a thermal vacuum chamber.

The thermal vacuum tests proved the housings were sealed sufficiently for the LASERs to properly operate for the intended mission duration. These LASERs were used as flight spares and two new units were fabricated for the flight units. These latter two units successfully passed the OPM environmental system test, and were thus qualified to fly.

3.3.4 Mission Status

3.3.4.1 Flight Performance

The TIS performed very well during the mission. Preliminary results of the data reveal

the instrument performed within specification. Figure 3-18 illustrates the percent change from pre-flight data for a gold mirror, a platinum mirror, and an aluminum-backed Kapton sample. Figure 3-19 illustrates the change in TIS for an Aluminum Magnesium Fluoride mirror over the mission as compared to the calibration sample. Other data are reported in the OPM Science Data Report.

3.3.4.2 Flight Anomalies

There were no hardware anomalies observed for the TIS during the mission.

The TIS software performed 27 runs during the mission, and performed nominally, with one minor exception. Some of the gain factors were recorded incorrectly on one of the 27 runs. One of the 1064nm specular readings from the calibration mirror was 3.798 V with a gain factor of 4. All other calibration mirror readings were about 3.8 V with a gain factor of 0. The gain factor of 4 was incorrect. For this same timeline, the specular gain factors on sample #3 were both significantly different than any before. Lastly, a gain factor of 5 was recorded on one reading. This anomaly did not repeat itself.

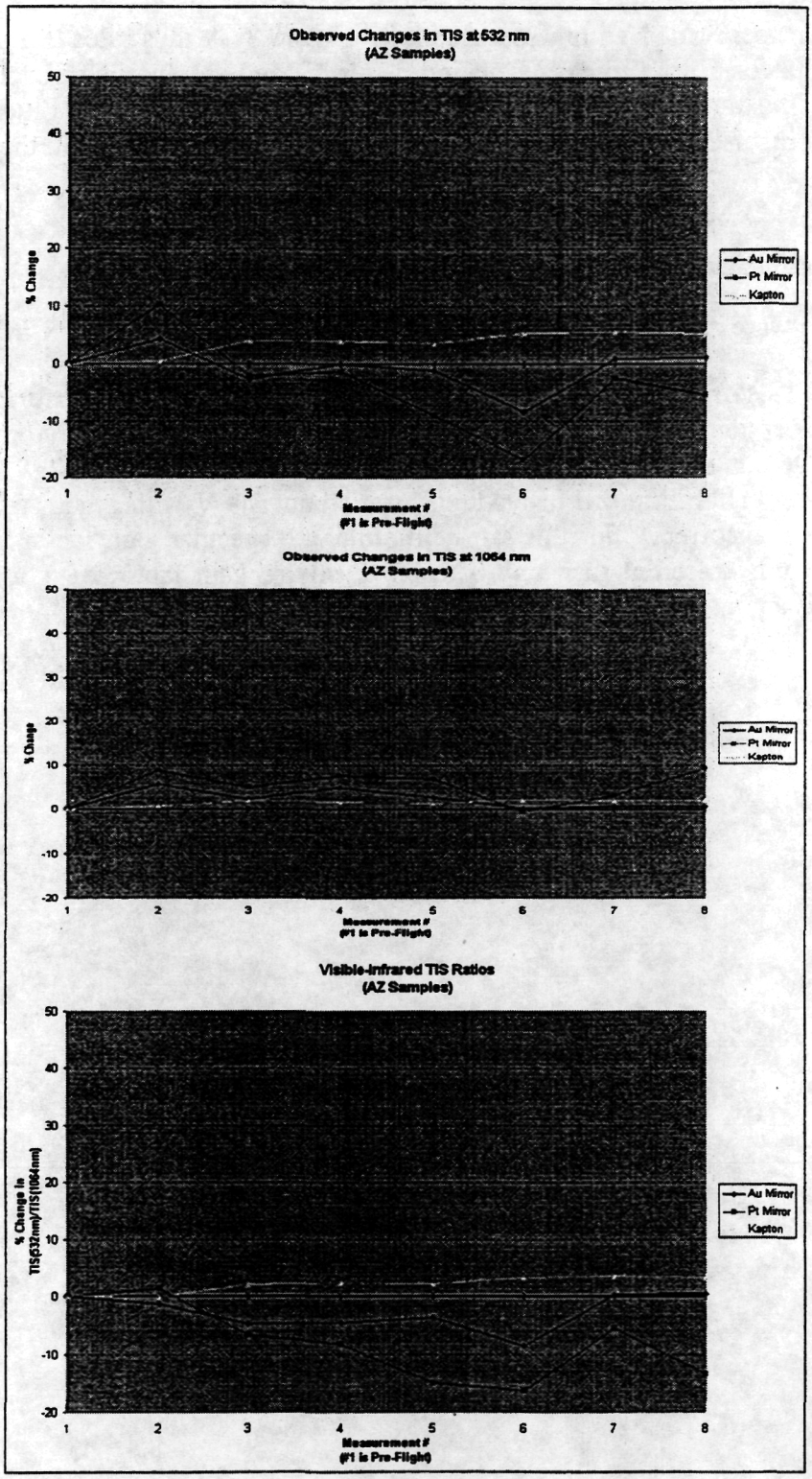


Figure 3-18. Examples of TIS Data.

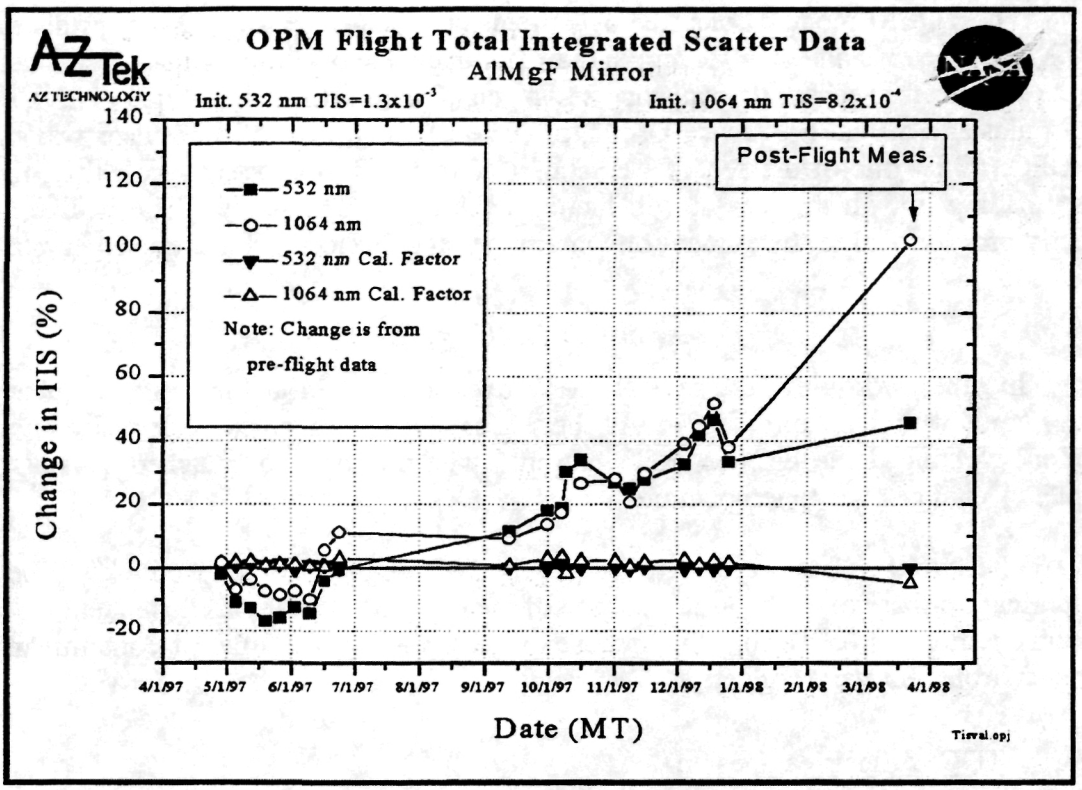


Figure 3-19. TIS Flight and Post-Flight Data for AlMgF Mirror

3.4 Molecular Contamination Monitor

The OPM Experiment used TQCM sensors to monitor the molecular contamination environment to which the flight test samples were exposed. The TQCM sensor is a standard off-the-shelf flight qualified item and is available commercially. Many TQCMs have been flown with success to measure molecular contamination.

TQCM sensors have become the standard for measuring molecular deposition (contamination) in the space environment. These sensors feature measurement of partial monolayers of contamination, wide range of operating temperatures typical of the space environment, and "self-cleaning" by driving off (at high temperature) volatile contaminants deposited on the sensor.

3.4.1 TQCM Design

There were two TQCMs on OPM. The purpose of a TQCM was to measure the mass deposition rate and total accumulation of contamination materials that deposited on its surface versus time. The TQCMs used on OPM were designed and built by Faradary Laboratories in La Jolla, California. The measurement and control electronics were designed by AZ Technology.

The TQCM module consisted of a precision matched set of quartz crystals that operated at 15MHz. The crystals were 1.27cm in diameter and were optically polished. Inside the module were a temperature sensor (thermistor), a two stage Thermo-Electric Device (TED), crystal drive electronics and a Beat Frequency Oscillator (BFO). The output of the sensor was the output of the BFO. Only one of the sensor's crystals was exposed to contamination flux; therefore, the mass loading, m, on the crystal will increase the output frequency. The beat frequency was directly proportional to the amount of contamination collected on the exposed crystal. This was given by:

$$m=1.56 \times 10^{-9}\ g/cm^2\ Hz$$

In other words, if both crystals were *exactly* matched at the same frequency, then the BFO output would be zero (DC). As the exposed crystal surface collected contaminates, its frequency changed, as did the BFO output. The use of two matched crystals minimized frequency changes due to temperature.

The two TQCMs were set to maintain -10°C and -30°C respectively. The amount of contamination that collected on the surface of the exposed crystal was dependent on the crystal's set-point temperature. During the space exposure, varying amounts of contaminants from the space environment were collected.

3.4.1.1 TQCM Electrical Design

The TED was used to control the temperature of the TQCM crystals. This allowed the TQCM to be driven to temperatures below ambient, so that it would collect more contaminants. Additionally, once the TQCM sensor became saturated, it could be driven hot (up to 100°C) to drive contaminants off the exposed crystal. The temperature control for the TED was located in the OPM PAC. Two second order closed loop analog control circuits controlled the TQCM TE cooler/heaters. A D2A inside the DACS set the reference voltage at the summing junction which in-turn controlled the temperature set-point. The analog temperature controller electronics then drove the TQCMs TED until the thermistor temperature feedback matched the desired reference temperature. During ground testing, the controller maintained the TQCM temperature within 1°C for the full range of 100°C to -40°C.

The frequency measurement was performed inside the OPM DACS. The measurement circuit used a programmable timer/counter chip (Am9513A) which could be programmed to measure period (for low frequencies) or measure frequency (for the higher frequencies). The resolution for this circuit was 1/2Hz from 1Hz to about 20KHz.

3.4.1.2 TQCM Mechanical Design

The TQCMs were mounted in the OPM front corner adjacent to the flight samples to monitor any molecular contamination incident on the test samples. The TQCMs were mechanically attached to a support bracket that was mounted to the OPM frame. Indium foil was used to insure good thermal contact of the TQCM sensors to this bracket. Good heat conduction

to the bracket was critical to the successful operation of the sensors. The mounting bracket also insured the top of the TQCM sensor was in the same plane as the flight samples.

3.4.1.3 TQCM Software Design

The TQCM software drivers were used to calculate TQCM beat frequencies and set TQCM operating temperatures. Each TQCM beat frequency was calculated and recorded once every minute. Each TQCM operating temperature was checked and, if necessary, adjusted once every minute. If a TQCM beat frequency reached levels greater than 30KHz, the TQCM software drove the sensor into a clean-up mode. In this mode, the sensor temperature rose to 80°C for 1 hour to attempt to drive contamination off of the exposed crystal's surface.

3.4.2 Testing

Initial ground testing for the OPM TQCM was performed on the bench. A breadboard TQCM controller was built, using analog feedback control theory, and connected to a TQCM TED. The breadboard controller behaved much like the mathematical predictions, but exhibited more sluggish response than desired. This sluggish behavior not only caused slow response, but more overshoot/undershoot than was desired. Slight tuning of the circuit, by changing resistor values to modify the controller's time constant, yielded the desired response. This design was then incorporated into a Flight PCA version.

Once the flight controller had been designed and assembled, the bench test was repeated. The flight controller behaved as expected on the bench. Further testing was performed to simulate on-orbit mission conditions by placing the TQCM in a vacuum chamber and testing performance. This testing revealed the TQCMs TED behavior was quite different in vacuum than in air. A great deal of time was spent learning how to tune the controller to operate the TQCM correctly in a vacuum.

3.4.3 Mission Status

3.4.3.1 Flight Performance

The TQCM environmental monitor subsystem performed well. The control system performed exceptionally well and maintained thermal control at the defined set points of -10°C and -30°C, within ±2°C. The temperature data appeared to have noise on the reading of approximately 5° peak-to-peak. This noise was not observed in either pre- or post-flight testing. If these variations were really a variation in sensor temperature, this would have also significantly affected the frequency of the sensor, which was not observed. Figure 3-20 shows the performance of the –30° TQCM sensor over several orbits on May 3, 1997. The OPM attitude data with respect to the sun is also shown. From this data the normal Mir attitude was solar inertial with the sun positioned just below the horizon for the OPM samples and TQCM sensors. The orbit to orbit variations of the sensor beat frequency during this period was due to

the heating of the Mir surfaces in the field of view. This resulted in a solar induced change of 90-100 Hz. This was typical of the maximum orbital variation observed for the Faraday Laboratories TQCM sensors. Also, from this data, it can be seen that for one orbit, the Mir attitude changed to where the OPM TQCM sensors (and test samples) were at a near normal exposure to the sun.

The TQCM hardware and software worked as expected during the OPM mission. Valuable contamination data were collected. TQCM sensor temperatures remained constant for the duration of the mission. The TQCMs did not collect enough contaminate film to enter the cleanup mode. The TQCM data is discussed in detail in the OPM Science Report.

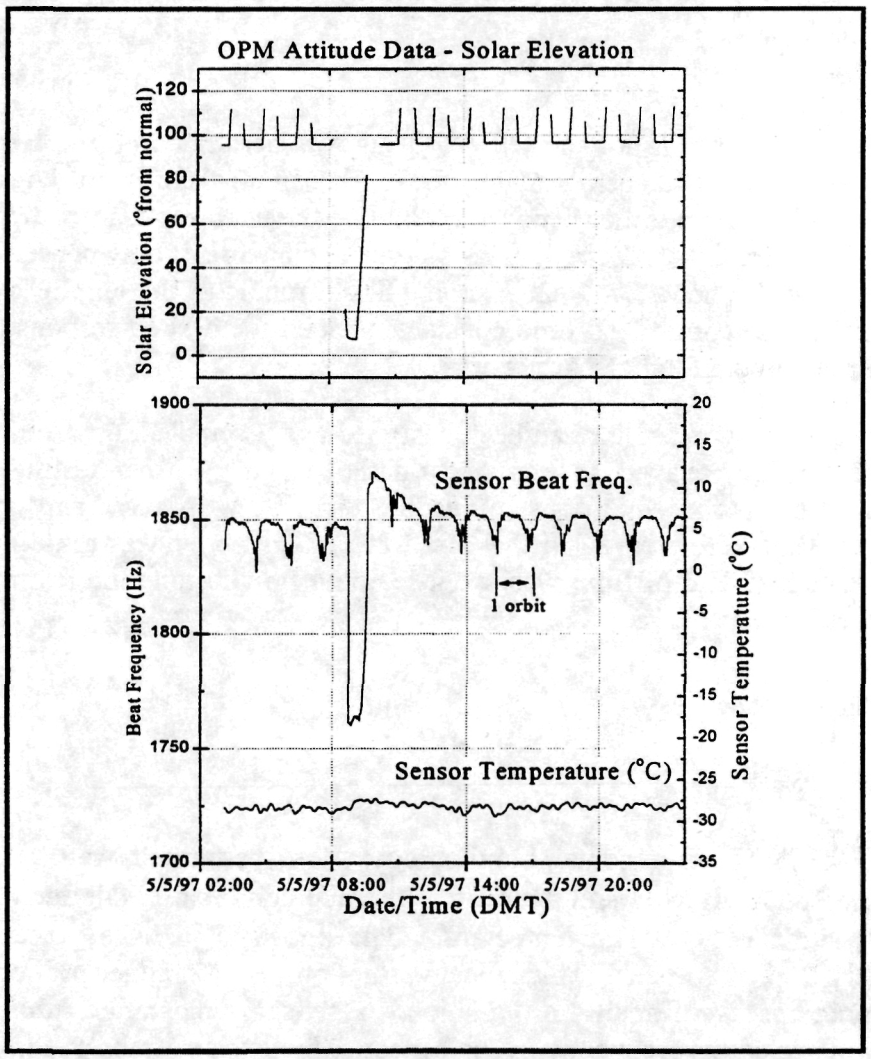


Figure 3-20. Comparison of TQCM and Attitude Data

3.4.3.2 Flight Anomalies

No anomalies in the TQCM subsystem were observed during the mission.

3.5 Atomic Oxygen (AO) Monitor

The effects of AO are one of the primary concerns for materials operating in the LEO space environment. To characterize the effect of AO exposure on materials, the total exposure or fluence and the time history of the exposure must be determined. To provide this required flexibility, the OPM AO monitor was designed to be sensitive enough to measure low AO flux levels where sensitive materials begin to exhibit changes. It must also provide a wide dynamic range for long duration OPM missions.

At the lower LEO altitudes (about 300km) where the Shuttle normally operates, the fluence rate is 10^{13} to 10^{16} atoms/cm^2/sec depending on the solar activity. The total fluence on typical Shuttle missions ranges from 6.5×10^{19} to 3.5×10^{20} atoms/cm^2.

At the higher altitudes (up to 500km) where the Space Station will operate, the fluence rate is significantly lower in the 10^{12} to 10^{14} atoms/cm^2/sec range, for a total fluence per year of 10^{19} to 10^{21} atoms/cm^2.

Given the wide range of potential AO fluence rates and the AO sensitivity of different materials, the OPM AO monitor sensitivity needed to be less than 10^{18} atoms/cm^2/sec and provide a wide dynamic range.

3.5.1 AO Monitor Design

The OPM AO monitor consisted of four carbon film sensors which were exposed sequentially to provide the needed sensitivity and wide dynamic range. The AO sensor used a carbon film as the active element for detecting AO. The carbon sensor was exposed to the AO environment and was eroded away by the reaction of carbon with AO. The resistivity of the carbon element was measured by the OPM system to determine the erosion rate of the element. Combining this rate with AO Reaction Efficiency (RE) for carbon, the total fluence of the exposure was determined. Carbon was chosen as the sensor material because it has zero order reaction kinetics with AO with the resultant products leaving the surface. It was also electrically conductive for ease of measurement. The AO sensors for the OPM were built by Dr. John Gregory of the University of Alabama in Huntsville (UAH). The RE for carbon has been measured at 1.2×10^{-24} cm^3/atom, and to lie in the range of 0.9 to 1.7×10^{-24} cm^3/atom depending on the temperature and form of the carbon.

The AO sensor assembly is shown in Figure 3-21. It used two carbon film elements: one of the elements was overcoated with a protective coating of Sodium Silicate ($NaSiO_4$) to prevent it from eroding and to account for temperature effects in the resistivity measurements of the sensor. The other element was left exposed to the environments where AO reacted with the carbon to release CO as the by-product. The resistance of each element and the temperature of the substrate were recorded by the OPM data system.

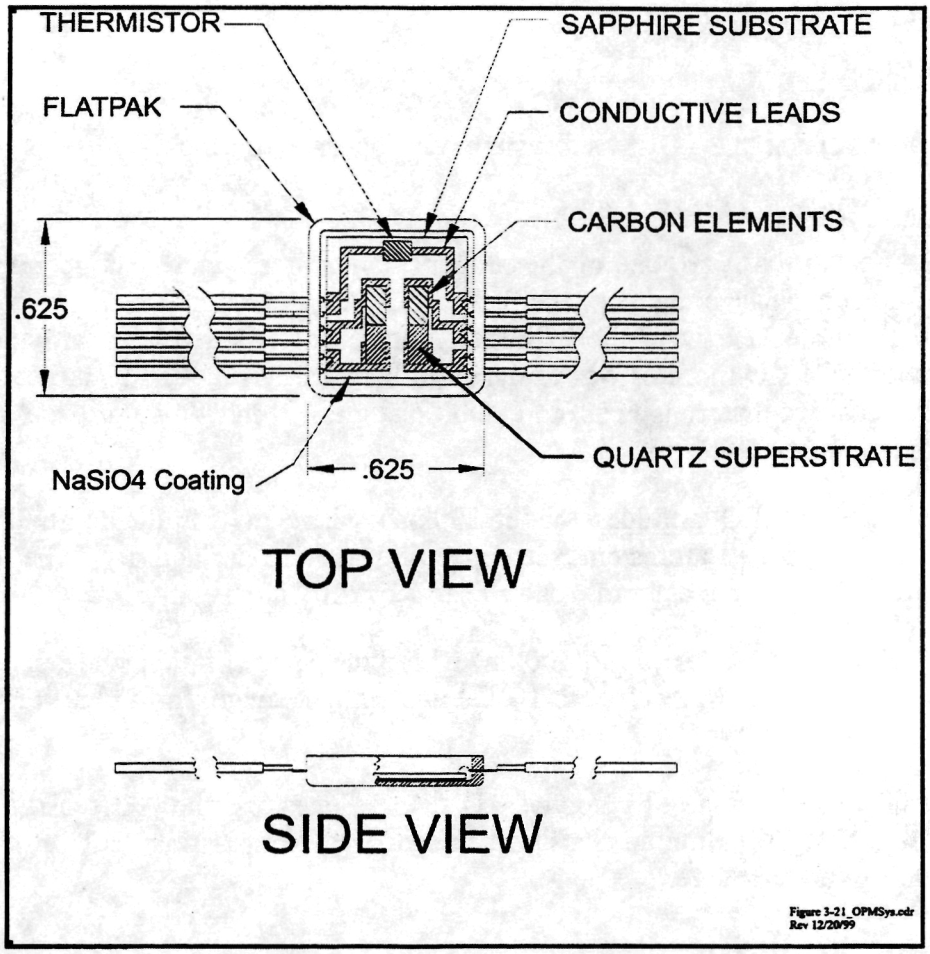


Figure 3-21. AO Sensor Assembly.

The thickness and dimensions of the carbon film can be selected for each mission to accommodate the expected total fluence. Using multiple sensors in the AO monitor, the full fluence can be accommodated even with the failure of one sensor. A trace of carbon film was deposited on a sapphire substrate in serpentine pattern to form the sensor.

The AO monitor assembly, shown in Figure 3-22, consisted of four sensors, one "blank", a motor-driven cover to selectively expose each sensor, and a sub-multiplexer PCB. The four sensors provided the sensitivity and dynamic range for the mission. A motor-driven cover provided the sensor selection capability. A sub-multiplexer PCB interfaced the AO monitor to the OPM cable harness and provided multiplexing of the AO sensors wires to the harness. During ground processing and launch, all sensors were protected by the AO cover plate and the "blank" sensor position was exposed. During the OPM initialization, the first sensor was moved to the exposure position. When the resistance of an element rose above a preset value (due to carbon erosion), the next sensor was to be moved into position. This preset high resistance value could be caused by the film thickness reaching a minimum value or by a sensor failure.

3.5.1.1 AO Monitor Electrical Design

The OPM AO monitor was designed to measure the fluence of AO. Each of the four sensors consisted of carbon film resistor pairs: One of the resistors was covered with $NaSiO_4$ while the other was exposed. As AO eroded the exposed sensor, the resistance increased. The coated or protected sensor was used as a reference for the starting resistance of that sensor. These sensors also included a thermistor to account for thermal effects (refer to Figure 3-21).

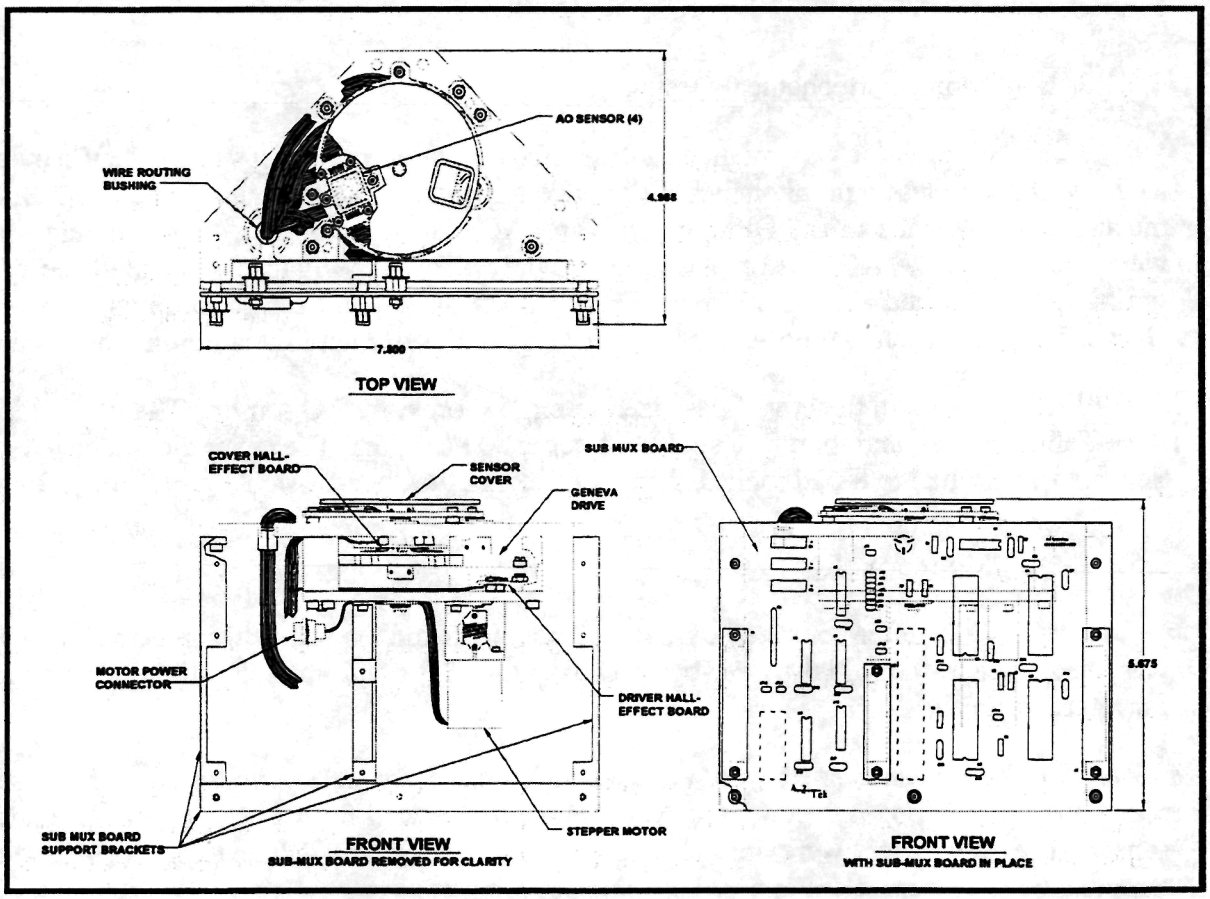


Figure 3-22. AO Monitor Assembly

The monitor had a five position cover with an exposure slot in the cover as one of the positions. In the initial starting position all four sensors were covered. Once in orbit and after power up, the cover was rotated to expose sensor number 1. As the sensor resistance increased, or "wore out" due to AO erosion, the cover was rotated to expose the next sensor. The cover drive consisted of a five step Geneva drive mechanism to effect precision positioning and repeatability. The Geneva was driven by a small space-rated stepper motor. The AO motor driver on the TQCM PAC PCA converted the digital control signals from the DACS to the required voltage and current levels for the motors. It functioned electrically identical to the

drivers on the reflectometer and VUV PAC PCAs. The Geneva drive rotation was software controlled by the DACS. Hall effect devices were used to provide a feed-back position as well as to indicate when the Geneva was in the "locked" position.

Resistance measurement was effected by a dual MUX design, which supported a "pseudo" 4-wire Kelvin measurements. The electrical design for these measurements are given in Section 2.4.1, Sample Carousel.

The sub-multiplexer PCA also had a difference amplifier to raise the thermister/AO sensor output voltage prior to routing the signal through the cable harness.

3.5.1.2 AO Monitor Mechanical Design

The AO monitor was mounted in the OPM front corner (opposite the TQCMs) adjacent to the flight samples to monitor the AO fluence imposed on the samples. The AO monitor was mechanically attached to the OPM frame. The AO sensors, mounted in commercial flatpacks, were clamped to the AO sensor plate (see Figure 3-23). The flatpacks enabled the connector wiring to be attached in a small area. One "blank" on the AO sensor plate assembly was the "launch" position such that no AO sensor was exposed to AO until the mission was initiated.

The aperture in the cover was sized to expose only the AO sensor. The connecting wires were Teflon coated, and therefore subject to some AO erosion. The cover clearance over the AO Sensors was limited to 0.040-inches, thereby reducing the "line-of-sight" portal for AO intrusion.

3.5.1.3 AO Monitor Software Design

The AO monitor consisted of 4 sensor positions and a blank position. The blank position was used prior to the initial power-on of OPM after EVA and upon deactivation in preparation for return to Earth.

The AO mechanism cover was rotated by the software to expose one of the sensor or blank positions. Upon power on, the AO sensors were tested for the next available "undepleted" sensor. The AO sensors were only exposed for 2 hours per day. While exposed, AO sensor and temperature data were taken at a rate of once per minute.

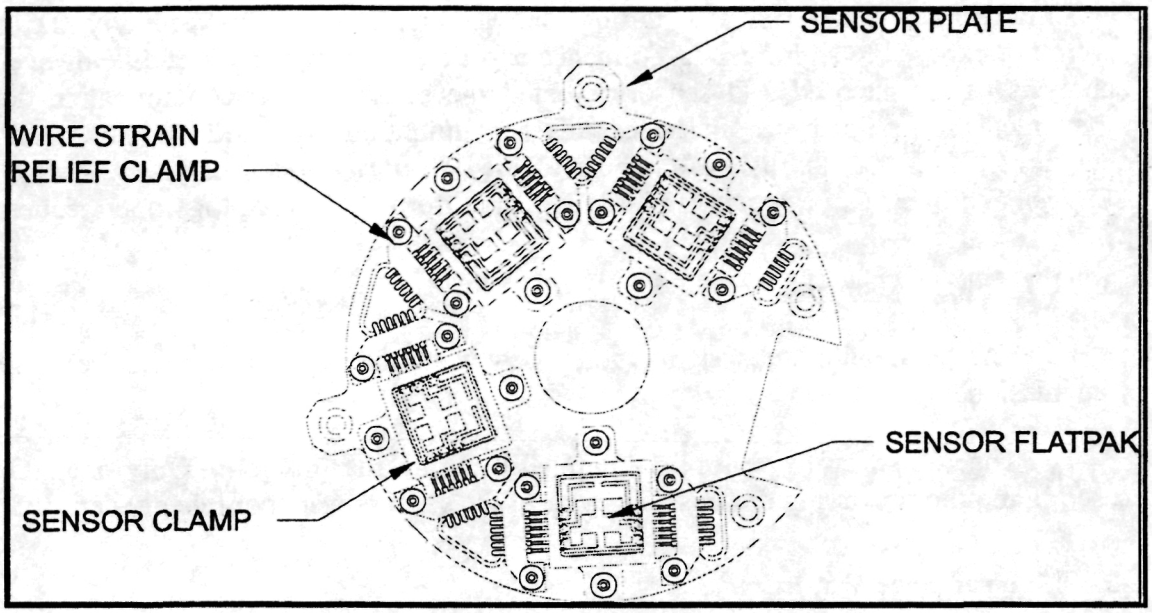


Figure 3-23. AO Sensor Plate Assembly.

3.5.2 Testing

Carbon resistance AO sensors have been flown successfully on short-duration Shuttle missions. While these sensors are well characterized for short missions, a potentially "long" six to nine month mission had not been proven. Therefore, two prototype AO sensors were fabricated and tested at Princeton University's Plasma Physics Laboratory. The samples were exposed for just over one hour to a 5eV neutral AO beam for a total fluence of approximately 2.4×10^{19} atoms/cm^2. At the end of the hour, the exposed samples had eroded away. The data indicated the exposed carbon sensors eroded linearly. One of the protected carbon sensors showed no effect to the AO while the second showed some erosion effects. This was believed due to experimental error or the coating not being as effective as desired.

This test proved the long-term viability of carbon sensors for AO monitors and that the flux could be calculated. Subsequently, these sensors were fabricated and flown on the OPM.

3.5.3 Mission Status

3.5.3.1 Flight Performance

The AO sensors were not exposed, as anticipated, to significant quantities of AO. The Mir Space Station attitude was stated to be a Nadir (gravity gradient) orientation most of the time, where the AO monitor would be exposed to a significant AO flux. Therefore, the AO sensors were protected by the AO sensor cover to reduce depletion and only exposed for one orbit per earth day. Instead, the actual attitude was predominantly more solar inertial where the

AO monitor saw only a "sweep" through the velocity vector. Consequently, the AO monitors were not exposed to significant AO fluence and little data were recorded. However, post-flight analysis of the exposed AO sensor revealed the sensor had a contamination deposit which prevented proper function. In effect, this contamination protected the carbon film from AO reaction. UAH has published a report entitled *"Fabrication and Analysis of OPM Atomic Oxygen Sensors, Final Report,"* and it is available from AZ Technology upon request.

3.5.3.2 Flight Anomalies

The AO monitor subsystem worked very well. There were no anomalies observed during the mission.

The AO software performed nominally during the mission. Only one AO sensor was used in monitoring during the mission; none of the sensors were completely depleted.

3.6 Irradiance Monitors

The OPM irradiance monitor was designed to measure incident energy from the sun, earth Albedo, and earth IR emission. It was also to provide a measure of the exposure time of the flight samples to the direct solar environment.

Two radiometers were used for irradiance measurements: one for the combined direct solar incidence and earth Albedo, and the second for earth-emitted energy (infrared). The design was a simple one using standard detectors and optics. The spectral range of the three energy sources (direct solar, earth Albedo, and earth emitted IR) overlap, and, therefore, could not simply be separately measured by the radiometers. The radiometer with the quartz lens was designed to see mainly the direct solar and earth Albedo. The radiometer with the germanium optics was designed to see mainly the earth emitted IR. Given the Mir attitude data obtained from the Russians, and knowing the OPM orientation on the Mir, the direct solar, earth Albedo, and earth-emitted energy could be calculated from these two radiometers.

3.6.1 Radiometer Design

The radiometers for this experiment consisted of thermopile detectors (a multiple-junction thermocouple) painted flat black covered with optics that selectively passed the external energy flux. Multiple junctions increased the sensitivity of the detector to the incident energy flux and gave a greater voltage output. Internal thermistors to the detector were incorporated to monitor the detector thermal response. The optics tailored the FOV of the radiometer to be as close to the same as the flight test samples. The lens material was selected to tailor the spectral response of the radiometer. For the solar spectral region of 0.2 to 3 microns, a quartz lens was used. A germanium lens was used for the infrared spectrum (between 2 and 20 microns). The irradiance monitor accuracy at near normal angles of incidence was not significantly degraded because of errors in attitude data. However, due to the near cosine response of the radiometer, the "system" accuracy approached five percent for low angles of incidence.

The radiometer performance criteria was:

	Solar	Infrared
Spectral Range	200nm - 3,000nm	2,000nm - 20,000nm
Optical Window	Quartz	Germanium
Accuracy	5%	5%
FOV	150°	150°
See Figure	3-24	3-25

The two radiometers were installed with baffles mounted over the lenses to block any reflected energy from its respective FOV of the OPM top cover.

3.6.1.1 Radiometer Electrical Design

The electrical design for the two radiometers was straight forward. The basic definition of radiometer is: a thermopile with a thermister and a lens. The thermopile consisted of several thermocouples, wired in series and painted optical black, that generated a voltage proportional to light intensity (temperature of the coating).

Each of these two radiometers had a pre-amp on the carousel sub-multiplexer PCA for signal conditioning prior to routing through the OPM cable harness to the DACS A2D. Each of these pre-amps had a time constant to make the response more sensitive to changes, and to remove the DC offset of each radiometer.

3.6.1.2 Radiometer Mechanical Design

The radiometers were mounted in the OPM sample carousel, as shown in Figure 2-13, and flush with the carousel top plane to enable the carousel to rotate inside the OPM. The radiometers were placed into a pilot hole in the carousel, pinned by a dowel, and bolted to the carousel. The outer diameter of each radiometer was established by the optical lens refraction path to the detector. The lens was mechanically clamped to the radiometer housing to comply with the "frangible" material safety issues of the Safety Panels. A wire clamp was bolted on the bottom of the radiometer housing to secure the detector wiring to the housing. A nine-pin connector connected the OPM harness (though the carousel sub-multiplexer PCA) to each radiometer. With this design, each radiometer could be removed intact from the carousel. Detailed drawings of the solar and earth IR radiometers are shows in Figures 3-24 and 3-25 respectively.

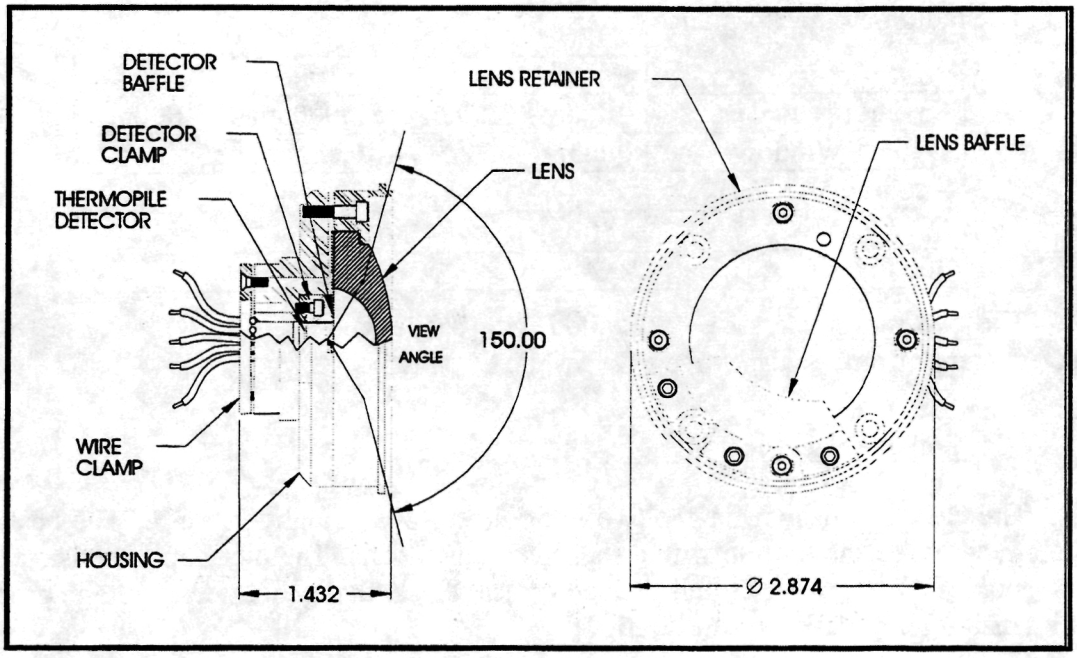


Figure 3-24. Solar Radiometer.

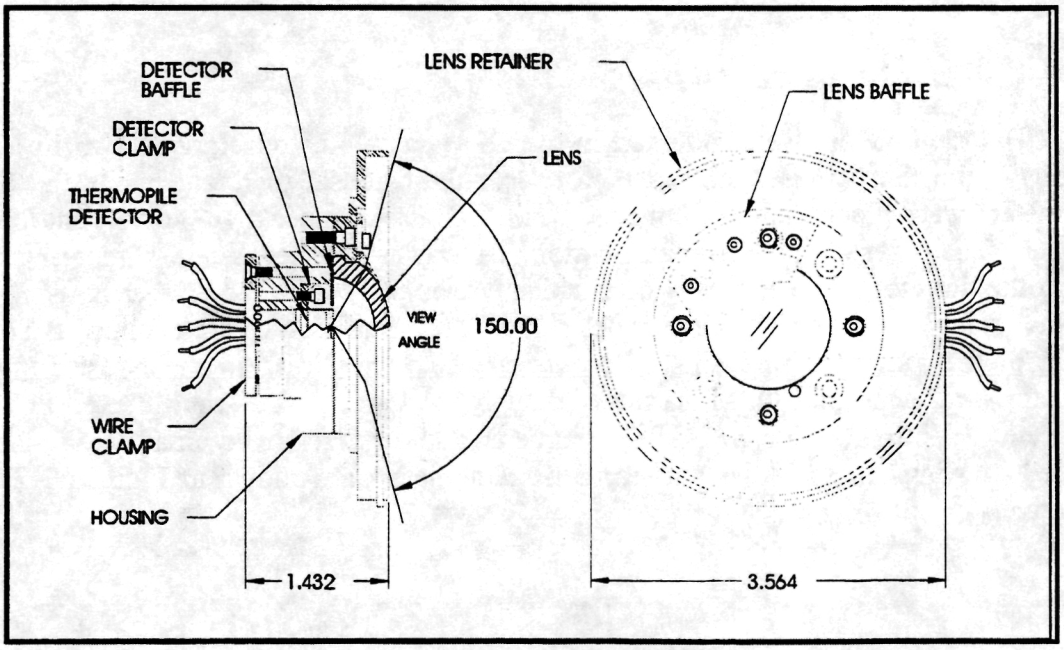


Figure 3-25. Earth IR Radiometer.

3.6.1.3 Radiometer Software Design

The radiometers were read once per minute during monitoring mode. The radiometer software performed nominally during the mission.

3.6.2 Testing

Both OPM radiometers were calibrated using equipment and laboratory facilities of the U.S. Army Radiation Standards and Dosimetry Laboratory at Redstone Arsenal. The radiometer electrical output produced by a known source of total irradiance was recorded for each unit under test. A standard 1,000 watt quartz-halogen Tungsten lamp was used as the calibrated source for the solar radiometer. A laboratory blackbody operating at 600° Kelvin was used as the source for the IR radiometer calibration. Because of the extremely wide fields-of-view associated with the radiometers, calibration using an extended source large enough to completely fill the FOV was considered to be impractical, although this was the preferred method for achieving direct calibration. Alternatively, the radiometer response to a small source was determined for all incidence angles up to and including the maximum field angle to determine any departure of the radiometer response from that of an ideal cosine receiver.

The radiometers were mounted on a rotary stage that permitted adjustment of the incident angle by rotating the radiometer with respect to the source. Angular response was determined for field angles of -100 to +100° at 5° intervals in both x and y axes. In order to establish repeatability of the measurements, three runs were made for each setup. The results were averaged to determine the calibration factors. Additional information regarding the radiometer calibration may be found in the *Radiometer Calibration Test Report, AZ Technology Report No. 91-1-118-142.*

3.6.3 Mission Status

3.6.3.1 Flight Performance

The radiometers were designed to measure solar and earth irradiance looking out from a satellite such as the European EURECA. The OPM location on the Mir had large veiwing angles to the Mir modules. The solar energy reflected from the Mir componments and the temperature of those surfaces resulted in irradiance levels on the radiometers that far exceeded solar and earth readings. This resulted in the radiometer data not being useful for exposure determination. Detailed attitude data provided by the Mir team allowed the accurate determination of solar exposure. See the OPM Science Data Report for these data.

3.6.3.2 Flight Anomalies

The infrared radiometer performed without any anomalies. However, the solar radiometer thermopile failed in June 1997 during a full-sun orbit. No further solar data was

recorded from this radiometer, but the thermistor remained operational.

The solar radiometer anomaly was investigated once the OPM was returned to ground. The fault revealed the thermopile detector resistance was "open." A spare detector was attached to the OPM cable harness and the OPM DACS was able to record viable data. The cause of the "open" detector is not resolved at this time.

4.0 POST-FLIGHT STATUS

The OPM returned to ground on STS-89 on January 31, 1998. The OPM was mounted in the same specially designed structure in a SpaceHab Double rack that was used for launch. The rack also held the OPM/Mir Interface Plate. Other OPM hardware was returned to ground in crew stowage bags. All OPM hardware was released to AZ Technology at the SPPF. The first opportunity for AZ Technology personnel to see the OPM hardware was on February 23, 1998. During the week of February 23-26, 1998, a visual inspection was performed on the OPM hardware, an inventory of hardware taken, the OPM de-integrated from the SpaceHab Double rack, and the first post-flight functional test performed. After the preliminary inspection and functional testing, the OPM was shipped to AZ Technology's facility in Huntsville, Alabama for further system checks, functional tests, and visual inspections.

4.1 Hardware Returned From Flight

The flight hardware inventory returned from the Mir Space Station included:

- OPM Assembly
- OPM/Mir Interface Plate
- EVA Cable
- IVA Cable
- Cable Bags (2 sets)
  - Cover Bag
  - EVA Cable Bag
  - IVA Cable Bag
- Software Bag
- Contamination cover
- Two Software diskettes (2 sets)
- Nomex transfer bag (backup unit)

The original nomex transfer bag that protected the OPM from launch through EVA deployment was believed to be lost inside the Spektr module. It was not returned to ground. The OPM/Mir Interface Adapter was left aboard Mir upon Russian request.

A visual inspection of the hardware revealed the following changes from launch:

The OPM/Mir Interface Plate contained obvious discolorations
The nomex transfer bag had miscellaneous pencil and pen marks
There was obvious discoloration (brown) on the OPM MLI Beta Cloth
The EVA Cable Beta Cloth had obviously discolored
The top cover thermal control coatings has numerous scratches and nicks.

The discolorations were subsequently photo documented by NASA photographers.

4.2 Post-Flight Functional Test at the SPPF

A short post-flight functional test was performed on the OPM assembly to check its health and status. During the setup for this test, the OPM was powered up and the carousel rotated to check and photograph the flight samples on the carousel. There were no major anomalies observed on the flight samples, except for one calorimeter that appeared to have lost some of its thermal control coating during the mission. While the OPM was powered on, the last measurement timeline data was downloaded from the DACS memory.

The short functional test was performed on a subset of the samples for each instrument to minimize the time required to conduct the test. This test confirmed two anomalies observed from the data taken during the measurement timelines while on orbit. The following malfunctions were verified during this ground test with the observed cause of the malfunction, determined during later testing at AZ Technology, given in parentheses: (1) VUV lamp (not striking), and (2) the solar radiometer (no signal). Further, one additional malfunction was discovered: there was no energy detected in one of the reflectometer lamp energy bands. A check of the last timeline data downloaded at the SPPF revealed this anomaly had occurred in the middle of the last timeline. No other malfunctions or anomalies were reported by this test. All other OPM subsystems worked as expected.

4.3 Post-Flight Functional Test at AZ Technology

This full length post-flight test was performed on the full complement of samples on the carousel to determine the characteristics of the flight samples after return from space. Prior to this test, AZ Technology worked with MSFC engineers to develop a procedure to determine the cause of the reflectometer lamp malfunction. During this investigation, the lamp was determined to have failed and it was replaced. A short test was then performed and measurement data recorded to ensure proper operation before the full length functional test. During the full length functional test, another malfunction was reported with the VUV subsystem. The filter wheel ceased rotating reliably. This anomaly was duly recorded for future characterization. All other systems and subsystems performed as expected.

4.4 Status Checks and Anomaly Investigations

After return of the OPM to AZ Technology in Huntsville, AL, the OPM was subjected to a battery of post-flight functional/status checks to characterize the health/status of the OPM hardware. Test Preparation Sheets (TPS) were developed to detail the desired steps taken for the status checks and/or anomaly investigations. Prior to the performance of each TPS, MSFC reviewed and approved each procedure. Through December 31, 1999, twenty TPS had been approved, and nineteen performed. The list of TPS are given in Table 4-1. TPS 015, to remove the TQCM sensors, was not performed. TPS020B was stopped short of completion because the stepper motor was not removed from the OPM. An engineering decision was made to leave the configuration as-is because a different higher output torque stepper motor most likely will have to be installed for a reflight.

Table 4-1. OPM TPS Log

TPS Log No.	TPS Identification	TPS Name	Status	Date Completed	Comments
1	AZ-TPS-OPM-001	Russian AT	Complete	09/27/96	
2	AZ-TPS-OPM-002	Removal of Volatile Organic Alcohols from OPM	Terminated	09/30/96	Toxicity Test Required
3	AZ-TPS-OPM-003	OPM Mission Simulation Test	Complete	10/14/96	
4	AZ-TPS-OPM-004	OPM Ground Processing at SPPF (STS-81)	Complete	10/24/96	
5	AZ-TPS-OPM-005C	OPM Ground Processing at SPPF (STS-89)	Complete	02/26/98	4 NCRs Opened
6	AZ-TPS-OPM-006C	OPM Return to AZ Technology	Complete	03/02/98	
7	AZ-TPS-OPM-007A	Post-Flight Functional Testing at AZ Technology	Complete	03/16/98	2 NCRs Opened. Tungsten Filament Failure
8	AZ-TPS-OPM-008A	Remove Flight Samples	Complete	04/24/98	Redlined TPS. TIS calibration sample not removed.
9	AZ-TPS-OPM-009	OPM Post-Flight Baseline Measurement Test	Complete	03/20/98	1 NCR Opened - Closed
10	AZ-TPS-OPM-010	Check EEPROM	Complete	03/30/98	
11	AZ-TPS-OPM-011	Download All Backup Data to GSE PC	Complete	04/08/98	
12	AZ-TPS-OPM-012A	VUV Lamp Troubleshooting	Complete	04/10/98	
13	AZ-TPS-OPM-013B	Solar Radiometer System Troubleshooting	Complete	04/09/98	Sensor Failure
14	AZ-TPS-OPM-014A	Final VUV Lamp Troubleshooting	Complete	05/28/98	Heater Circuit Failure
15	AZ-TPS-OPM-015	TQCM Sensor Removal from the OPM	Approved		TQCMs not removed
16	AZ-TPS-OPM-016	AO Sensor Removal from the OPM	Complete	07/20/98	
17	AZ-TPS-OPM-017A	VUV Filter Wheel Anomaly Investigation	Complete	07/10/98	
18	AZ-TPS-OPM-018A	Check VUV Filter Wheel Stepper Motor Torque/Load	Complete	11/17/98	
19	AZ-TPS-OPM-019A	Final VUV Filter Wheel Stepper Motor Checkout	Complete	12/14/98	
20	AZ-TPS-OPM-020B	VUV Flight Stepper Motor and Filter Wheel Torque Tests	Incomplete	5/3/99	Stopped at Step 5.5

5.0 SUMMARY

The OPM mission to Mir was a very successful mission. This success was due to the performance of the OPM system and instruments on a very difficult mission. The scientific results from this mission are discussed in the *OPM Science Data Report, AZ Technology Report No. 91-1-118-169.* A few of the OPM system highlights are:

- The core systems performed as designed. There were no anomalies in the core systems.
- The anomalies during the mission occurred at the end-component level in the instruments and monitors, not in the core systems. These include the reflectometer tungsten lamp, VUV Deuterium lamp, and solar radiometer detector.
- The OPM performed well in the space environment, and withstood unexpected conditions:
  - No power for two and one-half months; but core systems still powered up successfully and completed the mission.
  - Thermal margins were adequate. Station attitude went to full sun twice during the mission, creating over temperature conditions, but core systems remained operational.
  - Measurement data survived with few "upsets;" error correcting memory and memory scrubbing performed well.
- The software control program maintained good control over the autonomous OPM operation.
- The OPM returned intact. There were no frangible material issues. The external surfaces had some obvious "wear," but had not broken.
- There were no signs of "self-contamination." The OPM was "clean," or free from self-contamination.

The OPM was designed as a reusable flight instrument for multiple missions with minimal redesign and/or reconfiguration. A reflight opportunity for this materials laboratory to the new ISS is needed.

- There is an ongoing need for the contamination and materials degradation data. These data are necessary for the planning efforts for ISS materials life expectancy and potential refurbishment.
- These data are needed sooner than later. The OPM can be ready to refly in less than 24 months. This includes the OPM refurbishment, any design efforts to interface to ISS, and new sample materials.
- The OPM can accommodate other communication protocols and input voltages, as required.
- The OPM can quickly characterize this ISS AO, contamination, and Solar/Earth radiation environments, using proven subsystems.

ATTACHMENT 1

List of Available OPM Reports, Procedures and References

Page intentionally left blank

Page intentionally left blank

REFERENCES

1. Pezzaniti, J.L., Hadaway, J.B., Chipman, R.A., Wilkes, D., Hummer, L., and Bennett, J.M., 1990. *Total Integrated Scatter Instrument for In-Space Monitoring of Surface Degradation.* Proc. Soc. Photo-Opt. Instrum. Eng. 1329, 200-210.

2. Hadaway, J.B., Ahmad, A., and Bennett, J.M, 1997. *Final Design, Assembly, and Testing of a Space-Based Total Integrated Scatter Instrument.* Proc. Soc. Photo-Opt. Instrum. Eng. 3141, 209-219.

3. McHugh Photonics now manufactures the LASERS used in the OPM TIS instrument. When the project first began, Amoco Laser Company (ALC) manufactured the commercial units. Later, ALC was sold to ATx Telecom. When the LASERS used in OPM were sold to a competitor, AZ Technology worked through McHugh Photonics to complete this work.

List of Available OPM Reports:

OPM Report Title	AZ Technology Report No.	Release Date
Development Tests for the Amoco LASER company Solid-State Diode Powered LASERs	91-1-118-129	January 9, 1997
Radiometer Calibration Test Report	91-1-118-142	April, 1996
Thermal Data Book for the OPM Experiment	91-1-118-145	April 22,1997
OPM System Report	91-1-118-164	December 31, 1999
Mission Thermal Data Book	91-1-118-166	December 31, 1999
OPM Software Reference Manual	91-1-118-167	January 5, 1999
OPM Science Data Report	91-1-118-169	December 31, 1999
Fabrication and Analysis of OPM Atomic Oxygen Sensors, Final Report	Published by UAH, Laboratory of Materials and Surface Sciences	February 1999

List of Available OPM Procedures:

OPM Procedure Title	AZ Technology Report No.	Release Date
Electromagnetic Compatibility Test Procedure	91-1-118-138	June 25,1996
Thermal Vacuum Test Procedure	91-1-118-139a	July 8, 1996
Vibration Test Procedure and Data	91-1-118-140	July 8, 1996

REPORT DOCUMENTATION PAGE

Form Approved
OMB No. 0704-0188

Public reporting burden for this collection of information is estimated to average 1 hour per response, including the time for reviewing instructions, searching existing data sources, gathering and maintaining the data needed, and completing and reviewing the collection of information. Send comments regarding this burden estimate or any other aspect of this collection of information, including suggestions for reducing this burden, to Washington Headquarters Services, Directorate for Information Operation and Reports, 1215 Jefferson Davis Highway, Suite 1204, Arlington, VA 22202-4302, and to the Office of Management and Budget, Paperwork Reduction Project (0704-0188), Washington, DC 20503

1. AGENCY USE ONLY *(Leave Blank)*	2. REPORT DATE	3. REPORT TYPE AND DATES COVERED
	March 2001	Contractor Report (Final)

4. TITLE AND SUBTITLE
System Report for the Optical Properties Monitor (OPM) Experiment

5. FUNDING NUMBERS
NAS8–39237

6. AUTHORS
L. Hummer

7. PERFORMING ORGANIZATION NAMES(S) AND ADDRESS(ES)
AZ Technology, Inc.
7047 Old Madison Pike, Suite 300
Huntsville, AL 35806

8. PERFORMING ORGANIZATION REPORT NUMBER
M–1008

9. SPONSORING/MONITORING AGENCY NAME(S) AND ADDRESS(ES)
George C. Marshall Space Flight Center
Marshall Space Flight Center, AL 35812

10. SPONSORING/MONITORING AGENCY REPORT NUMBER
NASA/CR—2001–210882

11. SUPPLEMENTARY NOTES
Prepared for Materials Processes and Manufacturing Department, Engineering Directorate
Technical Monitor: Ralph Carruth

12a. DISTRIBUTION/AVAILABILITY STATEMENT
Unclassified-Unlimited
Subject Category 18
Standard Distribution

12b. DISTRIBUTION CODE

13. ABSTRACT *(Maximum 200 words)*

This systems report describes how the Optical Properties Monitor (OPM) experiment was developed. Pertinent design parameters are discussed, along with mission information and system requirements to successfully complete the mission. Environmental testing was performed on the OPM to certify it for spaceflight. This testing included vibration, thermal vacuum, electromagnetic interference and conductance, and toxicity tests. Instrument and monitor subsystem performances, including the reflectometer, vacuum ultraviolet, total integrated scatter, atomic oxygen monitor, irradiance monitor, and molecular contamination monitor during the mission are discussed.

The OPM experiment was launched aboard the Space Shuttle on mission STS–81 in January 1997 and transferred to the *Mir* space station. An extravehicular activity (EVA) was performed in April 1997 to attach the OPM experiment to the outside of the *Mir*/Shuttle Docking Module for space environment exposure. The OPM conducted in situ measurements of a number of material samples. These data may be found in the OPM Science Report. OPM was retrieved during an EVA in January 1998 and was returned to Earth on board the Space Shuttle on mission STS–89.

14. SUBJECT TERMS
space environment, environmental effects, optical properties, thermal control, *Mir*, space station

15. NUMBER OF PAGES
139

16. PRICE CODE
A07

17. SECURITY CLASSIFICATION OF REPORT	18. SECURITY CLASSIFICATION OF THIS PAGE	19. SECURITY CLASSIFICATION OF ABSTRACT	20. LIMITATION OF ABSTRACT
Unclassified	Unclassified	Unclassified	Unlimited

National Aeronautics and
Space Administration
AD33
George C. Marshall Space Flight Center
Marshall Space Flight Center, Alabama
35812